APPLICATION OF STABLE ISOTOPES AND GEOSTATISTICS TO PREDICT REGION OF GEOGRAPHIC ORIGIN FOR DECEASED MIGRANTS RECOVERED IN SOUTHERN TEXAS

by

Robyn T. Kramer, BA

A thesis submitted to the Graduate Council of
Texas State University in partial fulfillment
of the requirements for the degree of
Master of Arts
with a Major in Anthropology
July 2018

Committee Members:

Nicholas Herrmann, Chair

Eric Bartelink

Kate Spradley

FAIR USE AND AUTHOR'S PERMISSION STATEMENT

Fair Use

Duplication Permission

DEDICATION

To my *inamorato*, Walter Sipple, who was my rock and kept me going when times were tough. Thank you for everything, especially Alexa. I could not have achieved this without your love, laughs, adventures, and most importantly, your never-ending support and insistence that I never give up on my dreams. I love you.

I also want to dedicate this work to my father and grandmother for helping me fully experience graduate school—I am eternally grateful for your support and love. A special dedication to my partner-in-suffering, Mary Swearinger and the Sipple family for helping me move to Texas, for supporting Walter and me in every way, and for being the wonderful people they naturally are.

I want to dedicate this work to my sister, mother, little Thea, and my family in Alaska, Texas, Tennessee, North Dakota, Hong Kong, and Budapest. Even though we are spread around the world, you have been a wonderful support system. In addition to my family, this work is dedicated to my life cohort: Greg Merrill, Anna Guiles, Kristina Houchin, Minnie Lai, Lucien Gendrot, Linda Qiu, Grace Grimes and Stacey Lo. Thank you for your friendship and continuous support. This work would be eligible without Hoppy, who made me a Yerd—everything you taught me helped me succeed in Graduate School. Lastly, I want to thank and dedicate this work to the countless migrants that have lost their lives crossing the border. I hope my research helps you find your way home.

ACKNOWLEDGEMENTS

Thank you, Dr. Nicholas Herrmann, Dr. Kate Spradley, Operation Identification, and my cohort at Texas State University. The project would not have been possible without your advice, knowledge, and the resources you provided. Thank you Dr. Grady Early for your financial support through the Grady Early Endowment. I would like to thank the Graduate College at Texas State and Dr. Jim Garber for funding my research as well. Your support was necessary for this research and I greatly appreciate your contributions. A special thanks to Dr. Eric Bartelink for the helpful feedback, countless edits, funding, and collaboration. I would be nowhere without you and I am truly grateful for your guidance and your friendship.

Thank you, Gabriel Bowen, Eileen Miller, and the entire ITCE-NSF SPATIAL 2017 staff and students. Without the knowledge you all provided, this work would hold no weight. I earnestly thank you for your wisdom and guidance. Clément Bataille, thank you for sharing your global strontium isoscape rasters with me and for helping me adjust the r-code for the assignment model. I am truly grateful for your help and hope to continue working with you on future projects. Mike Wunder, thank you for allowing me to use and adjust the assignment code. Thank you, Lesley Chesson and IsoForensics, Inc. for preparing and analyzing the isotope samples. Lastly, I would like to thank the many contributors to research in strontium analysis, whose published work is used to calibrate the strontium model; a list of contributors is provided in Appendix B. Without your work, this project would be impossible. I sincerely thank you all for your research and data.

TABLE OF CONTENTS

Page

LIST OF TABLES

Table **Page**

LIST OF FIGURES

Figure **Page**

LIST OF ABBREVIATIONS

Abbreviation	Description
FACTS	Forensic Anthropology Center at Texas State
OpID	Operation Identification
EAAF	Equipo Argentino de Antropologia Forense
$\delta^{18}O$	Ratio of oxygen stable isotopes (^{18}O and ^{16}O)
$^{87}Sr/^{86}Sr$	Ratio of strontium stable isotopes
GNIP	Global Network of Isotopes
IAEA	International Atomic Energy Agency
SIPL	Stable Isotope Preparation Laboratory
PCOME	Pima County Office of the Medical Examiner
UBC	Undocumented Border Crosser
UAC	Unaccompanied Alien Child
FU	Family Units
BP	Border Patrol
FDB	Forensic Data Bank

I. INTRODUCTION

The land spanning the Mexico and US border totals 2,000 miles and experiences hundreds of thousands of border-crossings each year by migrants fleeing violence, seeking refuge and safety, in search of work, better healthcare, educational opportunity, and to reunite with family (Anderson, 2008; Spradley, et al. 2008; Holmes, 2013; DeLuca, et al. 2010). In recent years, migrants apprehended in Texas Border Patrol Sectors consist of males and females of varying age groups traveling from Mexico, Honduras, Guatemala, and El Salvador (United States Customs and Border Protection, 2016). The Pima County Office of the Medical Examiner (PCOME), Forensic Anthropology Center at Texas State (FACTS), Colibri Center for Human Rights, Argentinian Forensic Anthropology Team (EAAF), and South Texas Human Rights Center have joined together in an agreement to share information concerning migrant deaths with the goal of increasing the number of positive identifications and to better understand the scope and impact of migrant deaths (Anderson & Spradley, 2016; Spradley, 2014).

Currently, the primary methods used to estimate ancestry for unidentified skeletal remains are craniometric (Spradley, et al. 2008) and dental morphological analyses (Edgar, 2013), both of which are not currently capable of discerning between "Hispanics" of different country origins. This is mainly due to "the term Hispanic [being] a social construct with no precise genetic meaning" (Spradley et al., 2008:21). Instead, the U.S. Census Bureau classifies all members of the Caribbean, Mexico, Central America, and South America as "Hispanic" (Spradley et al., 2008). Promising attempts have recently been made by Edgar (2013) to differentiate between New Mexican Hispanics and South

Floridan Hispanics using dental morphological traits that are characteristic of those populations. In some cases, the cranium and/or the appropriate teeth necessary for ancestry estimations are not present, which prohibits either craniometric or dental morphological analyses. For cases missing essential skeletal elements required for ancestry estimation, stable isotope analysis can help estimate the regional geochemical signature of the skeletal elements and dental structures that are recovered with the individual. Stable isotopes are incorporated into the hard and soft tissues of people during life and can be extracted after death to inform the investigator of diet and migration patterns of the decedent. Therefore, I propose using stable isotope analyses as a tool to estimate geographic region of residence for deceased undocumented migrants recovered along the Mexico-US border in South Texas.

Strontium and oxygen isotope analysis can aid in the identification and repatriation of deceased migrants by excluding possible matches and isotopically narrowing the region of residence to specific areas within Central America, South America, the Caribbean, as well as Mexico. The use of isotopes to help identify migrants can be applied in conjunction with DNA, craniometric, and dental morphological data. Isotope analysis can rule out geographic regions that do not correspond to predictions based on isotope signatures from skeletal material. This eliminates time spent looking at missing person reports that may match the biological profile but are not congruent with the isotopic information for the individual.

Purpose of Research

The purpose of this research is to construct a general coarse-grained baseline strontium and oxygen isoscape model using data from existing literature by which unidentified deceased migrants can be mapped isotopically to estimate their region of geographic residence. Dr. Kate Spradley is the director of Operation Identification (OpID), a project with the aim of identifying and repatriating the skeletal remains of undocumented deceased migrants recovered in southern Texas. Stable isotope analysis can assist identification efforts by reducing the potential matches for unknown cases within the National Missing and Unidentified Persons (NamUs) database using residential history. The primary objective of my research is to determine how these individuals fit into the established models and see if their isotope signatures correlate with other lines of evidence.

Broader Impacts of Research

Hundreds of unidentified deceased migrants are found along the Mexico-US border each year and the number of deceased is increasing. Without knowledge of which region deceased migrants originate from within Central America, South America, and Mexico, it is nearly impossible to return their remains to their families. DNA analysis does not always provide an avenue to identification. Family reference DNA samples may not be available in the federal CODIS (Combined DNA Index System) database and therefore cannot be compared with the migrant samples. Forensic anthropologists and human rights groups work ardently to make public the biological profiles, pictures of personal effects, and descriptions of any identifying features of migrants to allow

potential family members to review and find their loved ones through online resources, such as NamUs (http://namus.gov/), the Colibri Center for Human Rights (http://www.colibricenter.org/), the Lost and the Found (https://lostandfound.revealnews.org/), and many others.

Isotopic data can aid in the identification efforts of these individuals by targeting geographic regions based on isoscape results and adding more information to the individual's case files. Isoscapes are maps that depict the spatial distribution of isotopes available in an area or region (Bowen, 2010; Bowen et al., 2013; West, 2006, 2010; Beard & Johnson, 2000). Adding the criteria of "location of residence" to online databases would allow for easy filtering of cases that do not fit the search criteria. For example, a family from Guatemala searching for their lost loved one could filter out the cases that indicate Mexico and El Salvador isotopic residential histories. Isotope analysis is a powerful tool that has the potential to aid in identification efforts; however, it has not been fully integrated in the forensic realm.

Research Design

Dental samples, specifically maxillary premolars, were extracted from deceased migrants that are temporarily curated by OpID at FACTS. The dentition was used in isotopic analysis that estimates the region of origin during childhood using local strontium and oxygen ratios. The dental isotope values will be run through a likelihood assignment model and mapped onto the baseline isoscape depicting the most probable region(s) of origin for each sample based on the variation in strontium (derived from bedrock, soil, catchment, and bioavailable sources) and oxygen (derived from precipitation values) for Mexico, Central America, and the Caribbean. The research

objectives are addressed in the following questions:

(1) Do migrants fit into the established isotope models for strontium ($^{87}Sr/^{86}Sr$) and oxygen ($\delta^{18}O$) variation for Mexico, Central America, and Caribbean?

(2) Do the isotopically estimated geographic residences of sampled migrants reflect the Border Patrol apprehension rates? Do they reflect recovery rates reported by the Pima County Office of the Medical Examiner in Arizona?

(3) Are the isotopic signatures of migrants found with regionally/country specific material culture consistent with their predicted region/country of origin?

(4) When comparing the craniometric data with the strontium data, are there observed patterns that reflect significant structuring within the OpID sample?

To address the first question, oxygen and strontium isotopes are used to construct isoscapes that depict variation in Central America, Mexico, and the Caribbean. Previous bioavailable strontium ($^{87}Sr/^{86}Sr$) data are collected from a variety of published sources to adjust the existing models of bedrock, water catchment, and soil strontium constructed by Bataille et al. (2012; in prep). Oxygen (^{18}O) precipitation data gathered from the Global Network of Isotopes in Precipitation online database encompasses precipitation isotopes collected since 1961. The temporal context for the precipitation data varies due to availability of the information; all available data are compiled and averaged to produce a

mean annual precipitation isoscape for the region and are available through IsoMAP (https://isomap.rcac.purdue.edu/isomap/) and waterisotopes.org.

Dental enamel samples, specifically from premolars, collected from five individuals (n=5) from the OpID forensic cases are extracted and prepared for isotopic analysis. Strontium and ^{18}O isotope values obtained from the teeth are analyzed to evaluate signatures incorporated into the teeth during the tooth's development. Strontium and ^{18}O from the diet are incorporated into human tooth enamel during tooth formation in childhood (Lee-Thorp 2008). The strontium ratio ($^{87}Sr/^{86}Sr$) of a tooth reflects the environmental $^{87}Sr/^{86}Sr$ values during the time of tooth formation and is therefore an indicator of childhood residency (Bentley 2006). Comparison of the isotope values extracted from the dentition in conjunction with isoscapes allow for an estimation of region of geographic residence for the individuals during their childhood. A likelihood assignment model established by Wunder (2005) produces probability densities for each sampled individual using the $^{87}Sr/^{86}Sr$ and ^{18}O data. The results of the assignment depict probability density heat maps showing the most likely region(s) of geographic residence for each sampled individual.

The second objective seeks to understand whether the proportions of migrants apprehended by Border Patrol country-wide reflect the population proportions of identified migrants recovered along the Texas-Mexico border and housed in the Operation Identification skeletal inventory at Texas State University. The published apprehension criteria available on the official Border Patrol website serves as the expected values for proportions of migrants coming into the US and can be used to test whether the same proportions of populations are migrating into the Texas region of the

southern border. A chi square test will be used because the data are categorical count data reported by three different institutions.

The third question concerns the associated cultural material recovered with the deceased migrants. The cultural material is used as a predictor for region of geographic residence and to assist in sample selection (e.g. an individual carrying quetzals is more likely to originate from, or at least had to travel through, Guatemala and not Mexico). If isotope values predict that an individual maps into the same region as the cultural material, associated artifacts recovered with the deceased migrants may be useful in assessing their region of geographic residence.

Lastly, measurements from the cranium (craniometric data), are routinely recorded for each case during the analysis performed by OpID. The craniometric data are examined to determine if spatial patterning of individuals occur in clusters, and if so, are the clusters related to other factors such as their strontium isotope values? Craniometric data from all available OpID cases are used to perform a principle components analysis to look at the structure of the OpID cases. The five unidentified migrants sampled for isotopes are highlighted to show their placement within the distribution. Then the first two canonical variates for the population structure are extracted, then combined with the strontium data for each case, and plotted in three-dimensional space to observe how the strontium data varies within the coordinate space. The aim of the analysis is to tease out any meaningful groupings within the OpID craniometric dataset and the strontium data for these select individuals. This analysis attempts to discern whether a relationship exists between bioavailable strontium in the environment and cranial morphology of the OpID cases. Individuals who share similar cranial morphology are expected to share similar

genetic and environmental histories and therefore, similar strontium ratios. However, this expectation will vary within populations based on geography. For example, Guatemalans living in the lowlands versus highlands will likely have simlar cranial morphology due to gene flow between nearby populations but are expected to have different isotope signatures due to the environment, specifically the geology. Additional considerations required for the analysis are the mechanisms that structure population genetics such as genetic drift, migration, gene flow, mating practices and natural selection that may obscure the effect that geographic context (i.e. strontium) has on the cranial morphology.

The overall objective of the research is to determine if a dual-isotope isoscape and likelihood assignment method can be used to estimate region of geographic residence for deceased unidentified migrants recovered along the Texas-Mexico border and improve the probability of making a positive identification. If successful, this method can be used for deceased unidentified migrants recovered across the southern border of the United States and effectively increase the number of identifications and repatriations.

Introduction to Isotopes in Anthropology

Before using isotopes to estimate the geographic origin of deceased undocumented migrants, it is necessary to understand the basic principles of isotopes: what they are and how they are measured. Isotopes are the name given to a single chemical element, such as oxygen or carbon, that vary at the atomic level by the number of protons to neutrons present (Hoefs, 2008; Schoeninger and Moore, 1992; Fry 2006; Katzenberg, 2008; McMurry and Fay, 2004). The number of neutrons and protons contribute to the overall mass of the atom. Although the isotopes may vary for any

element, they retain similar chemical properties to one another because they maintain the same number of protons and electrons (Schoeninger & Moore, 1992; Schwarcz & Schoeninger, 1991). The most widely recognized isotope, ^{14}C, is used in radiocarbon dating to determine the approximate age of organic materials by measuring the amount of ^{14}C present. Carbon-14 is an isotope of the neutral ^{12}C atom that has been bombarded with outside neutrons that change carbon's initial composition of six protons and six neutrons to six protons and eight neutrons. As atoms obtain more neutrons, their total mass increases. Therefore, there are light and heavy isotopes—if an atom has fewer neutrons than protons, it is called a light isotope. If an atom has more neutrons than protons like ^{14}C, it is considered a heavy isotope.

In addition to varying numbers of neutrons, isotopes can be stable or unstable. Stable isotopes do not decay, are abundant in nature, and are "natural parts of each one of us," (Fry, 2006:8). Unstable isotopes are radioactive and decay overtime (Katzenberg, 2008; McMurry and Fay, 2004; Hoefs, 1987). These are called unstable because the excess of neutrons causes an increase in kinetic forces within the nucleus causing the atomic structure to lose its stability (McMurry and Fay, 2004).

Two elements, strontium ($^{87}Sr/^{86}Sr$) and oxygen ($^{18}O/^{16}O$), are employed in this analysis. Isotopes are measured as ratios that compare heavy isotopes to light isotopes for an individual element using mass spectrometry (Schoeninger & Moore, 1992; Katzenberg, 2008). For example, the oxygen ratios measured in the migrant dental samples are calculated based on the ratio of the heavy to light isotopes as compared to an international standard ($\delta^{18}O = {}^{18}O/{}^{16}O$). All isotope ratios have a special notation, delta (δ), that "denote a difference measurement made relative to standards during the actual

analysis" (Fry, 2006:22). The equation below shows the method used to calculate the δ values for isotopes, in this case, oxygen (Fry, 2006).

$$\delta\,^{18}O = [\ ((^{18}O/^{16}O)\ \textit{sample} / (^{18}O/^{16}O)\ \textit{standard}) - 1\ ] * 1000\ ‰ \qquad (1)$$

The multiplication of 1000 allows for small differences in quantity to be amplified and are referred to as "permil" and denoted by the ‰ symbol. Calculations using this equation can produce negative or positive values. Computing a negative δ value means less of the heavy isotope remains in the standard than the material being measured. Conversely, obtaining positive δ values means that the sample is enriched in the heavy isotope relative to the standard (Fry, 2006). Table 1 depicts isotopes used in the research and their standards for measurement.

Table 1. Isotopes and Standards Used for Measurement.

Element	Standard	Standard Value	Source
Strontium ($^{87}Sr/^{86}Sr$)	Strontium carbonate (NBS-987 or NIST 987)	0.710245	Bentley et al., 2003
Oxygen ($^{18}O/^{16}O$)	Standard Mean Ocean Water (SMOW) or *Belemnitella americana* - Peedee formation (PDB or V-PDB)	2067.1×10^{-6}	Benson et al., 2006

Strontium

Strontium (Sr) is an alkaline earth metal (Group IIA) with an atomic mass of 87.62 ± 0.01 u (Faure and Powell, 1972). Strontium is formed by the decay of rubidium (Rb), a naturally occurring substance in geologic materials, and the quantity of Sr varies based on the age of a mineral (Faure and Powell, 1972; Beard and Johnson, 2000; Millard, 2003; Bentley, 2006; Price et al., 2002). Rb and Sr naturally occur in igneous,

metamorphic, and sedimentary rocks (Faure and Powell, 1972). Strontium closely resembles calcium (Ca) and readily replaces Ca in animal skeletons due to their similar structures including their ionic radii (Ca = 0.99Å vs. Sr = 1.13Å), electronegativities of 1.0, coordination numbers (Ca = 6 and 8, Sr = 8), and the presence of two valence electrons that tend to ionically bind to nonmetals (Faure and Powell, 1972).

Strontium ratios fluctuate and depend on the underlying bedrock geology, which tends to have heterogenous distributions (Faure and Powell, 1972). Sr ratios are calculated by the ratio of ^{87}Sr to ^{86}Sr. This ratio increases over time as a function of the primary Rb/Sr ratio of the parent bedrock material (Bataille and Bowen, 2012). Variation in Sr ratios also relies on whether the rocks originate from continental crust or the upper mantle. Faure and Powell (1972:24) discuss the different origins and state that Sr originating from the crust becomes enriched in ^{87}Sr in comparison to the rocks produced from the upper mantle. In 1977, Faure proposed equations that model the formation of Sr ratios in rocks originating from the mantel and crust. These equations are prevalent in model-based approaches for mapping regional and large-scale Sr variation today (Bataille and Bowen, 2012). It is important to acknowledge that the Sr values derived from bedrock can vary greatly from other bioavailable sources. Therefore, modeling bedrock variation alone is insufficient for studying migration of humans and animals; bioavailable Sr sources, such as water, soils, and plants, must be considered when mapping large-scale Sr variation (Bataille and Bowen, 2012).

Bioavailable Sr substitutes for Ca within the hydroxyapatite [$Ca_{10}(PO_4)_6(OH)$] structure of bone and tooth enamel (Faure and Powell, 1972; Likins et al., 1960; Price et al., 2015; Bentley and Knipper, 2005). Strontium in skeletal remains can be measured

and used to infer region of origin because it incorporates itself into living beings through the uptake of local water and food sources (Comar et al., 1957; Faure and Powell, 1972; Beard and Johnson, 2000; Budd et al., 2004; Price et al., 2002). Using current knowledge of bone turnover rates (Ambrose and Norr, 1993) and tooth mineralization (Knudson et al., 2009), strontium can provide a record of migration throughout life using different tissues. Teeth form during childhood and provide useful estimators for the location of where an individual lived during the tooth's formation (Bentley, 2006; Faure and Powell, 1972; Beard and Johnson, 2000; Price et al., 2002, 2015; Bentley and Knipper, 2005). Bone formation occurs throughout life and can be used to define more recent strontium signatures of an individual – different bones have varying turnover rates, meaning that a rib will show a more recent time frame than a femur (Hedges et al., 2007; Hill, 1998). Hair and fingernails are unique because they incorporate strontium from bath/sink water and do not accurately represent bioavailable strontium (Tipple, 2015).

Strontium isotope ratios characterize the underlying bedrock in geological formations. Variation in geological formations can be visualized in the form of a strontium isoscape, which shows the change in strontium ratios from one geologic formation to the next (West, 2010). Individuals can then be mapped onto the isoscape based on their $^{87}Sr/^{86}Sr$ ratios derived from bones, teeth, or hair/nail. For example, an individual from a mountainous region should have a significantly different strontium signature than a person living in a nearby valley. A limitation of this method is the susceptibility of Sr to geologic and anthropogenic processes that result in weathering, erosion, and mixing of heterogeneous strontium signatures. Using $^{87}Sr/^{86}Sr$ to construct

isoscapes relies heavily on the underlying bedrock composition, geological processes, and contributions from the lithosphere and hydrosphere to depict local bioavailability.

The use of $^{87}Sr/^{86}Sr$ allows forensic anthropologists to estimate probable regions of origin for a person, as well as their more recent migrations (Bataille and Bowen, 2012). Migration studies using $^{87}Sr/^{86}Sr$ analysis have been conducted for many regions around the world, such as Europe (Schweissing and Grupe, 2003; Bentley 2004; Bentley and Knipper, 2005; Bol et al., 2007; Kootker et al., 2016), Africa (Sealy et al., 1991; Sillen et al., 1995), Central America (Price et al., 2000, 2008, 2015; Wright, 2005, 2012; Freiwald, 2011; Thornton, 2011; Knudson and Buikstra, 2007; White et al., 2007; Bataille et al., 2012; Warner, 2016; Laffoon et al., 2017), South America (Knudson et al., 2004, 2007, and 2009) North America (Price et al., 1994; Ezzo et al., 1997) and Asia (Regan, 2006).

In 2000, Beard and Johnson constructed an isoscape displaying the isotopic variation for $^{87}Sr/^{86}Sr$ within the United States based on geological samples. The authors present three case studies from forensic and archaeological contexts to show the applicability of using the isoscape and conclude that geographic residence can be estimated using $^{87}Sr/^{86}Sr$ ratios of skeletal elements. The strength of the isoscape relies on the "isotopic distinctiveness" of differing geographic regions and the knowledge of local biologically available strontium composition (Beard and Johnson, 2000:1058). A limitation of my research is that the data will not represent every corner of Central America and Mexico, meaning that my isoscape will be coarse-grained and will rely on interpolation for areas lacking information. As new data is collected and added to the

isoscape, its accuracy and precision should both increase and the isoscape should become more useful in anthropological and forensic contexts.

Research using $^{87}Sr/^{86}Sr$ analysis in forensic settings has increased steadily and has been applied to provenancing unidentified individuals in a variety of contexts (Benson et al. 2006; Juarez 2008; Beard and Johnson 2000; Bartelink et al. 2014). Juarez (2008:46) discusses the difficulties with identifying undocumented border crossers due to the inability to narrow the search area to "more probable options." Using $^{87}Sr/^{86}Sr$ signatures of Mexican-born subjects with known origins from four specific states of Mexico, Juarez (2008) attempted to find regions of similar $^{87}Sr/^{86}Sr$ signatures in the data and concludes that a map with data is being compiled for later use in identifying undocumented border crossers. However, since this preliminary report in 2008, a strontium map has not been published.

Oxygen

Much like strontium, oxygen isotope ($\delta^{18}O$) values reflect the water that an individual takes into their system during life. However, $\delta^{18}O$ that becomes incorporated into human tissues has multiple sources: atmospheric diatomic oxygen, dietary/drinking water, and precipitation (Bentley and Knipper, 2005; Ehleringer et al., 2008). Molecules containing $\delta^{18}O$, found in drinking water and in the bulk diet, are cleaved from ingested proteins as they enter the stomach and small intestines and become an isotopic record of the gastric juices during digestion (Ehleringer et al., 2008). In animals, $\delta^{18}O$ becomes isotopically enriched in ^{18}O compared to the initial drinking water because it circulates through the vascular system, while $\delta^{18}O$ in plants uses a one-way transport system and

does not become enriched in ^{18}O (Ehleringer et al., 2010). The $\delta^{18}O$ ratios derived from hydroxyapatite phosphate and carbonate in bone and enamel are in equilibrium with $\delta^{18}O$ ratios of body water found in soft tissues (Knudson et al., 2009; Longinelli, 1984; Luz and Kolodny, 1985). Oxygen values obtained from skeletal materials should record the isotopic composition of gut water during digestion, which is assumed to be in isotopic equilibrium with body water (Ehleringer et al., 2008).

Dietary $\delta^{18}O$ is a proxy for environmental $\delta^{18}O$ and is influenced by evaporation, condensation, and precipitation (Bentley and Knipper, 2005; Knudson et al., 2009). "Water is taken up in liquid form. That source water carries a geo-location signal and is transported to different internal tissues or to external tissues" (Ehleringer et al., 2010). Therefore, $\delta^{18}O$ isotopes are an indicator of climate and diet, meaning that migration of individuals can be tracked if their $\delta^{18}O$ ratios are known. Maps illustrating the isotopic variation of $\delta^{18}O$ in precipitation are available through sources such as waterisotopes.org and the Global Network for Isotopes in Precipitation (GNIP). Coupling the provenancing power of the $\delta^{18}O$ and $^{87}Sr/^{86}Sr$ values should increase the precision and accuracy of the probability densities for each unidentified individual.

In 2008, Ehleringer and colleagues published an influential article demonstrating a predictive model that employs hydrogen (δD) and $\delta^{18}O$ in hair to predict region-of-origin for humans from 65 cities in the United States (Ehleringer et al., 2008). The $\delta^{18}O$ and δD isoscapes were created using tap-water collected across the continent. Oxygen atoms in hair may be derived from secondary water sources of the body because Ehleringer et al. (2008:2791) found the relationship between hair isotopes and tap-water was lower than expected if the isotopes had come from a primary water source in the

body. The authors conclude that the model explain more than 85% of the variation observed in hair samples (Ehleringer et al., 2008). The authors note the unexplained variation may be due to the "continental supermarket" producing nonlocal signatures in the samples (Ehleringer et al. 2008:2791).

Since the publication, numerous articles have followed that illustrate the use of $\delta^{18}O$ as a local geological signature. Wassenaar et al. (2009) produced an isoscape capturing the variation in deuterium (δD) and $\delta^{18}O$ for groundwater sources in Mexico. The authors acknowledged the large gap in spatially distributed data within the GNIP dataset concerning Mexico and test whether phreatic groundwaters are acceptable proxies of long-term precipitation inputs to the system. Wassenaar et al. (2009:135) conclude that the groundwater does reflect "seasonally weighted precipitation" and shows little alteration due to evaporative processes. The authors state that groundwater provides nearly 40% of water use in Mexico, but do not share the source of the statistic. Groundwater sources for $\delta^{18}O$ may be valuable when creating $\delta^{18}O$ isoscapes for establishing provenience for unidentified migrants. Future research efforts could be aimed at incorporating the groundwater isotope data into the existing precipitation isoscape to create an isoscape that compiles the raw data from both sources to produce a single "hybrid" mosaic isoscape for the region of interest (G. J. Bowen, personal communication, November 20, 2017).

Fractionation

A benefit of implementing strontium analysis in migration studies is that it integrates into the skeleton with little to no fractionation (Faure 1972; Kennedy et al.

2000; Price et al. 2002; Bentley 2006). Strontium isotope ratios in plants and animals are influenced by their trophic position. However, the isotopic values do not vary, meaning that strontium is resilient to fractionation. Therefore, the bones and teeth of an individual may display different amounts of strontium but have similar $^{87}Sr/^{86}Sr$ (Herz and Garrison 1998:272). Fractionation occurs during chemical reactions where isotopes are split apart or partitioned into their source atomic materials (Regan 2006; Fry 2006). Fractionation occurs as the isotope progresses through different levels of the food chain (Beard and Johnson 2000). For example, strontium travels from the bedrock to the water flowing over it, to the plant above and then it is ingested by the animal eating the plant or the human eating the animal or plant. The lack of Sr fractionation makes obtaining values less variable, meaning plants and animals should show the same Sr ratios.

The other isotopes, carbon and oxygen, do experience some fractionation. For carbon, DeNiro and Epstein (1978:495) state that "there is no large isotopic fractionation associated with the incorporation of carbon from the diet into an animal." However, Hoefs (1987) describes two processes where carbon fractionation occurs: the carbonate system and organic carbon system. Within the carbonate system, fractionation occurs when basic thermodynamic equilibrium events occur, such as $CO_2(aq) + H_2O \leftrightarrow H_2CO_3$. Bioapatite carbonate was found by Passey et al. (2005) to be enriched in ^{13}C by 6‰ to 15‰ relative to the dietary intake of an individual. The organic carbon fractionation takes place during photosynthesis and Hoefs (1987:70) admits that "$\delta^{13}C$-value for the input carbon cannot be measured precisely but can be estimated with a high degree of certainty." The author calculates the amount of -5‰ to account for the carbon fractionation (Hoefs 1987:70).

$\delta^{18}O$ values obtained from the atmosphere are relatively constant (Regan 2006; Fry 2006; McMurry and Fay 2004) and believed to be "representative of imbibed water" (Regan 2006:7) Therefore, the $\delta^{18}O$ values derived from skeletal remains should reflect the diet and water intake of the individual after fractionation events occur during evaporation, condensation, and precipitation (Bosl et al. 2006; Bentley and Knipper 2005). Oxygen isotopes vary with the environment and climate of a region. "The fractionation factor for oxygen (on the Earth's crust) shows an approximately inverse dependence on temperature," (Bentley and Knipper 2005:630), meaning that $\delta^{18}O$ values are dependent on latitude and altitude. Specifically, a concept called the Rayleigh distillation shows that $\delta^{18}O$ values decrease along increasing latitudes and altitudes, such as mountainous landscapes (Bentley and Knipper 2005). Therefore, $\delta^{18}O$ values should be heavy near coastal regions that receive the first precipitation events and become gradually depleted as you move inland because less water being dropped as rain.

Isoscapes

Isoscapes are geologic models that show the spatial distribution of isotopic variation for environmental resources available in the food web in a region (Bowen, 2010; Bowen et al., 2013; West, 2006, 2010; Beard & Johnson, 2000). Isoscapes attempt to model the natural processes producing isotope variation over space. Worldwide geological variation and precipitation patterns are understood and heavily researched, meaning that the isotopic value of strontium and oxygen at any location in the world can be estimated using existing knowledge. Other isotopes such as sulfur and lead are useful but there is not enough data at this point to construct predictive models. Research using

hydrogen isotopes has shown that they are useful in provenance studies (Warner et al., 2016; Ehleringer et al., 2008; Meehan et al., 2005, Bartelink et al., 2016). Hydrogen isotopes cannot be extracted from bioapatite in dental enamel and cannot be used for the current research. However, future research using hair and fingernail samples from the OpID cases can use hydrogen to aid in provenancing unidentified individuals.

Isoscapes are created by sampling a source, such as soil, plants, rivers, or local bedrock to characterize the isotope baseline value for a site or region. Using geostatistical methods, isotope values for untested sites can be predicted or inferred using Kriging interpolation (Bowen, 2010). Interpolation should be employed cautiously because it may not consider the additional sources that contribute to the bioavailability of an isotope, such as the atmosphere, climate, and distribution of soil and bedrock (Bataille et al., 2012).

Bataille et al. (2012) produced a model of strontium variation that accounts for chemical weathering of soluble strontium and the deposition of Saharan mineral dust and sea salt for the circum-Caribbean region. However, the model does not account for other bedrock sources, apart from surficial bedrock, and neglects continental atmospheric contributions to bioavailable strontium because their contributions have been shown to be much less when compared to Saharan mineral dust and sea salt (Bataille et al., 2012). Mineral dust is noted to experience high variability in deposition patterns, but over longer time intervals deposits appear to be uniform in the Caribbean region (Bataille et al., 2012).

For this research, Dr. Clement Bataille provided a new global $^{87}Sr/^{86}Sr$ isoscape model that encompasses multiple submodels that attempt to account for the contributions

to the bioavailable strontium pool, such as aerosol deposition, erosion, surficial bedrock, water catchment, and soil. Typically, strontium values are extracted from samples of unknown origins and compared against a reference strontium sample (Bataille et al. 2012) to estimate region of origin. By adding existing data from Mexico and Central America to the $^{87}Sr/^{86}Sr$ model of the circum-Caribbean and Central America, I will provide the forensic community with a dataset from which to compare isotopic data derived from unidentified individuals. As new isotopic information is gathered by researchers, it can be added to the reference database to increase the accuracy and precision of the isoscape and decrease the reliance on using interpolation for non-sampled regions. The assignment model used in this research employs both $^{87}Sr/^{86}Sr$ and $\delta^{18}O$ isoscapes to narrow search parameters and create more accurate and precise assignments for region of geographic origin for undocumented migrants recovered in southern Texas.

Likelihood Assignment Model

Dr. Michael Wunder (M. Wunder, personal communication, June 21, 2017) provided the likelihood assignment model employed to answer the research questions. The assignment method was first applied to Wunder and colleague's research concerning migration patterns of birds, specifically mountain plovers, using hydrogen (δD), carbon ($\delta^{13}C$), and nitrogen ($\delta^{15}N$) isotopes derived from feathers obtained from a known breeding range (Wunder et al., 2005). Previous attempts to predict region of origin relied on simple regression, regression trees, range matching, and assignment methods using likelihoods or probabilities (Wunder & Norris, 2008:550). When applied to provenancing bird feathers, the assignment model provided the strongest results when all three isotopes

were used in a probability framework (Wunder et al., 2005). Therefore, the dual-isotope approach for assignment used in this research provides stronger results than univariate assignment attempts.

Previous techniques to provenance archaeological and forensic cases included establishing local versus nonlocal ranges using faunal remains or local geology (Price et al., 1994; Price et al., 2002; Bentley et al., 2003; Hodell et al., 2004; Knudson et al., 2005; Knudson & Buikstra, 2007; Knudson et al., 2009; Sosa et al., 2014), trimming datasets to not include foreign $^{87}Sr/^{86}Sr$ values (Wright, 2005), and testing for outliers (nonlocals) using a variety of statistical techniques. These techniques promoted the use of model-testing for establishing provenance, however they lacked the process-based predictive modeling available in the Bataille et al. (2012) $^{87}Sr/^{86}Sr$ isoscape models. Wunder (2010:254-255) states that previous attempts to define geographic location using isoscapes "(1) arbitrarily describe large geographic ranges a priori and summarize isoscape values within each range, or (2) arbitrarily determine a minimum magnitude that is on the order of the measurement (analytical) error for measuring δ^2H." The former is too conservative, while the latter tends to not be conservative enough. Wunder (2010:255) suggests that the modelling approach provides an alternative route "by combining a stochastic component based on known, estimated, or hypothesized residual variance with a calibrated isoscape."

Assumptions of the Assignment Model and Isoscapes

Assumptions and expectations for the assignment model are outlined below and they are heavily influenced by Wunder (2010:253-254). These include:

1. The precipitation-based $\delta^{18}O$ isoscape "provides a reasonable process-model for the expected spatial pattern" in oxygen isotopes incorporated into human tissues (Wunder, 2010:253-254).
2. The $^{87}Sr/^{86}Sr$ isoscape illustrates a reasonable process-model for the expected spatial patterning of bioavailable strontium isotopes.
3. Values in the $\delta^{18}O$ and $^{87}Sr/^{86}Sr$ isoscapes are fixed and known, including the variance for each isoscape (Wunder, 2010:253-254).
    a. $^{87}Sr/^{86}Sr$ isoscape is model-based on geological processes and does not share the same assumptions concerning variance as a typical isoscape. A fixed variance calculated by subtracting a strontium raster encompassing the first quartile of variation from a strontium raster encompassing the third quartile of variation to produce the most conservative assignment estimations.
4. The fractionation that occurs as oxygen transfers from imbibed water and food water to enamel hydroxyapatite carbonate can be estimated empirically (Wunder, 2010:253-254).
5. The assumption that strontium isotope values do not change over time.
6. Lab practices of Isoforensics, Inc. reliably calibrate measurements using established standards (VSMOW and $^{87}Sr/^{86}Sr = 0.7045$).
7. Strontium ($^{87}Sr/^{86}Sr$) and $\delta^{18}O$ derived from premolars contain tracers of childhood diet and migration.
8. Other factors influencing $\delta^{18}O$ and $^{87}Sr/^{86}Sr$ ratios in unidentified migrants are considered unknown error or are not measurable (Wunder, 2010:253-254).

Theoretical Background

Spatial Analysis: Geology, Strontium, and Space

Charles Lyell published the *Principles of Geology* in 1833 where he discussed a major operating theory within geology, called uniformitarianism, which states that the forces shaping the Earth today are the same as the forces that shaped the Earth thousands, even millions, of years ago. In addition, Tobler's First Law of Geography states that objects located in proximity to one another will more closely resemble each other when compared to things that are farther away (Rogerson, 2015:144). These two laws provide the primary theoretical framework that most spatial analysts in geology or geography operate under. This research functions under these theories, but requires an additional theoretical framework concerning strontium variation established by Faure (1972).

Faure (1972:23-24) postulates that $^{87}Sr/^{86}Sr$ ratios can be used to geologically trace sources of magma if the following three conditions are met: "(1) the magma was generated in the upper mantle; (2) strontium in the magma was not contaminated with foreign strontium derived from another source; and (3) the strontium in the magma was isotopically identical to that of the solid mantle from which the magma was generated." In 1977, Faure presented two equations that define the evolution of strontium found in upper mantle and continental crust that have become the basis for modern modeling of $^{87}Sr/^{86}Sr$ variation (Bataille and Bowen, 2012). The theory proposed by Faure was further simplified by Beard and Johnson (2010) to model $^{87}Sr/^{86}Sr$ variation on a large, continental scale. Beard and Johnson (2010) accounted for age of the underlying bedrock to estimate the $^{87}Sr/^{86}Sr$ signature over large regions assuming that bedrock is the primary source for $^{87}Sr/^{86}Sr$. Beard and Johnson (2010) acknowledged that a better understanding

of weathering patterns for geological materials would improve the use of large-scale strontium maps for provenance studies because forces of weathering, such as surface water, aerosols, and soils can produce variation in bioavailable $^{87}Sr/^{86}Sr$ (Bataille and Bowen, 2012). In 2012, Bataille and Bowen proposed a GIS-based model of environmental $^{87}Sr/^{86}Sr$ fluctuation assuming the primary source of $^{87}Sr/^{86}Sr$ comes from the weathering of bedrock. The model considered the $^{87}Sr/^{86}Sr$ variation from bedrock and water and did not account for additional sources of bioavailable $^{87}Sr/^{86}Sr$ variation (Bataille and Bowen, 2012). The publication was an important step toward implementing GIS-based modeling to map bioavailable $^{87}Sr/^{86}Sr$ sources that have use in ecological, archaeological, and forensic provenance research.

Implementing geographical information systems (GIS) to answer biological and forensic anthropology research questions occurs infrequently (Devlin and Herrmann, 2008; Beard and Johnson, 2010; Abd, 2011; Calleja, 2016; Byrd, 2016; Spradley et al., 2012) despite its popularity in cultural resource management, archaeology, geology and geography. However, GIS is becoming more widely accepted as an important tool for understanding spatial patterns that occur in anthropological contexts. GIS provides "a powerful set of tools for collecting, storing, retrieving at will, transforming, and displaying spatial data from the real world for a particular set of purposes," (Burrough and McDonnell 1998:11). A caveat of analyzing data in GIS is that the data must be "spatially referenced to the Earth," meaning that each data point must be associated with a known point of location, such as UTMs, latitude/longitude, decimal degrees, etc. (Burrough and McDonnell 1998:11). Without spatial reference information, objects cannot be plotted into space and associations between them remain unknown.

Craniometric Evaluation

An aspect of the biological profile constructed by the forensic anthropologist for an unknown individual requires estimating ancestry using the skeletal elements present. Ancestry estimation methods can be broken into two categories, nonmetric (Hefner, 2009; Hefner and Ousley, 2014; Gill, 1998; Rhine, 1993) and metric traits (Howells, 1995; Relethford, 2001; Carson, 2006; Spradley et al., 2008; Relethford, 2010; Ousley and Jantz, 2012; Hefner et al., 2014). Ancestry estimations performed by forensic anthropologists refer to the geographic regions of origin for an individual's ancestral lineage. However, the legal system in the United States uses different categories that are based on social race classifications (such as Black, White, Hispanic, etc.) meaning that ancestry estimations provided by forensic anthropologists are sometimes used by officials within the medicolegal system to categorize unidentified individuals into ethnic and/or social race categories. Inferring social race can prove difficult, especially if someone's ancestry and self-reported social race or ethnicity do not agree with one another. In a study by Klimentidis and colleagues (2009), the researchers found that a sample of 170 Native Americans and Hispanics from New Mexico tended to underestimate their degree of genetic admixture with European and Native American groups, respectively. This poses an issue when attempting to estimate ancestry for an individual who may identify as "Hispanic" under the U.S. medicolegal system but also has European skeletal features. Traditional ancestry estimations tend to oversimplify human variation into three very broad geographic groups of African, European, and Asian/Native American. As mentioned previously, "Hispanic" is a social construct and encompasses a very large range of genetic variability (Spradley et al., 2008:21). Differences in skeletal morphology

for human populations arose by numerous evolutionary processes such as genetic drift, natural selection, mutation, and gene flow (Relethford 2001), which have produced the large amount of phenotypic and genetic variation in the modern world. Ancestry estimation form skeletal remains requires understanding the theory of population genetics and its association with the race concept because ancestry encompasses both biological and social aspects of an individual.

Historically, biological determinists believed humans could be separated into "races" that were discrete and natural entities (Caspari, 2003). The introduction of the modern synthesis to the field of anthropology promoted a period of scrutiny where "races" were reassessed as "populations". However, the new term "populations" remained a typological and essentialist way of thinking because people remained separated into categories that were based on geographically isolated populations (Caspari, 2003). Today, these controversial ideologies are rejected, and race is viewed as a social construct that influences a person's perception and interpretation of the world (Gravlee, 2009; Armelagos and van Gerven, 2003). In addition, human genetic diversity on a global level does not align with the antiquated view of discrete populations. Instead, it has been shown that most genetic variation occurs within groups, rather than between groups (Gravlee, 2009; Relethford, 2010).

Though these racial classifications hold little weight in anthropology today, Gravlee (2009) argues that race can become biology because racial divisions are deepened by physical and symbolic structures within societies by enforcing the embodiment of racial inequalities imposed by existing socio-cultural constructs. It is important to understand that ancestry estimations from skeletal remains refer to

morphometric traits that are inherited and reflect geographically patterned genetic variation (Christensen et al., 2013) and should not be used to justify racial classifications. Though some anthropologists have criticized the use of ancestry within the field (Sauer, 1992; Kennedy, 1995), forensic anthropologists must make a "race" classification to be used for comparing against missing person reports in the medicolegal context.

Population genetics theory is concerned with understanding the structure and history of gene flow and mate selection for populations. Craniometrics have been shown to be an acceptable representation of genetic markers that aid in ancestry estimations (Relethford, 1994; Algee-Hewitt, 2016; Roseman & Weaver, 2004). The data consist of measurements taken from designated landmarks on the cranium that represent a variety of heritable phenotypic traits that are polygenic, meaning they are controlled by numerous genes, and are population-specific (Carson, 2006; Devor et al., 1986). Measurements taken during craniometric analysis can be statistically assessed using the FORDISC 3.1 software to estimate ancestry for an individual (Jantz & Ousley, 2005). The program produces posterior probability values that show the probability that an unknown individual belongs to one of the groups represented in the reference sample (Spradley et al., 2008; Jantz & Ousley, 2005). In addition, the provided typicality probability indicates the likelihood that the unknown individual belongs to one of the reference groups (Ousley and Jantz, 2012). Therefore, an unknown individual will be classified into a group even if they are not a member of the group, reinforcing the importance of properly interpreting the posterior probabilities and associated typicalities (Spradley et al., 2008).

Using principal components analysis, craniometric data are used to detect morphological patterns within the sample of deceased migrants recovered by OpID.

Essentially, this portion of the project aims to use morphology to map population structures that are distributed across landscapes that should have some correlation (though not directly) with geological $^{87}Sr/^{86}Sr$ values. It is expected that individuals who are near each other in coordinate space may share genetic and environmental histories that produce similar cranial morphologies. The objective of the analysis is to find individuals that are similar and group them together with the main goal of minimizing within-group variation and maximizing between-group variation (Rogerson, 2015). The goal of the craniometric analysis for this project is to observe how the craniometric and $^{87}Sr/^{86}Sr$ data plot out in x-y-z space. It has been shown in the literature that cranial morphology is highly heritable and is also influenced by the environment (Carson, 2006). This research proposes that cranial shape may be associated with geographic regions that have distinct strontium signatures. If similar patterns do appear when the craniometric and isotope data are combined, craniometric data could be used to identify meaningful groupings that can guide the selection of future samples to be analyzed using isotope analysis. In this way, the analysis tests whether craniometric data can be used as an additional predictor for region of geographic origin.

II. MATERIALS AND METHODS

In a recent article, "Investigating human geographic origins using dual-isotope ($^{87}Sr/^{86}Sr$, ^{18}O) assignment approaches," Laffoon et al. (2017) expand on the strontium isoscape from Bataille et al. (2012) to provenance identified persons using ^{18}O and $^{87}Sr/^{86}Sr$ variation for the circum-Caribbean region (Laffoon et al., 2017). The results found in Laffoon et al. (2017) demonstrate that the dual-isotope method is a viable option for provenancing studies because it was able to successfully define regions of most likely origin that included the actual known origin for the three sampled individuals. This thesis employs the same technique but applies the method to individuals of unidentified origin.

The research project involved many steps outlined in the following sections. The first section explains the steps involved in obtaining and preparing the oxygen (^{18}O) and strontium ($^{87}Sr/^{86}Sr$) isoscapes. The next section discusses methods used to select the skeletal data sample and the methods used for enamel preparation. The third section concerns the likelihood assignment model created by Wunder (2005) and the alterations made to the code for this application. The final section describes the craniometric analysis used in conjunction with the isotopic data to identify any observable patterns between the strontium values and the craniometric data.

Isoscape Treatment

Strontium ($^{87}Sr/^{86}Sr$) Isoscape

Two $^{87}Sr/^{86}Sr$ models are used to estimate the $^{87}Sr/^{86}Sr$ signature at any given locale using submodels that consider differing sources of bioavailable $^{87}Sr/^{86}Sr$ in the environment (Bataille and Bowen, 2012). Bataille personally provided two $^{87}Sr/^{86}Sr$ models for the research; one model is an improved version of the Bataille and Bowen

(2012) model and the other includes an additional erosion sub-model.

Strontium ($^{87}Sr/^{86}Sr$) data associated with spatial-reference points from previous studies within the existing literature are used to calibrate two $^{87}Sr/^{86}Sr$ isoscape models produced by Bataille (in prep). The data collected comes from a variety of published sources (listed in Appendix A and B) including archaeological, natural, and faunal samples that represent the bioavailable $^{87}Sr/^{86}Sr$ for the region of interest. If the data came from a thesis or dissertation, the authors were contacted to obtain permission to use copyrighted material. Otherwise, all other data comes from articles published in professional journals and are cited accordingly.

The research required calibrating Bataille's strontium model to better reflect the bioavailable $^{87}Sr/^{86}Sr$ for Mexico and Central America. Calibrating the models requires compiling nearly 1,000 spatially-referenced bioavailable strontium values for the region of interest from published literature (Appendix A). Compiling and organizing the existing $^{87}Sr/^{86}Sr$ data requires a significant amount of effort to "disaggregate" data into a comparable sampling interval (Bowen, 2009:144). Strontium data interpreted as "nonlocal" to the region were omitted to reduce biases and outliers (Wright, 2005). The calibrated $^{87}Sr/^{86}Sr$ isoscape is used to estimate the unknown region of geographic origin for the unidentified migrants. A list of articles used for the bioavailable data is provided in Appendix B. Once collated, a generalized linear model is performed between the bioavailable $^{87}Sr/^{86}Sr$ data (from existing literature) and the $^{87}Sr/^{86}Sr$ data from Bataille's strontium model.

The $^{87}Sr/^{86}Sr$ data from Bataille's model is collected by plotting the collected data onto the model in ArcGIS via ArcMap and then extracting the values from the model

raster where the plotted points are located. The extraction of data from the same location allows for the comparison of the bioavailable $^{87}Sr/^{86}Sr$ values and the expected $^{87}Sr/^{86}Sr$ values. Figure 1 illustrates the linear regression between the observed bioavailable data and the expected model data. Wunder (2010:258) states that "few individual isotope data observed at a single geographic location are expected to align exactly with the isoscape value for that locale." Therefore, the linear regression is expected to have a moderate correlation value between the two variables due to the presence of noise that results from random processes (Wunder, 2010:258). The line equations are factored into the strontium models using the ArcTool, Raster Calculator, to multiply the model raster by the slope of the line plus the intercept to rescale the models ensuring that they better reflect the bioavailable strontium data. Maps of the original strontium model and the adjusted model are shown in Figures 2, 3, and 4.

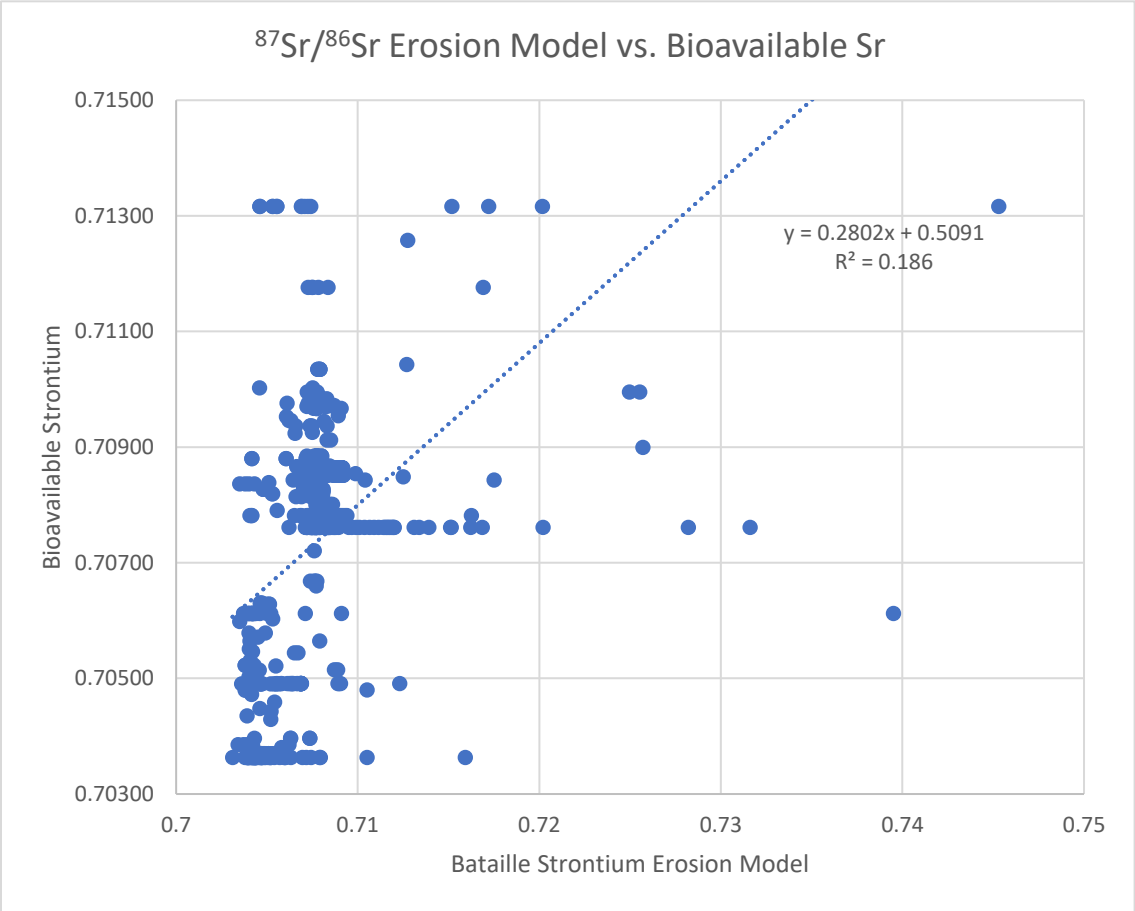

Figure 1. Linear Regression for $^{87}Sr/^{86}Sr$ Model with Erosion.

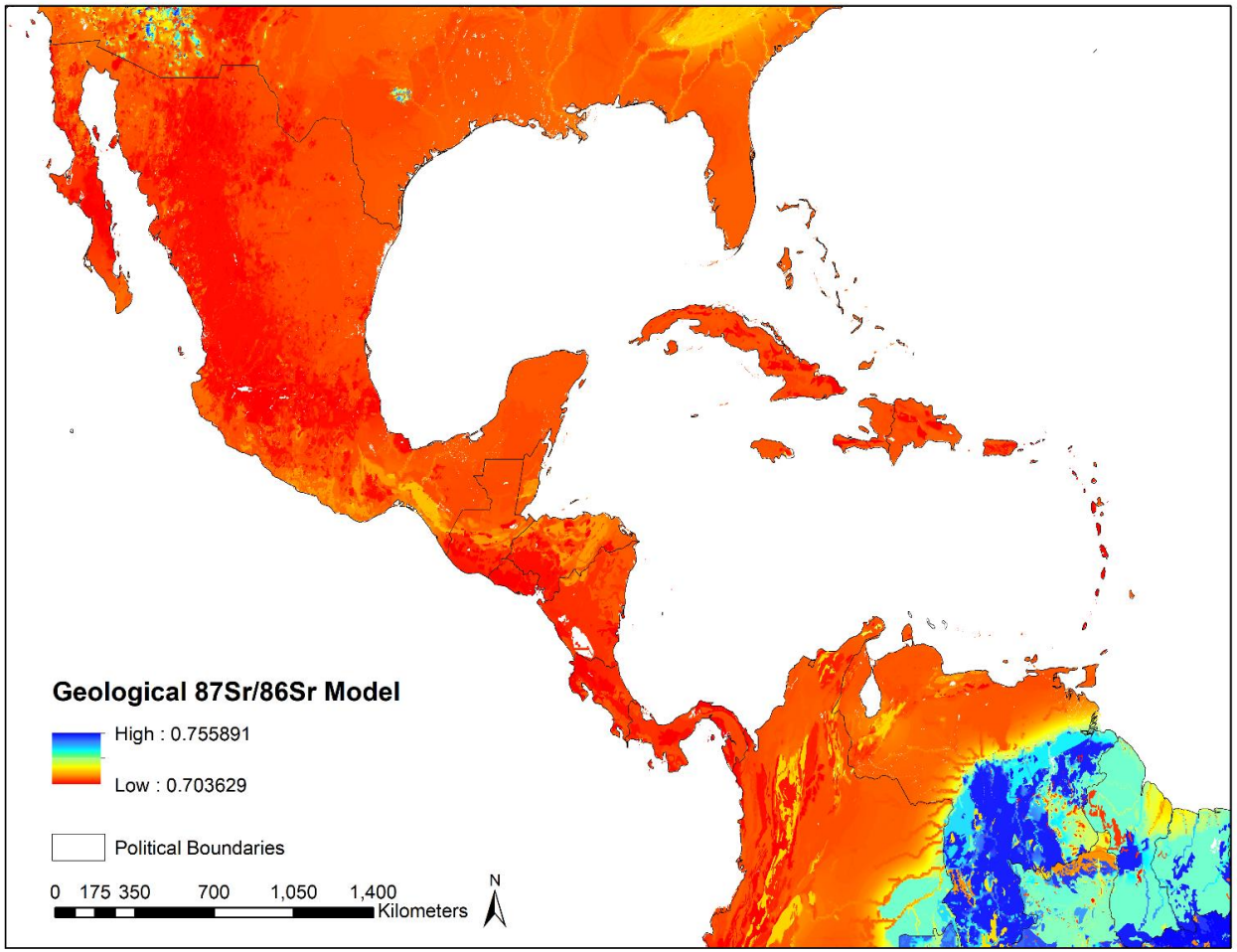

Figure 2. Original Strontium ($^{87}Sr/^{86}Sr$) Isoscape provided by Dr. Clement Bataille for Mexico and Central America. Raster provided by Bataille and map created in ArcMap 10.5.

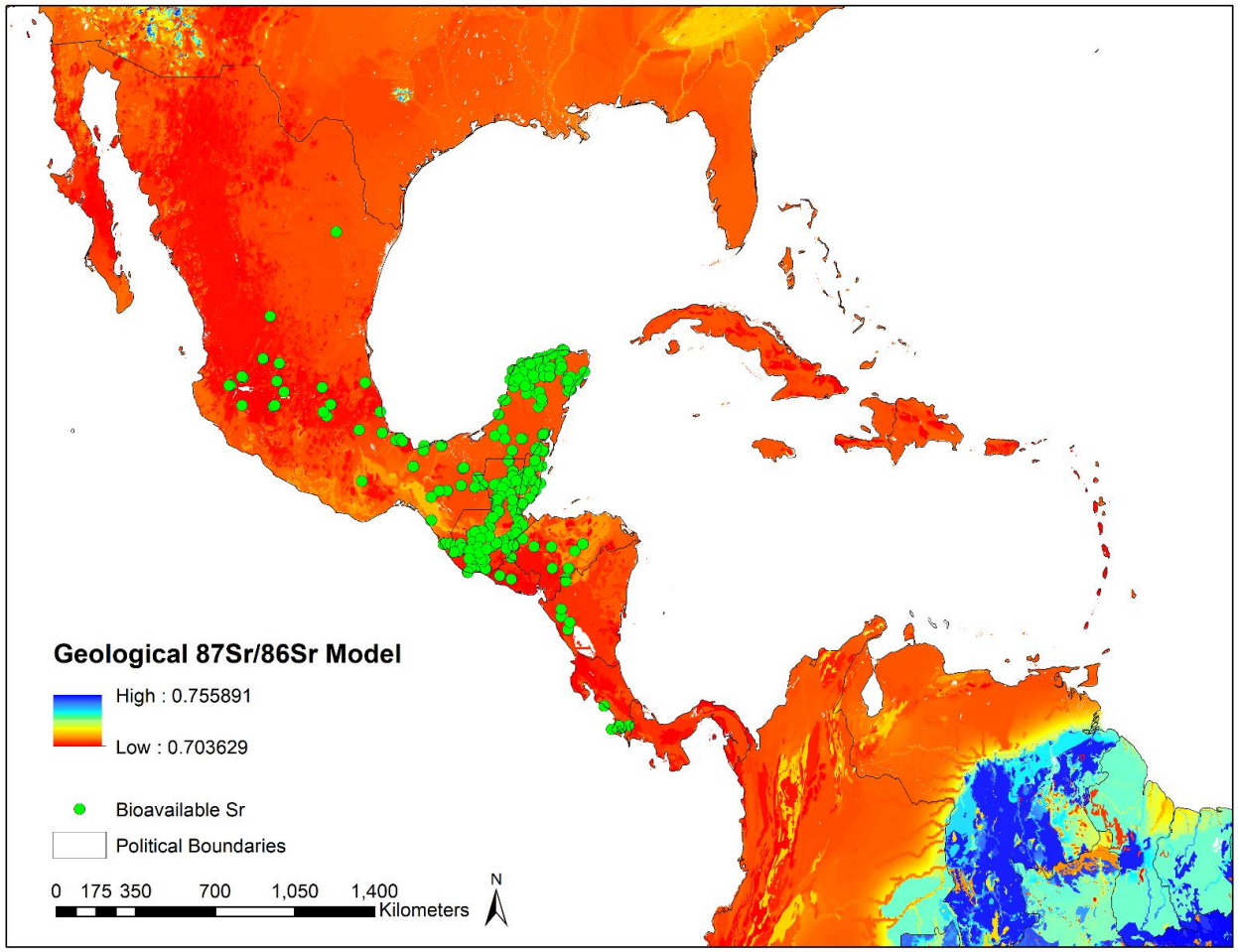

Figure 3. Original Strontium ($^{87}Sr/^{86}Sr$) Isoscape with bioavailable $^{87}Sr/^{86}Sr$ data obtained from published literature plotted. Raster provided by Bataille and map created in ArcMap 10.5.

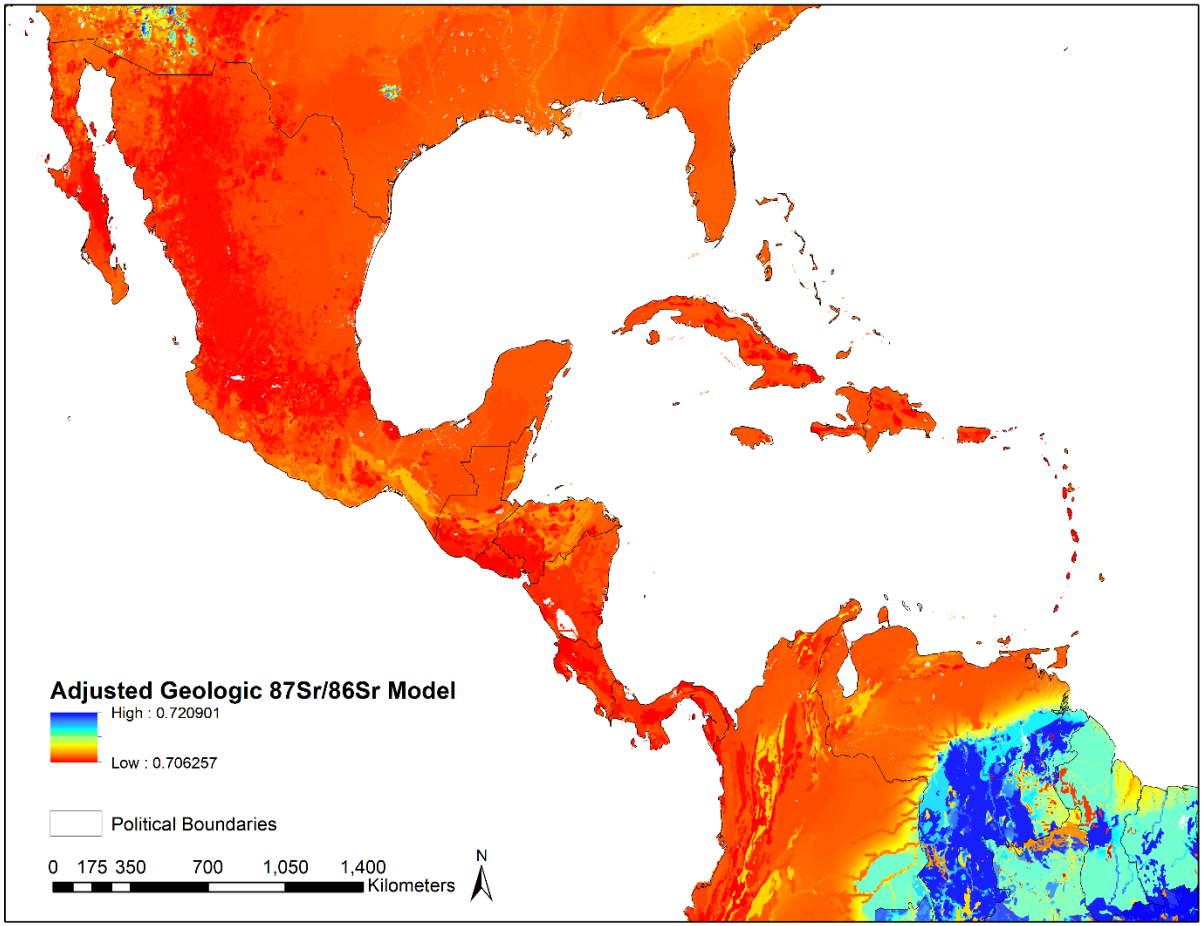

Figure 4. Adjusted Strontium ($^{87}Sr/^{86}Sr$) Isoscape for Mexico and Central America. Raster provided by Bataille, adjusted by author, and map created in ArcMap 10.5.

Oxygen ($\delta^{18}O$) Isoscape

The next step involves obtaining the global mean annual precipitation oxygen ($\delta^{18}O$) isoscape that is available to the public through multiple sources, such as waterisotopes.org and IsoMAP (http://isomap.org). The precipitation isotope data used to construct the $\delta^{18}O$ isoscape has a temporal range from 1960 to 2010 and is available through the Global Network of Isotopes in Precipitation (GNIP) database that can be accessed via the International Atomic Energy Agency (IAEA) water resources program website (http://iaea.org/water). The database encompasses global precipitation isotope data for a temporal range from the 1960s to the present for Central America, Mexico, and the Caribbean. The sparsity of precipitation $\delta^{18}O$ data for the region reduces the accuracy and precision of geostatistical estimations (Bowen, 2010:144). To compensate for the "spatiotemporal heterogeneity" of the $\delta^{18}O$ data, Bowen and colleagues (2010:144) use "long-term average values rather than data for specific months or years" to increase the density of the spatial data across space and time.

The global $\delta^{18}O$ isoscape used in the research has a 90 meter resolution and the $\delta^{18}O$ values are in permil using the V-SMOW scale. The isoscape raster is interpolated from point data using detrended interpolation that allows for the prediction of values for non-sampled sites based on principle of Tobler's Law (Bowen, 2010; Rogerson, 2015:144). Bowen and colleagues at the University of Utah have created the IsoMAP (and waterisotopes.org) database with the purpose of providing a source of point estimates for modern $\delta^{18}O$ precipitation values for paleoclimate, ecology, and forensic studies and as a source of data for hydrologic models.

The $\delta^{18}O$ precipitation isoscape shapefiles are retrieved from the IsoMAP online

database, imported into ArcMap, and trimmed to include Central America, Caribbean, and Mexico (Figures 5 and 6). No other adjustments are made to the isoscape. The lack of precipitation data for Mexico and Central America may represent a source of error and produce larger regions of probable geographic origin than desired.

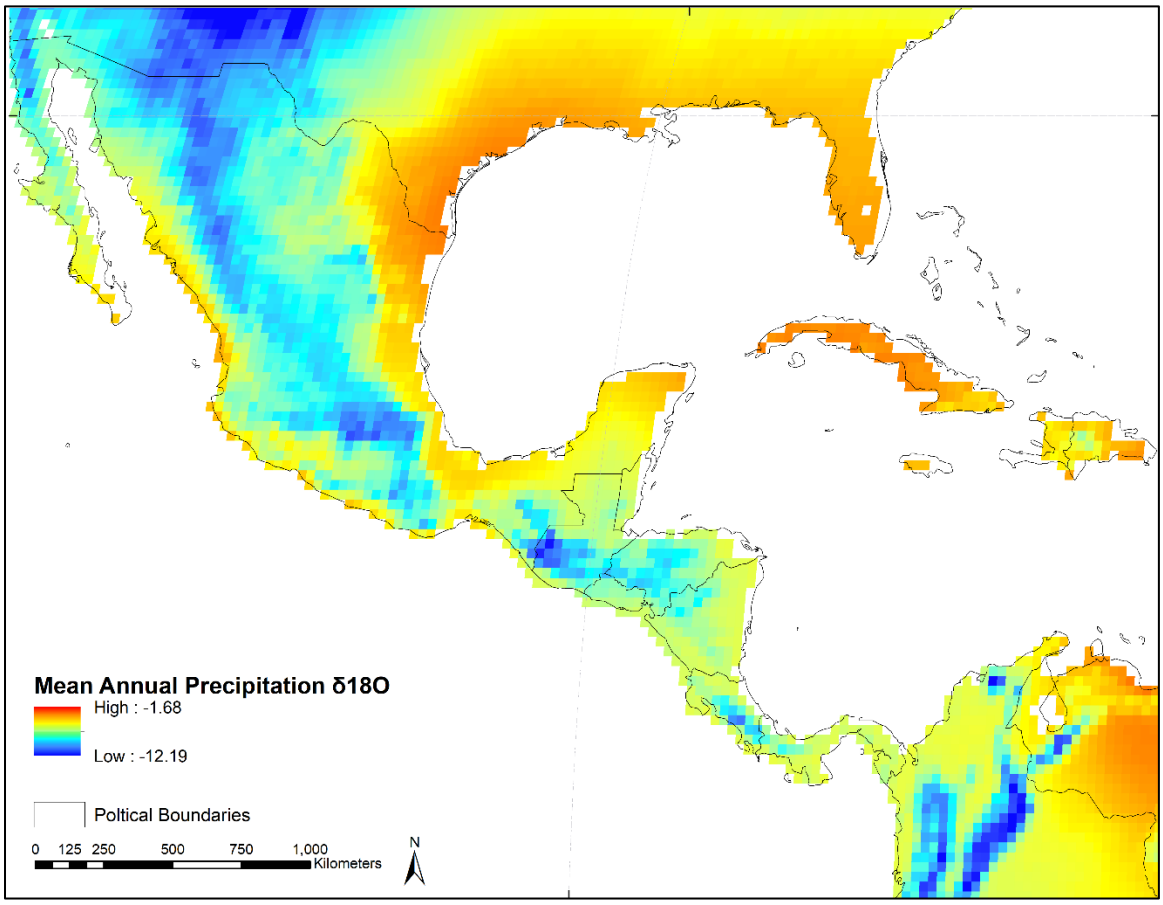

Figure 5. Mean Annual Precipitation Oxygen (δ18O) Isoscape for Mexico and Central America. Map created in ArcMap 10.5.

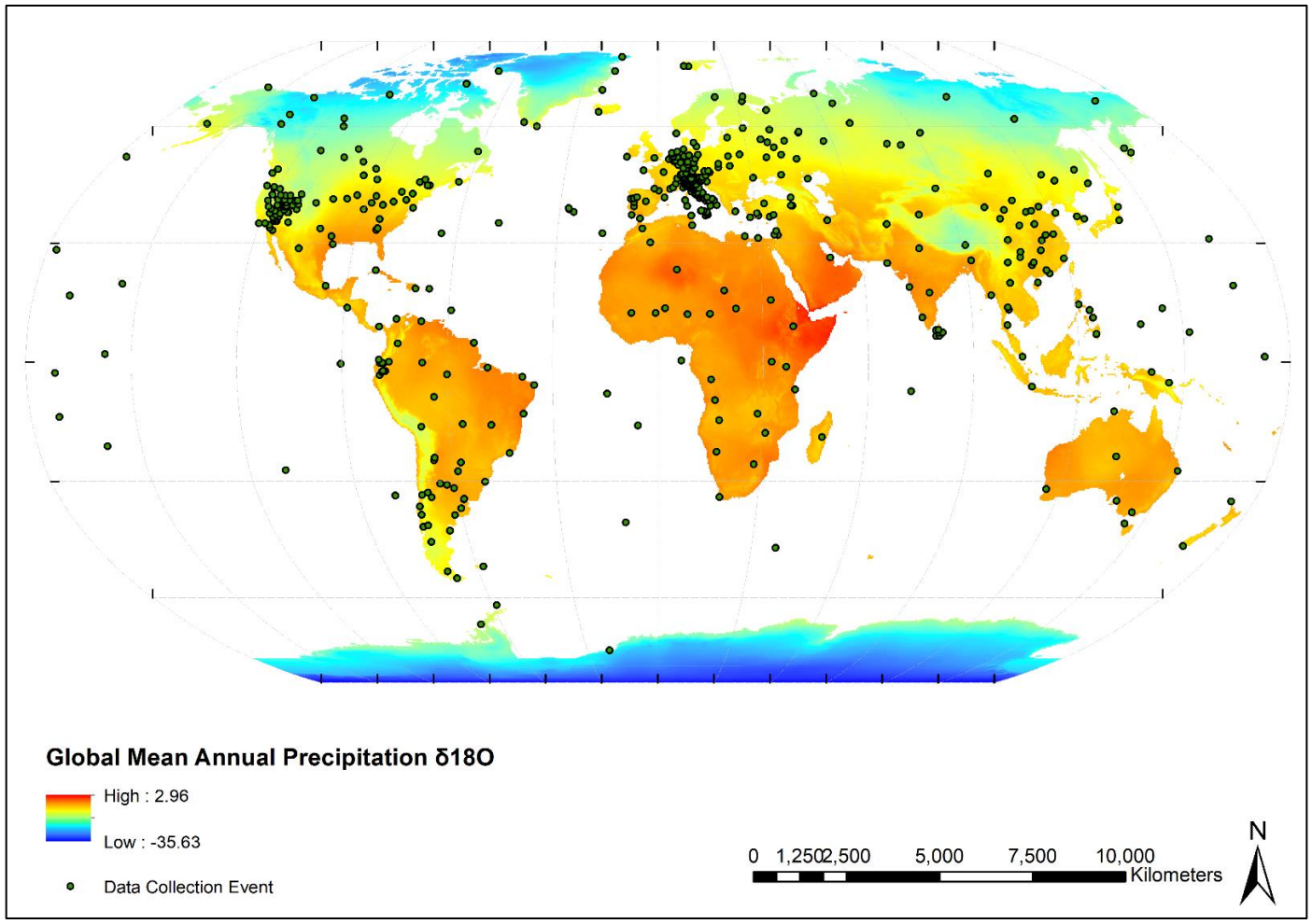

Figure 6. Global Mean Annual Precipitation Oxygen (δ18O) Isoscape. Map created in ArcMap 10.5.

Sample Selection

The sample comes from the OpID skeletal remains housed at the Forensic Anthropology Center at Texas State (FACTS). OpID achieves its identification mission along the southern Texas border by means of "community outreach, forensic anthropological analysis, and collaboration with governmental and non-governmental organizations," (Operation Identification, 2017).

The human skeletal remains were recovered from Brooks County, located near a Border Patrol checkpoint, during three field seasons (2013, 2014, and 2017) by students, professors and volunteers. The OpID cases consist of over 270 individuals and continues to increase as more exhumations take place. Recently, OpID has formed a cooperative relationship with Starr and Cameron Counties in South Texas and exhumations are planned for January and May of 2018. As of January 1st, 2018, 27 individuals have been successfully identified by OpID with one case pending verification via DNA evidence.

Cases that were identified at the time of sample selection were not able to be sampled for the analysis because the remains are being repatriated to the families and/or countries and are not subjected to destructive analysis without the family's approval. Therefore, the unidentified cases are examined to determine which are suitable for the isotopic analysis. To minimize the destruction to the skeletal remains, the samples selected must also work for three additional research projects using the OpID cases. Two of the projects concern age estimation methods and are based at Texas State University. One is non-intrusive and the other is destructive for single-rooted dental samples. Therefore, the five samples chosen for this research needed to fulfill the criteria set by the primary investigators of three Texas State University projects. These criteria include:

having a single-rooted tooth, lacking taphonomic damage, the presence of ribs and pelvis associated with the dentition, and the presence of appropriate teeth with preference given to maxillary premolars. The third project examining OpID samples is isotope-based but compares the isotopic values of the dentition and the bones (preference given to the left fourth metatarsal, with some substitutions). Lastly, the cases selected must have completed anthropological and dental reports by OpID staff including dental casts, dental metrics, DNA samples, skeletal and dental inventories, and photographs.

The five cases selected fulfill the requirements for all four research projects and have associated cultural material to address the research question concerning artifacts as predictors for region of geographic origin. After the five samples were sent to the lab for isotope analysis, two of the five cases (OpID-0383 and OpID-0608) selected for the project were successfully identified by OpID. The two identifications allow for the validation of the dual-isotope assignment model by comparing their predicted region of origin to the actual region of origin reported by the families of the identified individuals. Table 2 lists the dental samples (preference given to the maxillary premolars) extracted from five individuals to be analyzed for $^{87}Sr/^{86}Sr$ and $\delta^{18}O$.

Table 2. Cases Selected for Isotopic Analysis.

OpID Case Number	Associated Cultural Material	Tooth Extracted	Crown Completion[1]
OpID-0383	Mexican Flag Bandana	Maxillary PM2 – 13	7.5 years
OpID-0422	Quetzal – Guatemalan currency	Maxillary PM1 – 12	6.5 years
OpID-0477	Dollar – US currency	Mandibular PM2 – 29	7.5 years
OpID-0485	Pesos – Mexican currency	Maxillary PM1 – 5	7.5 years
OpID-0608	Quetzal – Guatemalan currency	Maxillary PM1 – 5	7.5 years

[1]Source for age at time of crown completion: AlQahtani et al. 2010

Once analyzed, the isotope values from the samples are plotted onto the isoscape to estimate their probable regions of geographic residence. If the isoscape successfully narrows region of geographic residence, OpID should add a new level of sampling for deceased migrants during their intake protocol, meaning a single tooth be extracted for isotope analysis from every case.

Associated Cultural Material

Of the 200 individuals, only 44 were recovered with country-specific associated cultural materials. One goal of this research is to test whether the associated material acts as a predictor for region of geographic origin for the five selected samples (n=5). It is likely that migrants may carry forged documents stating they are citizens of Mexico. If apprehended, it is more convenient for migrants to be deported to Mexico, rather than back to Central American countries (M. K. Spradley, personal communication, May 1, 2017). After searching through each case file, country-specific associated cultural material could be sorted into four groups: money, clothing, form of identification, and other.

Most of the materials are associated with Mexico; this pattern is expected because each person crossed the border from Mexico. It is important to consider the directionality of money. For example, an individual recovered carrying Guatemalan currency, quetzals, may be assumed to be from Guatemala or a more southern country. Sample selection focuses on individuals that are predicted to originate from countries in Central America since their associated cultural materials hold greater weight than the large amount of Mexican associated cultural material in the OpID cases. Table 3 below shows the

prevalence of each type of cultural material for the 44 cases and which country they are most likely coming from. Referring to Table 2 (above) shows the cultural material associated with each of the five samples.

Table 3. Country-Specific Associated Material for OpID Cases.

	Currency	Clothing	Form of Identification: (licenses, reg. cards)	Other: (flags, etc.)	Total
Mexico	21	4	2	3	30
Guatemala	6	1	-	-	7
Honduras	-	1	-	-	1
El Salvador	-	1	2	-	3
Nicaragua	-	-	1	-	1
Other	1 (Euros)	-	1 (Dom. Repub.)	-	2
Total:	28	7	6	3	**44**

Isotopic Preparation

Dental samples, listed in Table 2, are extracted from each of the five sampled individuals. Isotope ratios derived from dental crowns should reflect the isotopic signatures that were incorporated into the tooth enamel during their mineralization (Hillson, 1996). Maxillary premolars are preferred for sampling because they have large crowns, tend to be single-rooted, and form during childhood as shown in Table 4 (Price et al., 2015; Turner et al., 2009).

Table 4. Age Range in Years for Dental Crown Formation.

Tooth	M3	M2	M1	PM2	PM1	C1	I2	I1
Age	8.0- 15.0	2.5-8.0	0.0-3.5	2.0-8.5	1.0-7.5	0.3-7.0	0.8-5.5	0.0-5.0

Source: Hillson, 1996

Once dental samples were extracted from each of the individuals, each sample was sectioned into two parts, separating the crown from the root. The roots were reserved for a fellow graduate student performing cementum increment analysis for age estimation, while the crown will be used for the isotope analysis. The crown was removed using a precision saw available at the Grady Early Forensic Anthropology Research Lab. The crown samples were paired with their accompanying metatarsals and then packaged, labeled, and sent to Dr. Eric Bartelink, one of the researchers performing isotope analysis on the sample from the Stable Isotope Preparation Laboratory (SIPL) at California State University, Chico (CSU, Chico). Lab assistants at SIPL removed the metatarsals from the labeled packages and sent the crown samples to Isoforensics, Inc., a forensic lab specializing in isotope analysis. Isoforensics performed all sample preparation and analyses to obtain $^{87}Sr/^{86}Sr$ and $\delta^{18}O$ values. Table 5 summarizes the isotope data derived from dental enamel for the five samples.

Table 5. Isotope Data for Research Samples.

Case number	$^{87}Sr/^{86}Sr$	$^{87}Sr/^{86}Sr$ SE	$\delta^{18}O_c$ (VPDB)	$\delta^{18}O_c$ SE
OpID-0383	0.70748	0.00001	-3.53	0.179
OpID-0422	0.70600	0.00001	-4.51	0.180
OpID-0477	0.70680	0.00001	-3.29	0.081
OpID-0485	0.70697	0.00001	-6.01	0.183
OpID-0608	0.70595	0.00001	-5.04	0.181

The $\delta^{18}O$ values derived from the dental samples were first converted from oxygen derived from carbonate ($\delta^{18}O_c$) using the Vienna Pee Dee Belemnite (VPDB) standard to $\delta^{18}O_c$ using the Vienna Standard Mean Ocean Water (VSMOW) shown in

equation 2 below discussed by Alison et al. (1995:157). Next, the $\delta^{18}O_{c\ (VSMOW)}$ was converted to oxygen derived from phosphate ($\delta^{18}O_p$) using equation 3 shown below established by Iacumin and colleagues (1996:4). Equation 4 was used to convert the $\delta^{18}O_p$ into the oxygen isotope composition found in food water ($\delta^{18}O_w$) following Daux and colleagues (2008:1143).

$$\delta^{18}O_{c\ (VSMOW)} = \delta^{18}O_{c\ (VPDB)} * 1.03092 + 30.92 \quad (2)$$

$$\delta^{18}O_p = 0.98 * \delta^{18}O_{c\ (VSMOW)} - 8.5 \quad (3)$$

$$\delta^{18}O_w = 1.54(\pm 0.09) * \delta^{18}O_p - 33.72\ (\pm 1.51) \quad (4)$$

The table below shows the $\delta^{18}O$ conversion between different oxygen isotope composition for each of the research samples. Once converted, the oxygen isotope data were run through the assignment model.

Table 6. Conversion of Oxygen Isotope Data for Samples.

Case number	$\delta^{18}O_c$ (VPDB)	$\delta^{18}O_c$ (VSMOW)	$\delta^{18}O_p$ (VSMOW)	$\delta^{18}O_w$ (VSMOW)
OpID-0383	-3.53	27.28	18.24	-5.64
OpID-0422	-4.51	26.27	17.25	-7.16
OpID-0477	-3.29	27.53	18.48	-5.26
OpID-0485	-6.01	24.72	15.73	-9.50
OpID-0608	-5.04	25.72	16.71	-7.99

Likelihood Assignment Model

A global $^{87}Sr/^{86}Sr$ isoscape model created and provided by Bataille (C.P. Bataille, personal communication, June 20, 2017) was used to assign $^{87}Sr/^{86}Sr$ values of the

unidentified migrants from the OpID cases. The $^{87}Sr/^{86}Sr$ model is an improved version of the Bataille and Bowen (2012) model because it considers the effects produced by erosion. In addition to the $^{87}Sr/^{86}Sr$ isoscape, the global mean annual $\delta^{18}O$ in precipitation isoscape from IsoMAP is used in the assignment model to predict regions of geographic origin for the unidentified migrants in the OpID cases. The two isoscapes are incorporated into a bivariate assignment model that produces probability densities using maximum likelihood estimations for provenancing studies (Wunder, 2012). The likelihood-based model increases the accuracy of the geographic assignment because it uses Bayesian statistics to produce estimations using previous data (Wunder & Norris, 2008). For further information concerning the assignment model, refer to publications by Wunder and colleagues (Wunder et al., 2005; Wunder & Norris, 2008; Wunder, 2010; Wunder, 2012).

The likelihood-based assignment model aims to address the first question proposed: Do migrants fit into the established isotope models for $^{87}Sr/^{86}Sr$ and $\delta^{18}O$ variation for Mexico, Central America, and Caribbean? The R-code for the assignment model was provided by Wunder during the Spatial-Temporal Isotope Analytics Laboratory short course at University of Utah during the summer of 2017. The R-code has been adjusted to import isoscape rasters created in ArcMAP. The original code creates the isoscapes in R-studio. However, the rasters were created in ArcMap to improve the primary investigators experience with ArcGIS software and because ArcGIS software has a faster learning curve and friendlier interface than R-studio for those less-inclined toward statistical coding software.

Craniometric Evaluation

To complete the craniometric assessment, all interlandmark distances were collected for the OpID forensic cases. Rather than imputing data for missing variables, measurements with missing variables or incorrect values were dropped from the analysis to reduce bias. The OpID dataset was analyzed in DISPOP, a program developed by R. L. Jantz (2000) to assess craniometric variation between and within groups. Running the dataset through DISPOP produced a Mahalanobis distance matrix, principal coordinates, and a classification for the unknown OpID crania. The principal coordinates were combined with the strontium data for the OpID cases to produce a 3D scatterplot to visualize the genetic and isotopic variation between and within the groups present in the cases. Two different 3D scatterplots were created; one using the default DISPOP dataset and the second using a modified DISPOP dataset including more appropriate reference groups for analyzing the OpID cases.

DISPOP uses multiple variables to assess variation between and within each of the reference groups in the program that includes the following default datasets: W. W. Howell's, Native American groups, 20th century American Blacks and Whites, Terry and Todd collection of Blacks and Whites, and West African groups (Spradley, 2006:72-73). Jantz and Owsley (2001) state that when using DISPOP, groups with similar genetic structures should be used to produce appropriate covariance matrices. Therefore, during the first DISPOP analysis, the OpID cases were run against the following reference groups: Peru, West Africa, American Black, American White, and Mexican American. The second run used a modified dataset comprising 20th century Black, White, positively identified Mexicans, and Guatemalans. These groups are predicted to be more genetically

similar to the OpID cases and more substantial results are expected from the analysis. The cranium of OpID-0422 is highly fragmented, preventing it from being digitized and included in the craniometric analysis.

III. RESULTS

Question 1

To determine if migrants fit into the established $^{87}Sr/^{86}Sr$ and $\delta^{18}O$ isotope models for Mexico, Central America, and Caribbean, the five unidentified samples were run through the dual-isotope assignment model adjusted from Wunder (2005). The enamel isotope data for an identified case, OpID-0373, was run through the assignment model to determine if the model accurately predicted the individual's known region of origin, El Salvador. The isotope data ($^{87}Sr/^{86}Sr = 0.70664$ and $\delta^{18}O_c = -4.2$) for the case was converted to the appropriate reference scale ($\delta^{18}O_w$) and run through the assignment model. The results shown in Figure 7 below provide evidence in support of the assignment model's ability to accurately predict region of origin for individuals within the OpID cases. It is important to acknowledge that the model may not work for all cases and has only been tested on a few cases with known regions of origin. The color gradient bar on the right side shows the probability density of the individual being from that location; dark purple and blue being the most probable and tan being the least probable.

The predicted regions of origin for OpID-0373 primarily fall within the borders of El Salvador with a linear trend of light and dark blue dots highlighted in near the southwestern border of Texas (Figure 7). The success of the assignment model to predict El Salvador as a region of origin deomstrated that the assignment model may have similar success with the unidentified cases selected from this research. It is important to emphasize that the assignment model is fallible and should not be used as the only means of narrowing region of origin; other lines of evidence should always be considered in conjunction with the dual-isotope assignment results.

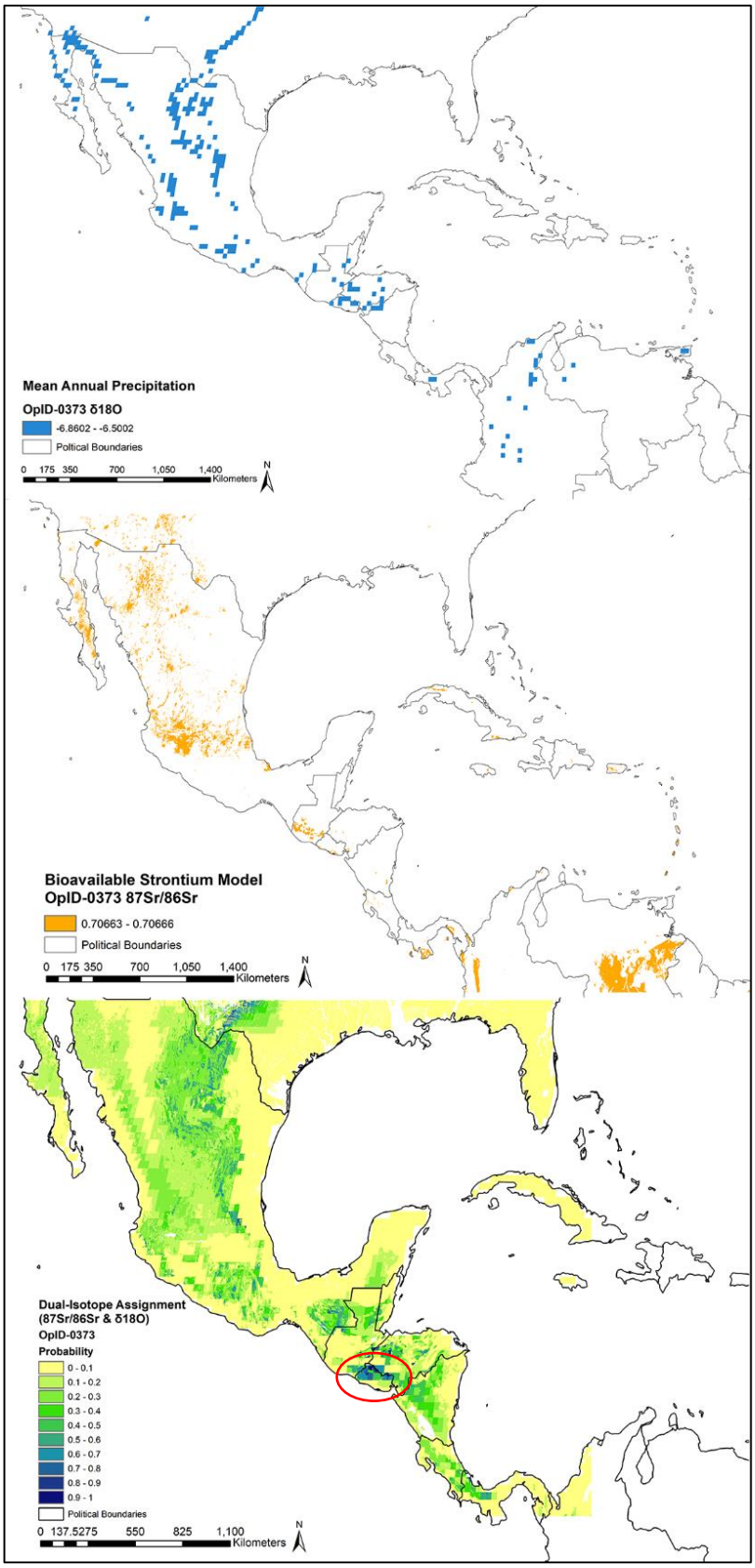

Figure 7. Isotope Assignment for OpID-0373. Top map shows the prediction using only $\delta^{18}O$ isotopes. The center map shows the prediction using only $^{87}Sr/^{86}Sr$ isotopes. The bottom map shows the dual-isotope assignment using both isotopes. The case plots into the Sierra Madre Mountains in Northern El Salvador marked by the red circle. All images created in ArcMap 10.5 by author.

Maps illustrating the prediction probability output for each case are shown in Figure 8-12. For all figures, the top map shows the predicted regions of origin using only the $\delta^{18}O$ isotope data, the center map shows the predicted regions of origin using only the $^{87}Sr/^{86}Sr$ isotope data, and the bottom map shows the multivariate prediction using the dual-isotope approach. Areas of highest probability are shown in blue for the dual-isotope assignment, while least probable regions of geographic residence are shown in contiguous color range from yellow to green. Full page maps are available in Appendix C. For each of the individuals, the assignment model successfully predicted regions of interest that can be used to filter missing person reports that match the biological profile and isotopic information for the unidentified individual.

Areas of high probability are highlighted in dark blue for the predicted region of origin for each sampled case. Since the commencement of the research, two of the five cases have been positively identified, OpID-0383 and OpID-0608. Both have been identified as Mexicans who were raised in Mexico—specific regions of childhood have not been released preventing further assessment of the model's accuracy and precision for origin predictions. The assignment for OpID-0383 predicts Panama as the region of origin and has no high probability areas within Mexico (Figure 8), while OpID-0608 primarily plots into Guatemala and Honduras (Figure 12). The incorrect predictions may be due to the large extent used in the assignment—if the extent was limited to Mexico, more regions of high probability may be produced than when the extent includes Mexico and Central America. For the other three unidentified cases, the accuracy of their predictions is unknown until positive identifications are made.

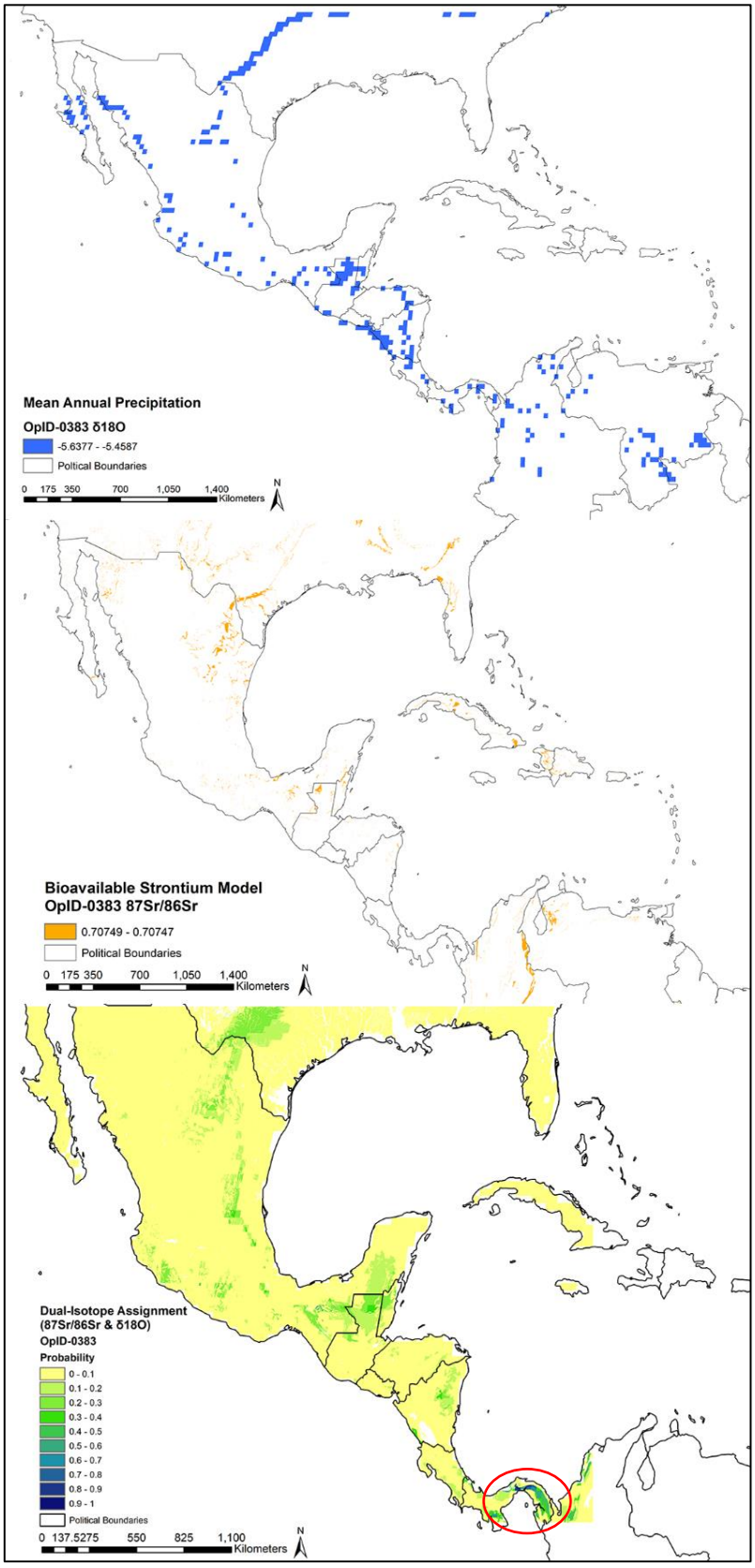

Figure 8. Isotope Assignment for OpID-0383. Top map shows the prediction using only $\delta^{18}O$ isotopes. The center map shows the prediction using only $^{87}Sr/^{86}Sr$ isotopes. The bottom map shows the dual-isotope assignment using both isotopes. OpID-0383 has been identified as being of Mexican nationality. Sadly, the assignment model does not work and plots them into the hill region of Panama between the Panama Canal and the San Blas Mountains marked the red circle. All images created in ArcMap 10.5 by author. Full page maps are available in Appendix C.

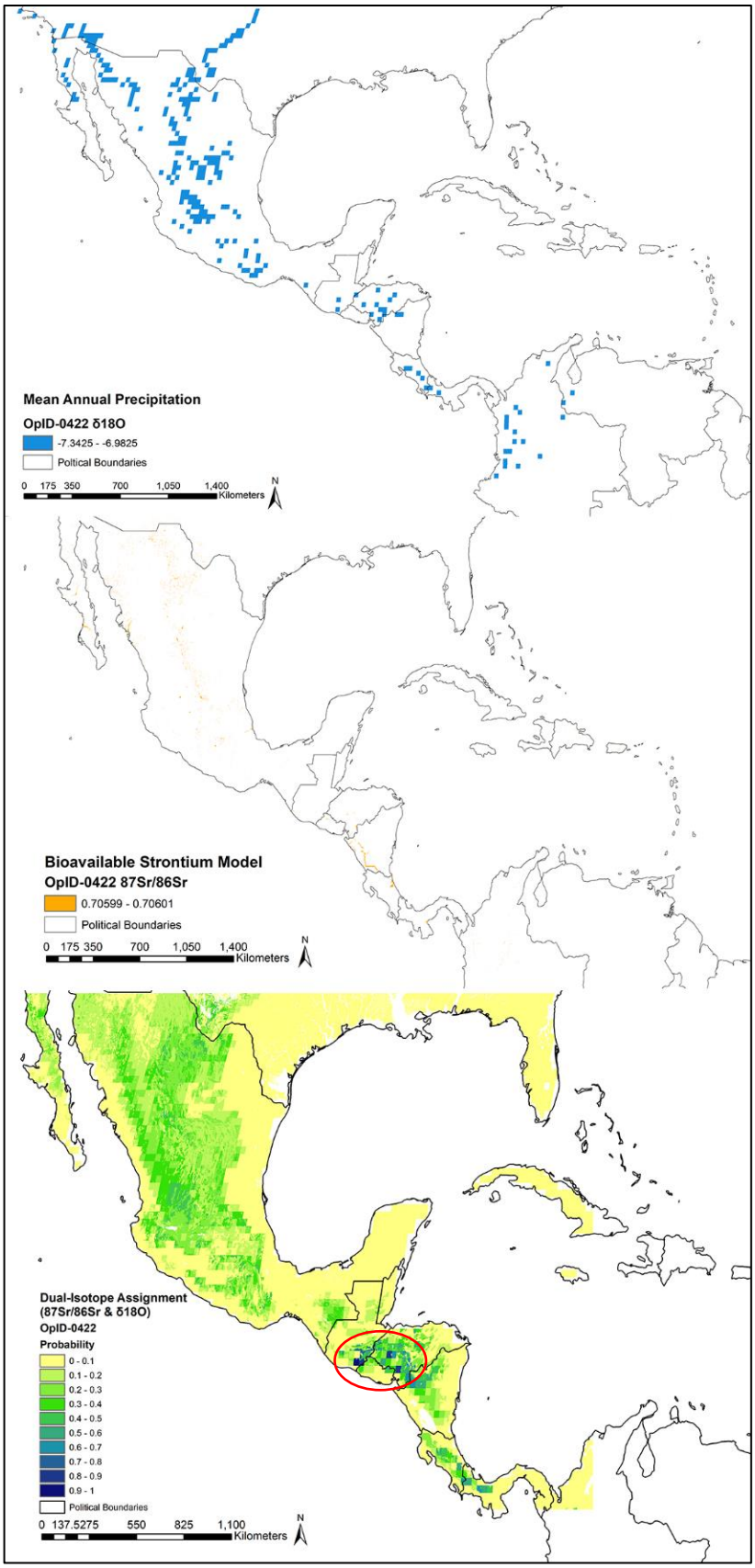

Figure 9. Isotope Assignment for OpID-0422. Top map shows the prediction using only $\delta^{18}O$ isotopes. The center map shows the prediction using only 87Sr/86Sr isotopes. The bottom map shows the dual-isotope assignment using both isotopes. OpID-0422 plots into the Sierra Madre Mountain range located in southwestern Guatemala and western Honduras marked by the red circle. All images created in ArcMap 10.5 by author. Full page maps are available in Appendix C.

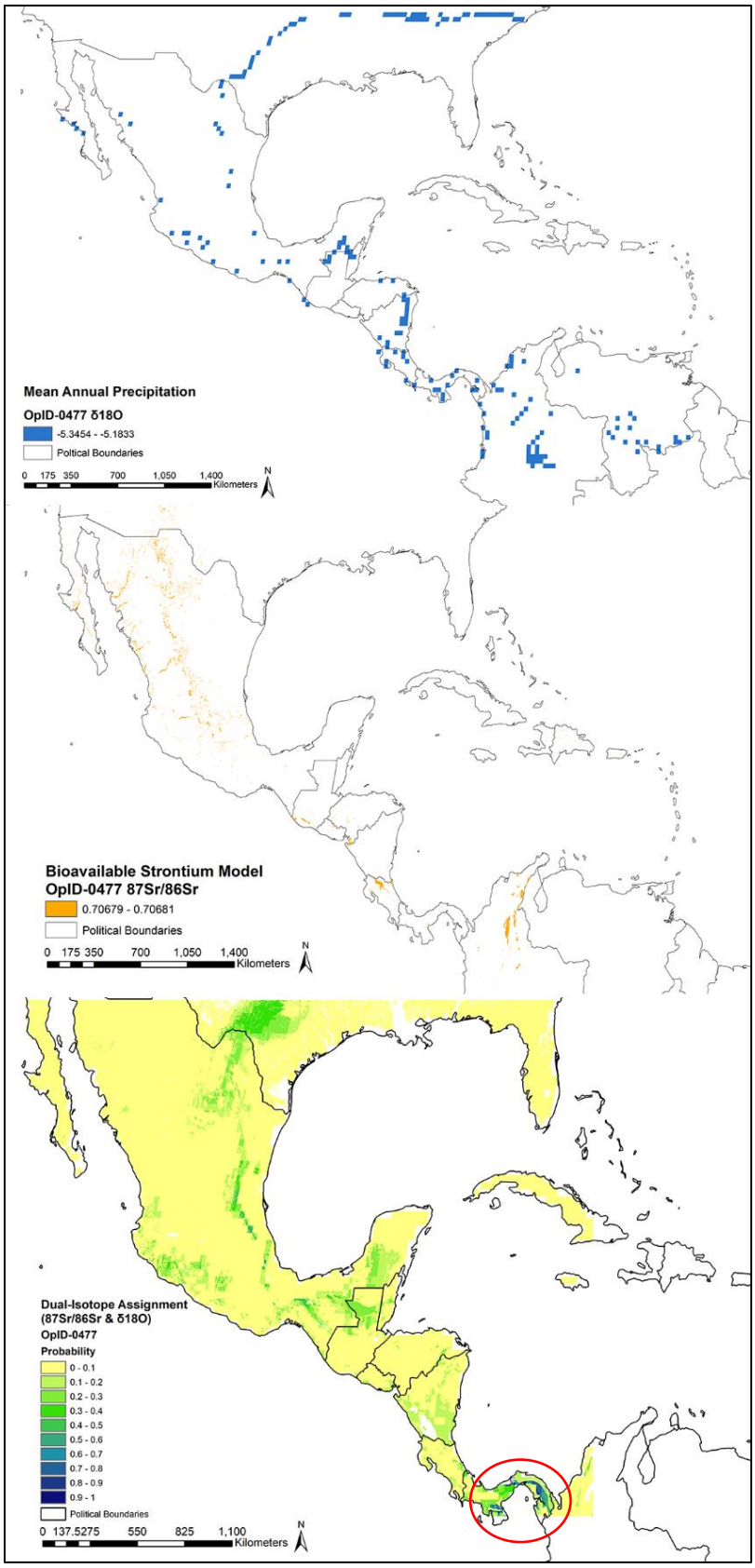

Figure 10. Isotope Assignment for OpID-0477. Top map shows the prediction using only $\delta^{18}O$ isotopes. The center map shows the prediction using only $^{87}Sr/^{86}Sr$ isotopes. The bottom map shows the dual-isotope assignment using both isotopes. OpID-0477 plots into the hill region of Panama between the Panama Canal and the San Blas Mountains marked by red circle. Due to the density plot being like the prediction for OpID-0383, OpID-0477 may be of Mexican nationality as well. All images created in ArcMap 10.5 by author. Full page maps are available in Appendix C.

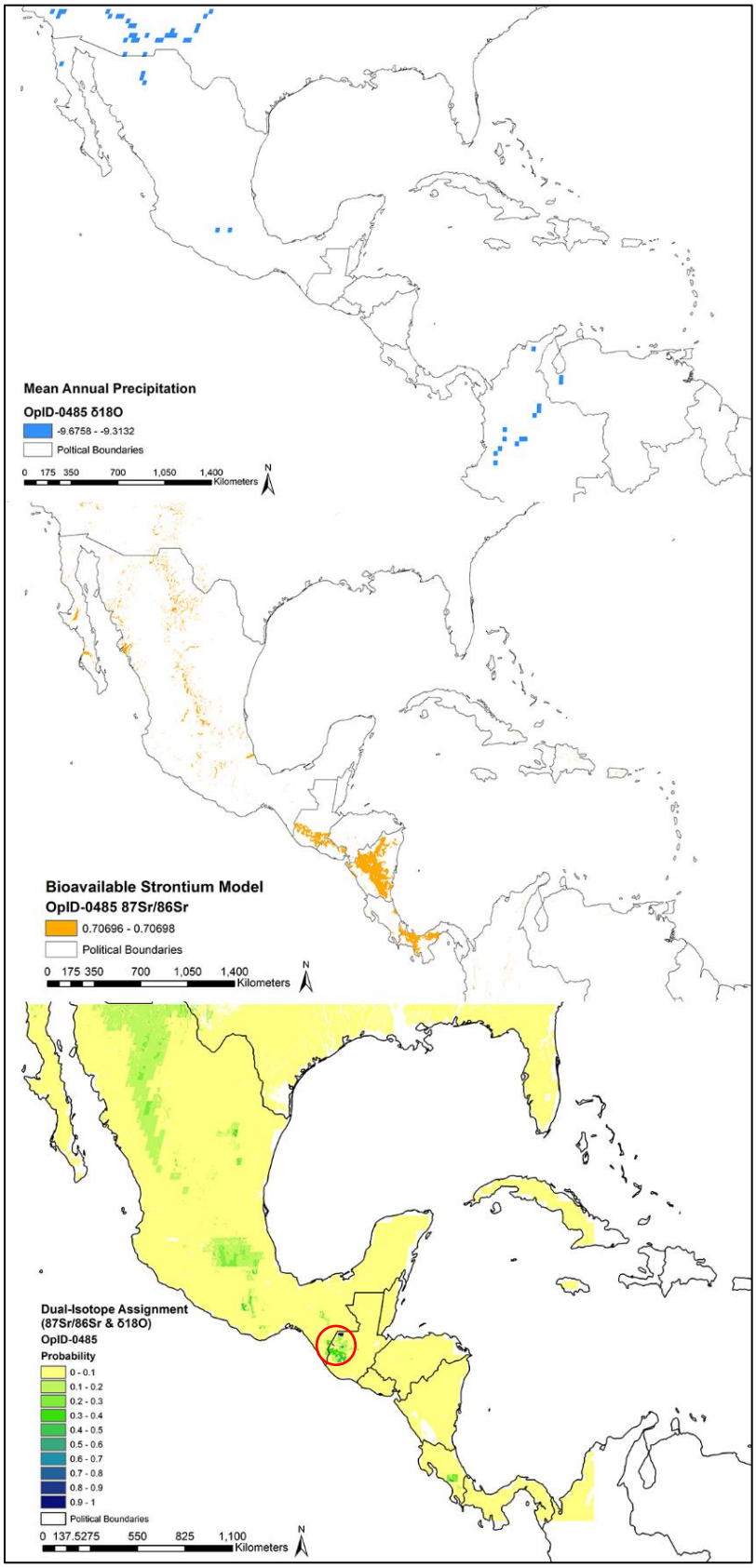

Figure 11. Isotope Assignment for OpID-0485. Top map shows the prediction using only $\delta^{18}O$ isotopes. The center map shows the prediction using only $^{87}Sr/^{86}Sr$ isotopes. The bottom map shows the dual-isotope assignment using both isotopes. OpID-0485 plots into a small part of northwestern Guatemala located in the highlands of the Cuchumatanes Mountains marked by the red circle. All images created in ArcMap 10.5 by author. Full page maps are available in Appendix C.

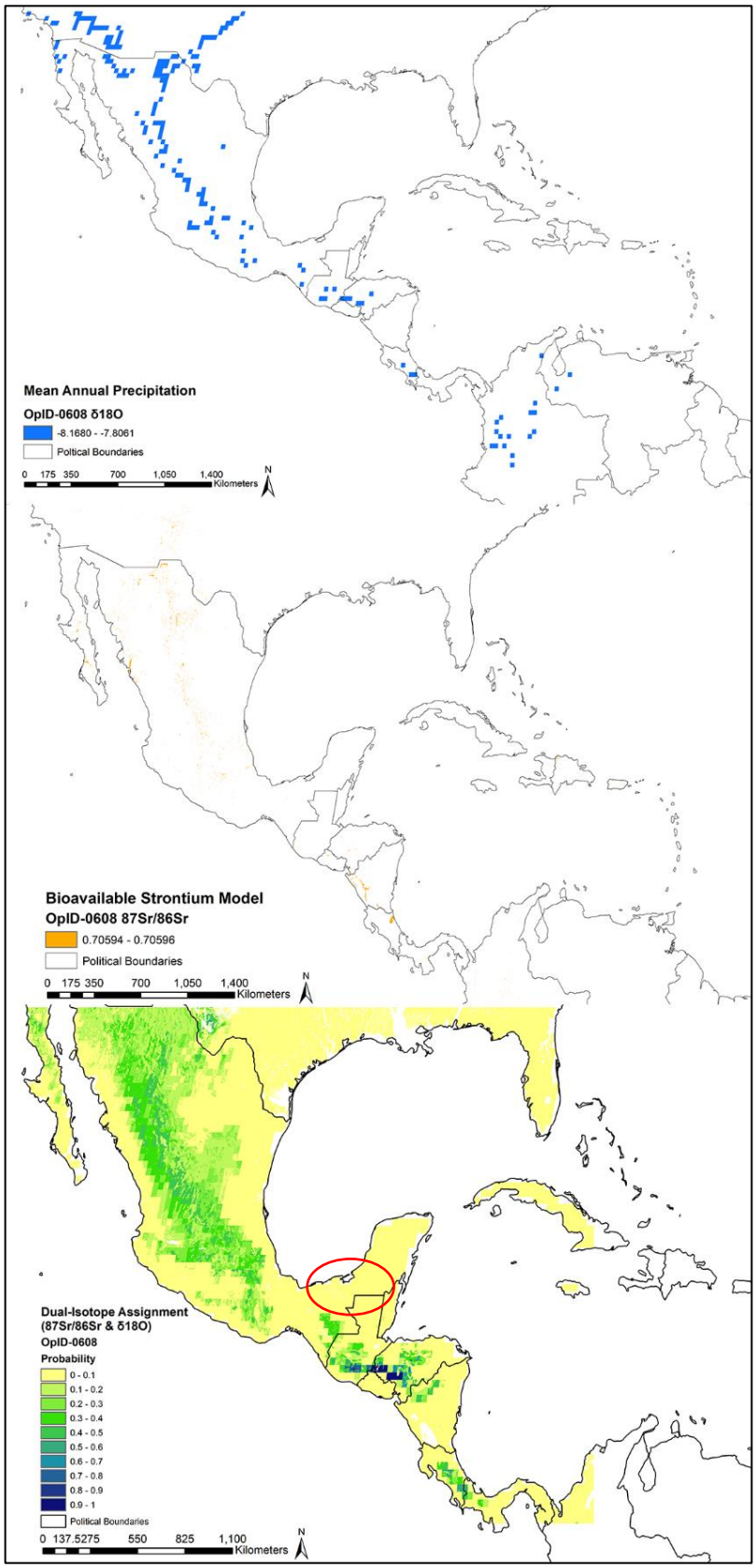

Figure 12. Isotope Assignment for OpID-0608. Top map shows the prediction using only $\delta^{18}O$ isotopes. The center map shows the prediction using only $^{87}Sr/^{86}Sr$ isotopes. The bottom map shows the dual-isotope assignment using both isotopes. OpID-0608 has been identified as being of Guatemalan nationality and the assignment model strongly plots the individual into the Sierra Madre Mountain range of Honduras and Guatemala meaning the model was successful at predicting region of origin. All images created in ArcMap 10.5 by author. Full page maps are available in Appendix C.

Question 2

To address the question of whether the Border Patrol apprehension rates reflect the same proportions of nationalities present in the OpID skeletal sample, statistics retrieved from the Border Patrol website are obtained for the 2017 fiscal year. The question seeks to explore whether the Southwestern sector of the border experiences similar migration proportions as the identified deceased migrants recovered by OpID in South Texas. In addition, nationalities of undocumented border crossers (UBCs) identified by PCOME are compared to observe if differences in migrant nationality profiles occur between Arizona and Texas. Table 7 shows the total recovered and identified UBCs from 2001 to 2016 obtained from the Annual Report 2016 of the PCOME, the identified deceased migrants for OpID as of November 2017, and the overall Border Patrol (BP) apprehension rates of living migrants for the fiscal year of 2017. Figure 13 illustrates the differences in proportions of reported nationalities between the three institutions.

Table 7. Nationalities of Apprehended and Recovered Migrants.

Nationality	PCOME	OpID	BP
Mexico	1403	5	15,407
Guatemala	154	7	41,980
El Salvador	45	9	44,626
Honduras	37	2	30,694
Other	37	3	283,887
Total	1,676	26	416,594

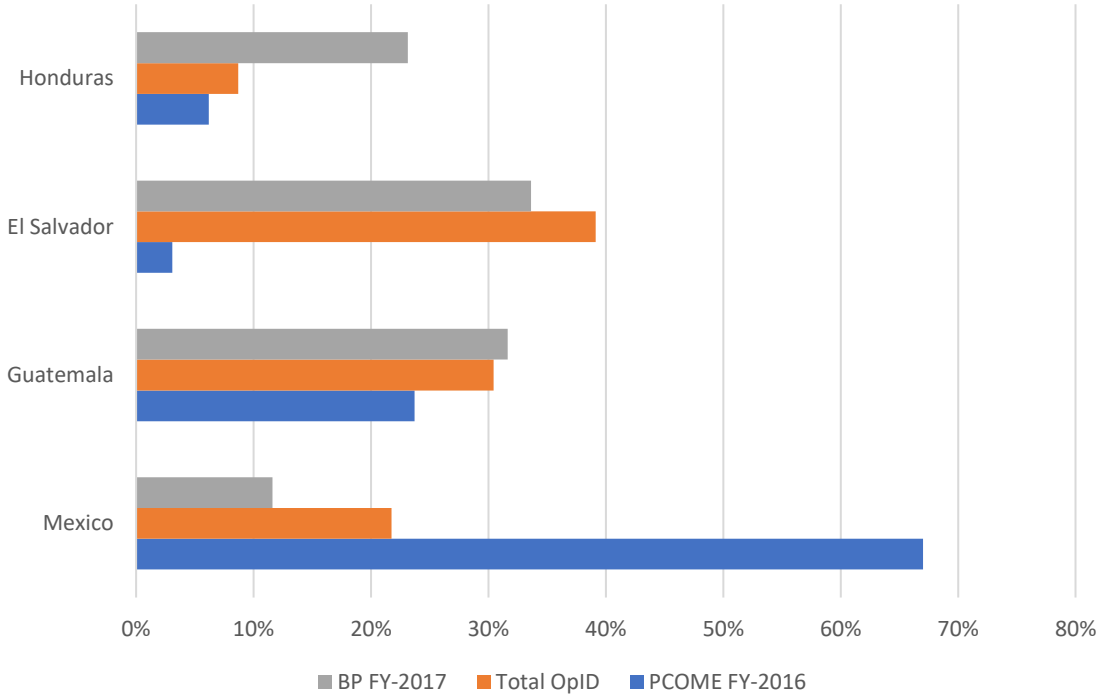

Figure 13. Recorded Proportions of Recovered and Apprehended Undocumented Migrants by Country for Border Patrol (Fiscal Year-2017), OpID, and PCOME.

Overall, the percentages are very dissimilar to one another for each nationality, except for Guatemalans which has similar proportions for all three institutions. The OpID sample has recovered a larger proportion of El Salvadorans than PCOME and the BP. The published statistics for the BP are vague when it comes to apprehensions—the total counts for nationalities are reported in Unaccompanied Alien Child (UAC) and Family Units (FU). The UAC and FU groupings reported by the Border Patrol produce ambiguous totals that may not accurately reflect the true proportions of individuals recovered. For this analysis, the UAC and FU totals were added to obtain the total number of migrants apprehended for each nationality. Lastly, the Border Patrol does not

differentiate between apprehensions performed at the border versus in the interior. Therefore, the BP total numbers used in the analysis may consider both border and interior apprehensions.

A chi-squared test of homogeneity was performed in R-Studio to assess whether the proportions have similar distributions of nationalities (Verzani, 2005:262). The "Other" category was dropped from the analysis due to the ambiguity of which groups are included within the category for the BP statistics. Also, the large number of "Others" for the BP may be inflated through the inclusion of non-Latin American migrants apprehended across the United States. The R script is provided below to show the process and results of the test.

```
> PCOME = c(1403,154,45,37); OpID = c(5,7,9,2); BP = c(15407,41980,44626,
30694)
> x = rbind(PCOME,OpID,BP)
> colnames(x) = c("Mexico", "Guatemala", "El Salvador", "Honduras")
> x
          Mexico Guatemala El Salvador Honduras
PCOME       1403       154          45       37
OpID           5         7           9        2
BP         15407     41980       44626    30694

> chisq.test(x)

                  Pearson's Chi-squared test

data:  x
X-squared = 8114.7, df = 6, p-value < 2.2e-16

Warning message:
In chisq.test(x): Chi-squared approximation may be incorrect
```

The outcome of the chi-squared test produces a statistically significant results ($p<0.000$). However, the warning message appears due to the values for some cells being less than 5 (Verzani, 2005:262). To confirm the test is significant despite the small cell values, a simulation was computed to observe if the p-value changes significantly

between the two runs. The results below show that the p-value remains significantly small (p-value = 0.0004998) and the null of no difference can be rejected.

```
> chisq.test(x, simulate.p.value = TRUE)

Pearson's Chi-squared test with simulated p-value (based on 2000
replicates)

data:  x
X-squared = 8114.7, df = NA, p-value = 0.0004998
```

The chi-square test illustrates that a significant difference exists between the three institutions but does not show which institutions are significantly different from one another. Additional chi-square tests, shown in Table 8, are run comparing the migrant nationality profiles for two institutions at a time. The results show that PCOME reports statistically different proportions of nationalities than the deceased migrants recovered by OpID in Southern Texas and the BP apprehensions in the Southwestern border sector (Table 8). The PCOME has recorded a much larger portion of Mexican migrants than either OpID or the BP illustrated in Figure 13 (Pima County Office of the Medical Examiner, 2016). Thus far, the migrants identified from OpID are primarily of Central American origin. Additionally, Mexicans compose only 4% of migrants apprehended and reported by the BP (United States Border Patrol, 2017).

Table 8. Chi-square (X^2) Results Between Institutions.

Institutions	X^2	P-value	Results
OpID - PCOME	117.71	0.0005	Significant
BP – PCOME	8111.7	0.0005	Significant
OpID – BP	4.321	0.2209	Not Significant

Question 3

This section addresses the question: are the isotopic signatures of migrants found with regionally/country specific material culture consistent with their predicted region/country of origin? To answer the question a simple comparison is made between the region predicted using the associated cultural material and the region predicted using the stable isotope data. Table 9 summarizes the findings.

Table 9. Comparison of Predicted Origin from Associated Material and Isotopes.

OpID Case Number	Associated Cultural Material Prediction	Isotope Assignment Prediction Regions	Prediction Agreement
OpID-0383	Mexican Flag Bandana	Panama	No
OpID-0422	Quetzal – Guatemalan currency	Guatemala/Honduras	Yes
OpID-0477	Dollar – US currency	Panama	Maybe
OpID-0485	Pesos – Mexican currency	Guatemala	No
OpID-0608	Quetzal – Guatemalan currency	Guatemala/Honduras	Yes

The predictions between the associated cultural material and isotopic data are in partial agreement with one another. The two individuals carrying Guatemalan currency, OpID-0422 and OpID-0608, plot within Guatemala and Honduras. However, the two individuals carrying material associated with Mexico, OpID-0383 and OpID-0485, plot into Panama and Guatemala, respectively. Two cases, OpID-0383 and OpID-0477, have origin predictions of Panama but also have moderate probabilities of being from southern Texas highlighted substantially in green on both maps, Figure 8 and 10, respectively. If the prediction of southern Texas is correct for OpID-0477 then the associated cultural material and isotope data predict the same region of origin three out of five times for the five samples. However, 60 percent is not significant enough to definitively say that the associated cultural material accurately predicts region of origin. The incongruency between the isotope model predictions and the cultural material predictions may be the

result of the isotope model estimating region of childhood residency instead of adulthood residency. The individuals may have lived in regions that match the region of the associated cultural material later in life and lived in the regions predicted by the isotopes during their childhood. It is impossible to know for sure unless residential history information can be gathered on the cases from the surviving family members.

The cultural material associated with OpID-0383 matches their known region of origin, Mexico. Additionally, the other identified case, OpID-0608 had associated cultural material that accurately predicted their established region of origin, Guatemala. The cultural material for OpID-0608 and OpID-0383 matches their established regions of origin on both occasions while the isotope assignment model only accurately predicted the region for one of the cases. This provides evidence that the associated cultural material is a strong predictor for region of origin and should be considered during the analysis if found associated with the case.

Question 4

DISPOP Analysis Using Standard Reference Groups

The final question compares craniometric data with strontium data to observe if there are patterns that reflect significant structuring within the OpID sample using 27 measurements. Two 3D scatterplots are used to observe population structures of principal coordinates and strontium data. The first 3D scatterplot uses the most genetically similar groups available in the standard DISPOP dataset, including W. W. Howells, Native American groups, 20th century American Blacks and Whites, Terry and Todd collection of Blacks and Whites, West African groups, and contextually identified Mexicans from PCOME. The first two canonical variates contribute to 11.77% and 8.83% of the morphological variation, respectively. The canonical variates are placed into a csv. file with strontium data for the OpID cases and a 3D scatterplot is produced in R Studio using the code below and shown in Figure 14.

```
Function ()
{library(plot3D)
  x <- DISPOP$P_Coor1
  y <- DISPOP$P_Coor2
  z <- DISPOP$Strontium

  Mex<-subset(DISPOP,Known_Origin=="Mexico")
  Hon<-subset(DISPOP,Known_Origin=="Honduras")
  Gua<-subset(DISPOP,Known_Origin=="Guatemala")
  ElS<-subset(DISPOP,Known_Origin=="El Salvador")
  Ecu<-subset(DISPOP,Known_Origin=="Ecuador")

  scatter3D(x, y, z, colvar = z, col = "blue", add=F, bty = "g", theta =
45, phi = 20, xlab = "Principal Coordinate 1", ylab = "Principal
Component 2", zlab = "Strontium",ticktype = "detailed", type = "h", pch =
20, main = "Percentage of Variation in PCoord and Strontium",
zlim=c(0.70495,0.7080))

points3D(Mex$P_Coor1,Mex$P_Coor2,Mex$Strontium, cex=1.15, pch=19,
   add=T, col="green",colvar=NULL)
points3D(ElS$P_Coor1,ElS$P_Coor2,ElS$Strontium, cex=1.15, pch=19,
   add=T, col="yellow",colvar=NULL)
points3D(Hon$P_Coor1,Hon$P_Coor2,Hon$Strontium, cex=1.15, pch=19,
   add=T, col="red",colvar=NULL)
points3D(Gua$P_Coor1,Gua$P_Coor2,Gua$Strontium, cex=1.15, pch=19,
   add=T, col="purple",colvar=NULL)
points3D(x[1:5], y[1:5], z[1:5], cex=1.25, pch=19, add=T, colvar
   = NULL)
text3D(x[1:5], y[1:5], z[1:5], c("PE", "AB", "AW", "MX", "WA"),
   adj = -0.25, add=T, cex=1, phi = 20, theta = 40)              }
```

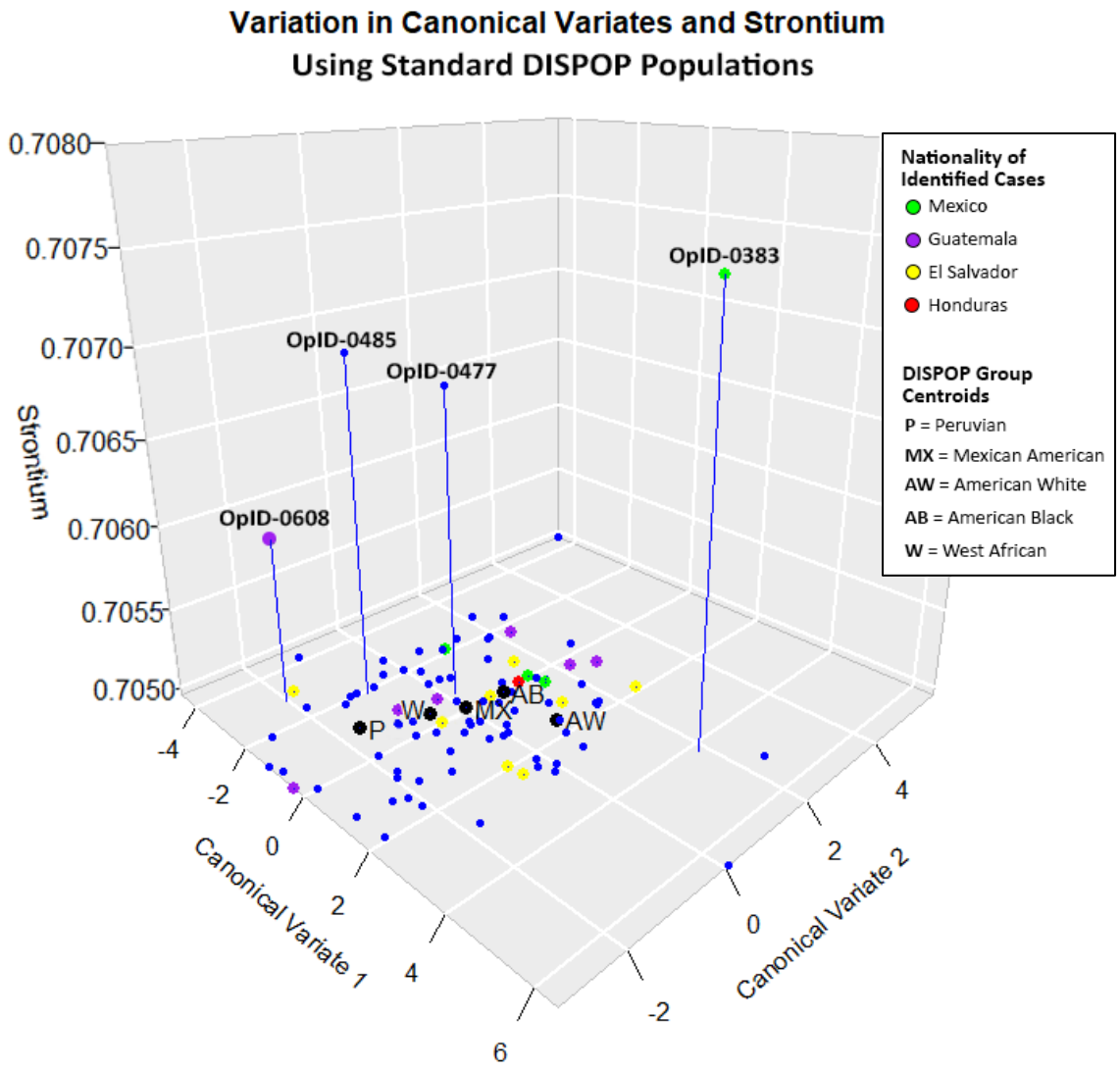

Figure 14. Variation in Canonical Variates and Strontium Data Using Standard DISPOP Reference Groups. Analysis completed using select reference populations from the standard DISPOP populations including, Peruvian, West African, and American Mexican, Black, and White groups. OpID-0422 was not used in the analysis due to the fragmented state of the cranium.

According to Figure 14, the overall population structure of the OpID forensic cases moderately clusters together near the DISPOP reference group centroids with a few outliers. There are eight outliers in total that are summarized in Table 10. The Mahalanobis distance matrix computes the expected distance (D) of any individual "drawn at random from a population with the same covariance matrix as the pooled within matrix of reference samples," (Jantz, 2000). The DISPOP program calculates the mean distance (D=7.6514, SD=1.3343) for the unknown OpID cases and reference samples selected and then states that "distances greater than 9.2401099 can be considered significant" because they fall outside the first standard deviation from the expected distance of 7.2801. The significance level for discerning outliers is set at any distances greater than 10 to include two standard deviations from the mean (i.e. the 95% confidence interval). The individual, OpID-0383, is the only outlier for the OpID cases selected for this project and clearly deviates from the other cases when looking at the 3D scatterplot in Figure 14.

Table 10. OpID Cases with Greater Than 10 Significant Differences in the Mahalanobis Distance Matrix for Standard DISPOP Analysis.

OpID Case	# of Significant Differences
OpID-0423	64
OpID-0484	63
OpID-0419	40
ME15-183	31
OpID-0431	20
OpID-0383	14
OpID-0462	14
OpID-0368	11

Among the identified cases shown in color in Figure 14, there appears to be no significant cluster patterns. The individuals identified as El Salvadoran (in yellow) are

grouped primarily near the Mexican American, American Black, and American White group centroids meaning they are most like these groups morphologically and least like the Peruvian and West African reference groups (Figure 14). No notable clusters occur in the Guatemalan, Honduran, and Mexican identified OpID cases. Posterior and typicality probabilities are calculated for each of the four OpID cases and results are provided in Table 11. Posterior probabilities explain the likelihood that the unknown individual belongs to each reference group and the probabilities sum to one (Ousley & Jantz, 2005). The typicality probability indicates the likelihood that the unknown individual belongs to a group (Ousley & Jantz, 2005).

Clustering of cases OpID-0477, OpID-0485 and OpID-0608 demonstrate that they are morphologically similar to one another, unlike OpID-0383 which is isolated from the other cases (Figure 14). The posterior and typicality probabilities for OpID-0477, OpID-0485 and OpID-0608 predict group membership to the Mexican American reference group (Table 11). On the other hand, OpID-0383 has a high posterior probability of 0.9968 for belonging to the American White reference group but is highly atypical of the American White group (typicality = 0.0367) and even less typical of the other reference groups (Table 11).

Cases OpID-0383 and OpID-0608 have been identified as individuals of Mexican and Guatemalan nationality, respectively. The cranial morphologies differ significantly for the two cases meaning they are most likely from populations that do not interact with one another and therefore do not experience gene flow through marital exchanges. In addition, the strontium values for OpID-0383 and OpID-0608 are drastically different (0.70748 and 0.70595, respectively) meaning they are most likely from geologically

distinct regions of Mexico and Guatemala. Higher $^{87}Sr/^{86}Sr$ values are expected in mountainous regions, while lower values are expected in lowland regions. Exact locations of residency are not known for the cases at this time, but the distinct isotope values from OpID-0383 and OpID-0608 are not surprising because Mexico is an enormous country that encompasses a large spectrum of geology from the numerous Sierra mountain ranges on the western coast to the lowlands of the Yucatan Peninsula in the east. Mexico and Guatemala share a border—therefore southern Mexico should share similar geology and strontium ratios with Northern Guatemala. Since OpID-0383 and OpID-0608 have such different strontium values, it is likely that OpID-0383 does not originate from southern Mexico and more likely spent their childhood in central or northern Mexico. An additional explanation for the large variability between the $^{87}Sr/^{86}Sr$ values for these two cases may be due to water insecurity in regions of Mexico (Ramey & Juarez, 2018). If water insecurities are causing the variable range of strontium values, Case-0383 may be from southern Mexico.

Table 11. Classification of OpID Cases Using Standard DISPOP Populations.

		Peru	AmBlack	AmWhite	MexAm	Wafrica
OpID-0608	Distance	36.6160	47.6480	58.9050	35.2380	52.1700
	Posterior	0.3337	0.0013	0.0000	**0.6648**	0.0001
	Typicality	0.0809	0.0059	0.0002	**0.1066**	0.0017
OpID-0485	Distance	24.8850	42.9520	44.2840	23.2230	53.0620
	Posterior	0.3035	0.0000	0.0000	**0.6965**	0.0000
	Typicality	0.5255	0.0195	0.0141	**0.6203**	0.0013
OpID-0477	Distance	41.1880	44.5920	41.4020	27.8300	68.1420
	Posterior	0.0013	0.0002	0.0011	**0.9974**	0.0000
	Typicality	0.0297	0.0130	0.0283	**0.3669**	0.0000
OpID-0383	Distance	79.9580	58.7890	40.2680	51.7760	90.9650
	Posterior	0.0000	0.0000	**0.9968**	0.0032	0.0000
	Typicality	0.0000	0.0002	**0.0367**	0.0019	0.0000

DISPOP Analysis Using Modern Forensic Reference Groups

The second DISPOP analysis employs a modern dataset derived from the Forensic Data Bank (FDB) that were provided by Dr. Kate Spradley (2018). The modern forensic reference groups are expected to be more appropriate for modeling the population structure of the OpID forensic cases. The reference groups include 20th century Black, White, positively identified Mexicans from PCOME, and Guatemalans. The first two canonical variates contribute to 11.08% and 8.3% of the variation for the sample, respectively. The 3D scatterplot from the second run is shown in Figure 15.

The overall population structure of the OpID forensic cases clusters less than the previous analysis most likely due to the morphological similarities between the populations (Figure 15). Three of the modern forensic group centroids (Mexican, Guatemalan and Black groups) cluster together, while the White group centroid is morphologically distant from the other populations. Within the unknown OpID cases analyzed, there are nine outliers that fall outside the 95% confidence interval from the calculated mean distance of D=6.9527 and a SD=1.1605 shown in Table 12.

Table 12. OpID Cases with Greater Than 10 Significant Differences in the Mahalanobis Distance Matrix.

OpID Case	# of Significant Differences
OpID-0484	52
OpID-0423	29
OpID-0419	20
OpID-0431	18
OpID-0368	15
ME15-183	15
OpID-0510	12
OpID-0387	12
OpID-0383	11

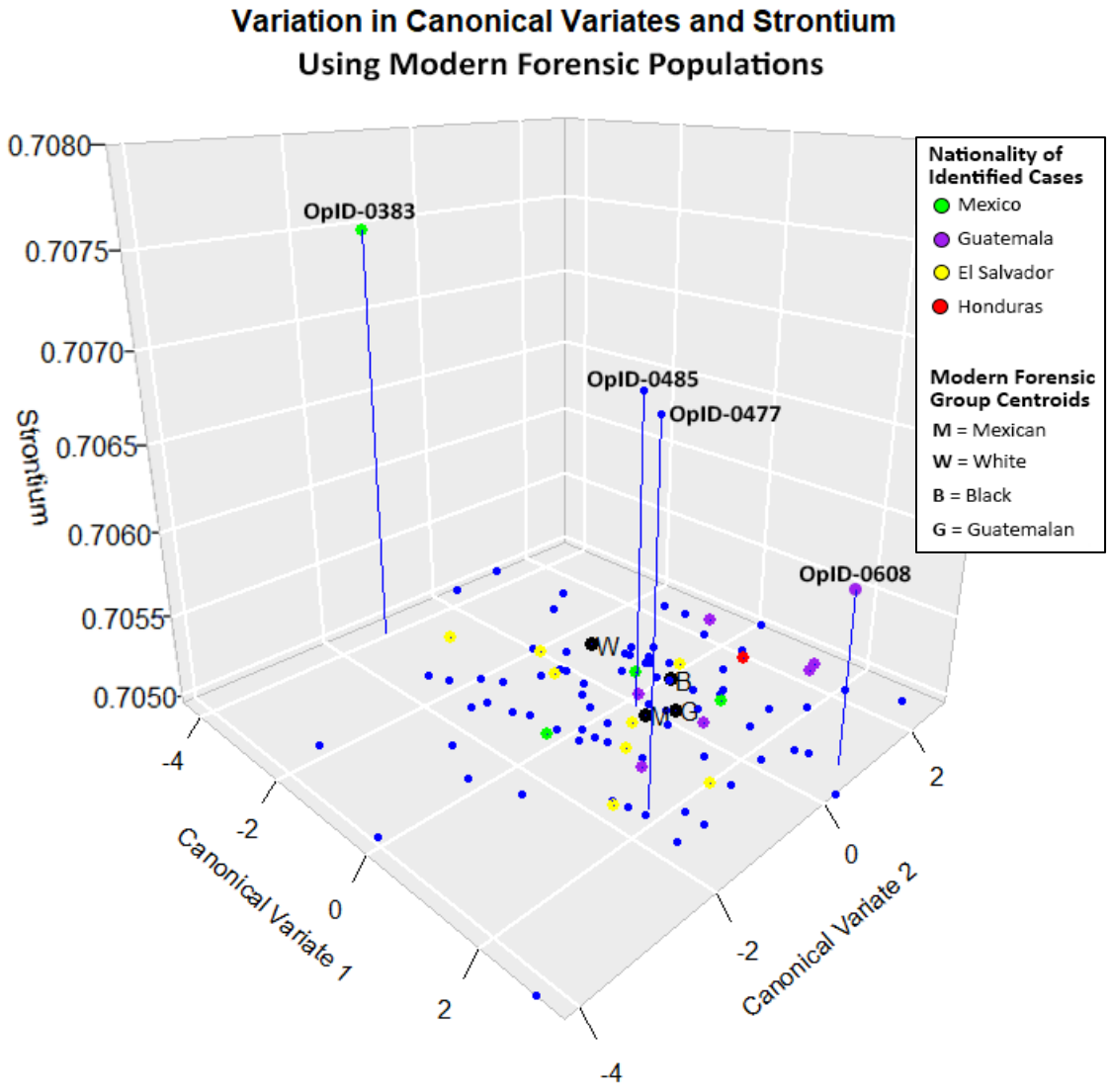

Figure 15. Variation in Canonical Variates and Strontium Data Using Modern Forensic DISPOP Reference Groups. Analysis completed using select reference populations from a modified DISPOP dataset that includes forensically significant populations including, Guatemalan, Black, White, positively identified Mexicans. OpID-0422 was not used in the analysis due to the fragmented state of the cranium.

Once again, there appears to be no significant cluster patterns among the identified OpID cases highlighted in color (Figure 15). The lack of clustering may result from the lack of genetic drift and/or the isolation of groups represented in the unknown OpID cases. The genetic relationships of modern populations, like the OpID forensic cases, are most likely heavily influenced by genetic admixture from different populations present within North and Central America. A major difference between Figure 14 and Figure 15 is the placement of OpID-0485, OpID-0477 and OpID-0608. In Figure 15, the OpID-0485 and OpID-0477 appear to be more morphologically similar to one another than they are with OpID-0608. In Figure 14, the three samples appeared to be equally distant using the canonical variates. When referring to the posterior and typicality probabilities for the samples, OpID-0485, OpID-0477 and OpID-0608 all classify as Guatemalan, except OpID-0485 which has slightly higher posterior and typicality probabilities for belonging to the Mexican reference group (Table 13). Like the previous run, OpID-0383 has a high posterior of belonging to the White reference group and is moderately typical of the White reference group with a value of 0.0994 (Table 13).

Additionally, the $^{87}Sr/^{86}Sr$ values for OpID-0477 and OpID-0485 are very similar to one another which provides evidence that these two samples may be from similar geographic regions and genetic groups. Lastly, using the modern DISPOP reference groups produces an accurate classification of OpID-0608 as Guatemalan. Overall, the modern forensic reference groups may be more successful at revealing morphological similarities and differences for the OpID forensic cases because the reference groups are more representative of the OpID cases than the standard DISPOP reference groups.

Table 13. Classification of OpID Cases Using Modern Forensic DISPOP Populations

		Black	Guatemalan	Mexican	White
OpID-0608	Distance	32.0350	21.0380	24.3850	39.7800
	Posterior	0.0034	**0.8391**	0.1575	0.0001
	Typicality	0.1920	**0.7400**	0.5540	0.0410
OpID-0485	Distance	36.5370	19.5270	19.2050	40.9740
	Posterior	0.0001	**0.4598**	**0.5401**	0.0000
	Typicality	0.0822	**0.8134**	**0.8277**	0.0312
OpID-0477	Distance	37.4460	21.1350	26.6360	35.1800
	Posterior	0.0003	**0.9389**	0.0600	0.0008
	Typicality	0.0681	**0.7350**	0.4286	0.1078
OpID-0383	Distance	55.4000	52.7560	48.2950	35.5960
	Posterior	0.0001	0.0002	0.0017	**0.9980**
	Typicality	0.0007	0.0015	0.0050	**0.0994**

IV. DISCUSSION

Research Summary and Conclusions

This research demonstrates the potential value of strontium and oxygen isotope analysis to aid in identification and repatriation efforts for deceased unidentified migrants recovered in southern Texas and along the Mexico-U.S. border. Data derived from isotope analysis can aid identification efforts by predicting geographic regions of origin that will add residential history information to the case file to eliminate missing person reports that are not congruent with all available evidence and, overall, improve the chances of making an identification. The isotope assignment model approach to the identification of human skeletal remains is needed because it provides an important piece of information, specifically residential history, that can eliminate missing person reports whose residential history does not match the isotopically predicted region of residence.

The issue of recovering unidentified deceased migrant remains is not limited to southern Texas—all states sharing a border with Mexico are experiencing the effects of this humanitarian crisis. It is important to note that the migration issue is not contained to the U.S; Mexico and Central American countries also experience the migration of individuals seeking refuge and fleeing violence occurring primarily in El Salvador, Honduras and Guatemala. Identification efforts have been underway for many years by international organizations such as the EAAF, the Peruvian Forensic Anthropology Team (EPAF), the Guatemalan Forensic Anthropology Foundation (FAFG), the Center of Forensic Analysis and Applied Sciences (CAFCA) and the Archbishop's Human Rights Office of Guatemala (ODHA).

The major take-home message of this research is that isotope provenancing and

associated cultural material are additional lines of evidence that can be extremely useful for deciding where to focus identification efforts. Once regions or countries are predicted, dialogues can begin with non-governmental organizations to obtain family reference DNA samples for missing person reports whose information match the forensic anthropological report for the unidentified individual. The results from the final question concerning craniometric analysis support the conclusion that multiple lines of evidence are required to accurately identify each case because the OpID cases are a heterogenous group composed of migrants from a variety of regions and socio-political situations. There is not one fool-proof method that can be relied on for obtaining positive identifications; instead, all information must be considered and weighed by the analyst to decide if an unidentified case is a potential match for a missing person report. Isotope data and associated cultural material are powerful pieces of evidence that can greatly inform identification efforts.

Question 1

The isotope assignment model was successful for predicting probable regions of origin for each of the OpID cases. Of the five cases, two have been identified and the model successfully plotted one case, OpID-0608, into its country of origin, Guatemala. However, the model was unsuccessful at plotting OpID-0383 into its country of origin, Mexico. The limited isotope data for Mexico most likely influenced the inaccurate geographic origin prediction due to massive data interpolation. Green dots shown in Figure 6 represent water isotope collection points and there are only two precipitation water stations that record isotopic data for Mexico located in Chihuahua (northern

Mexico) and Veracruz (southeastern Mexico). In addition, only one precipitation station exists for Central America located near San Salvador in El Salvador. If more stations were placed in under-sampled regions, the accuracy of the isotope assignment model would increase dramatically.

Question 2

The second objective is to better understand how the nationality profiles of migrants differ from state to state and the overall southwestern sector of the border. The total recovered migrant nationalities are obtained for the identified cases from PCOME and OpID, while the apprehended FU and UAC data for the fiscal year of 2017 are used for the BP. The analysis found that OpID and the southwestern sector of the BP report similar proportions of migrant nationalities, while PCOME reports significantly more Mexican migrants than the other two institutions. The rates and proportion of migrants vary from state to state, specifically Arizona and Texas, and are influenced by a variety of unknown factors, such as country of origin, reason for migration, age, socioeconomic status, sex, etc. At this time, OpID has similar proportions of individuals from Central America and Mexico which may change as more identifications are made. It is important to understand the nationality profiles of recovered deceased migrants because they can be used to better understand the pressures causing the migration. A tumultuous history of structural violence, organized crime, and foreign intervention throughout Latin America has stimulated mass migrations to the U.S. for decades. The reasons for migrating will differ from region to region and better understanding where individuals are coming from will aid in understanding the scope of the issue and potentially bring awareness to the

events affecting migration and producing the humanitarian crisis at the border.

Question 3

The third objective is to compare the regions of origin predicted using the isotope assignment model to the regions predicted using the associated cultural material. After comparison, the country-specific associated material did not predict the same region of origin as the isotope assignment model consistently. However, this does not mean that the cultural material should be ignored. The lack of agreement between the isotope assignment model and the associated material predictions may be due to the prediction timeframe each type of evidence represents. The assignment model uses isotopes derived from teeth that depict geographic childhood residency, while the associated cultural material represents a later time during adulthood for the individual, just prior to their death.

For the two identified cases, OpID-0608 and OpID-0383, the cultural material is consistent with their established region of origins, Guatemala and Mexico, respectively. This provides strong evidence that the cultural material is an important variable to consider when establishing regions of origin. It is important to understand that associated cultural material is considered circumstantial and should be supported with additional evidence to back a positive identification.

Question 4

The final objective of the research was to observe how the strontium isotope data covaries with the overall population structure of the OpID cases. Canonical variates

derived from craniometric analysis run in the DISPOP software were used with the strontium data to create 3Dplots showing the isotopic and morphological variation within the sample. The OpID cases were run through two different DISPOP reference group datasets. The first run used the standard DISPOP reference groups composed of data derived from the following skeletal collections: W. W. Howell's, Native American groups, 20th century American Blacks and Whites, Terry and Todd collection of Blacks and Whites, West African groups, and contextually identified Mexicans from PCOME. The second run used a modified DISPOP reference group dataset composed of 20th century Black, White, positively identified Mexicans from PCOME, and Guatemalans. The modern forensic reference groups were more successful at revealing morphological similarities and accurately classifying the unidentified migrants because the groups are more representative of the OpID cases than the standard DISPOP reference groups.

Overall, the observed patterns within the craniometric and strontium data are not tightly clustered, indicating there is no correlation between cranial shape and strontium isotope ratios. Instead, the strontium values exhibit a large range of variation for the OpID cases. The four individuals sampled (OpID-0422 was not included in either DISPOP analysis due to fragmentation of the cranium) showed quite a bit of variation in cranial shape and isotope values providing evidence that the OpID cases come from variety of regions within Mexico and Central America and cannot be treated as a homogenous group.

Limitations

It is important to recognize that isoscapes created using geostatistical methods do not depict the data, but instead illustrate "a set of expectations from the isoscape model," (Wunder, 2010:251). The very limited data for both $^{87}Sr/^{86}Sr$ and $\delta^{18}O$ in Mexico most likely influenced the geographic origin predictions due to data interpolation. There are only two precipitation water stations that record isotopic data for Mexico: one is located in Chihuahua in Northern Mexico and the other is located in Veracruz in Southern Mexico near the Yucatan peninsula. Bowen (2010:142) states that $\delta^{18}O$ data experiences "significant unevenness of the data in space and time" which limits it's "relevance to mapping applications." The deficiency of $\delta^{18}O$ data limits the accuracy and precision of geostatistical applications which perform estimations better with increased data density (Bowen, 2010:144). If more stations were placed in under-sampled regions of Mexico the accuracy and precision of the assignment model would increase dramatically. Much like the $\delta^{18}O$ data, $^{87}Sr/^{86}Sr$ data is severely lacking for Mexico and Central America. As more research takes place in these regions, the accuracy and precision should increase for the $^{87}Sr/^{86}Sr$ model after it is rescaled with the bioavailable $^{87}Sr/^{86}Sr$ data.

An additional limitation for the predictive model includes the isotope "noise" produced by the global supermarket that can introduce nonlocal food, and therefore nonlocal isotopes, into the diet (Ehleringer et al. 2008:2791). If people are consuming nonlocal foods and water sourced from distant regions, the assignment model will fail and plot the location of the food resources and not the actual location of the individual exploiting those resources. Lastly, the extent used for the assignment model may reduce the probability densities for likely regions of origin. If a smaller extent was used, regions

will show higher probability densities than produced by the assignment using the continental extent. As discussed previously in the Results chapter, the incorrect predictions for OpID-0383 and OpID-0608 are most likely a product of the large extent used for the assignment. If the extent was limited to Mexico, more regions of high probability would appear than when the extent includes Mexico and Central America.

Future Research

The research utilizes isotope analysis to predict region of geographic origin and represents an important first step to better understanding migrant residency from childhood into adulthood. Migrants recovered near the Mexico-U.S. border are a heterogenous group, constantly migrating, that originate from a variety of regions and backgrounds. It is important to better understand the mobility of migrants to reveal the pressures producing the mass migrations of people out of their native countries and to aid in identification efforts for the unidentified.

Future applications of the assignment model are abundant and do not need to be constrained to anthropological settings. The model would benefit the most from increasing the spatial resolution of the $\delta^{18}O$ isoscape. I propose creating a hybrid $\delta^{18}O$ model using mosaic modeling to combine the groundwater isoscape produced by Hobson et al. (2009) with the global precipitation isoscape currently available through IsoMAP. Creating the hybrid model will greatly increase the spatial resolution for Mexico which currently relies too heavily on kriging interpolation to estimate $\delta^{18}O$ values. In addition, I believe adding additional isotopes (sulfur, lead, carbon, etc.) into the assignment would greatly benefit the assignment model's ability to predict region of geographic origin for unknown samples.

The assignment model has many possible applications for the bioarchaeology of Mexico and Central America. In addition, similar assignment models can be made for other regions of the world once the global strontium model is published by Clement (in prep). The isoscape assignment model can be used to track migration of past populations using $^{87}Sr/^{86}Sr$ and $\delta^{18}O$ values derived from dental enamel and bone apatite, assuming the bone has not been subjected to major diagenetic alterations. The model should work for temporal ranges extending back to the Last Glacial Maximum because the global temperature has been relatively stable since this climatic event meaning the $\delta^{18}O$ have remained relatively stable.

Overall, the models are not perfect. They are predictive and attempt to model natural processes that are ever-changing. As new advances in geologic modeling are discovered, the isoscapes and assignment model will need to be adapted to consider the new information.

Recommendations

For future projects following the same trajectory as this study, I recommend the following procedures:

1. When selecting teeth for analysis, target teeth that have no signs of caries, dental calculus, or postmortem cracking because these features introduce the possibility of contamination and diagenetic alteration. The specific tooth selected is also important to consider since different teeth represent different windows of childhood residence.
2. Make casts of each extracted tooth to ensure future research can be performed using dental morphological trait analysis.

3. The teeth in this analysis were used for histological analysis for age-at-death estimations—the crowns were separated from the roots using a precision saw. Preserving the root for further analysis is highly recommended for unidentified forensic cases.
4. If possible, collect hair and bone samples from each case to be used for isotope analysis to track adult migration of the individual. Left fourth metatarsals were extracted with each dental sample for this research.
5. Once extracted, place samples into individually labelled tubes or plastic bags to prevent commingling.
6. Samples for this analysis were sent to Isoforensics, Inc at the University of Utah for oxygen and strontium isotope preparation and analysis. There are a variety of other labs that can be used but ensure that all samples are processed at the same lab to account for inter-laboratory variability (Pestle et al., 2014).
7. Strontium data provided in the Appendix should be used to rescale the strontium isoscape model (Bataille, in prep). As new isotope data is published, add any additional geo-referenced strontium data to assist in the rescaling.

APPENDIX SECTION

APPENDIX A. PUBLISHED STRONTIUM DATA FOR ISOSCAPE ADJUSTMENT

Median 87Sr/86Sr	SE	Sampled Material	Latitude	Longitude	Datum	Source Paper
0.704595	0.0006	Rabbit bone	19.6925	-98.8438	WGS84	Price et al. 2000
0.704588	0.0009	Rabbit bone	19.6925	-98.8438	WGS84	Price et al. 2000
0.704689	0.0006	Rabbit bone	19.6925	-98.8438	WGS84	Price et al. 2000
0.704591	0.0007	Rabbit bone	19.6925	-98.8438	WGS84	Price et al. 2000
0.70464	0.0008	Rabbit bone	19.6925	-98.8438	WGS84	Price et al. 2000
0.704717	0.0013	Rabbit bone	19.6925	-98.8438	WGS84	Price et al. 2000
0.704612	0.0007	Rabbit bone	19.6925	-98.8438	WGS84	Price et al. 2000
0.704709	0.0008	Rabbit bone	19.6925	-98.8438	WGS84	Price et al. 2000
0.704654	0.0006	Rabbit bone	19.6925	-98.8438	WGS84	Price et al. 2000
0.7047958	0.00001	Human bone - not sp	19.6925	-98.8438	WGS84	Price et al. 2000
0.705061	0.0006	Human long bone	19.6925	-98.8438	WGS84	Price et al. 2000
0.705071	0.0006	Human long bone	19.6925	-98.8438	WGS84	Price et al. 2000
0.704672	0.0013	Human long bone	19.6925	-98.8438	WGS84	Price et al. 2000
0.704759	0.0006	Human long bone	19.6925	-98.8438	WGS84	Price et al. 2000
0.704736	0.0006	Human long bone	19.6925	-98.8438	WGS84	Price et al. 2000
0.7046508	0.00001	Human tooth	19.6925	-98.8438	WGS84	Price et al. 2000
0.7046479	0.00001	Human long bone	19.6925	-98.8438	WGS84	Price et al. 2000
0.704703	0.00002	Human bone - not sp	19.6925	-98.8438	WGS84	Price et al. 2000
0.7046624	0.00001	Human bone - not sp	19.6925	-98.8438	WGS84	Price et al. 2000
0.704678	0.0007	Human long bone	19.6925	-98.8438	WGS84	Price et al. 2000
0.704625	0.0005	Human long bone	19.6925	-98.8438	WGS84	Price et al. 2000
0.704624	0.0007	Human long bone	19.6925	-98.8438	WGS84	Price et al. 2000
0.704615	0.0005	Human long bone	19.6925	-98.8438	WGS84	Price et al. 2000
0.704633	0.0007	Human long bone	19.6925	-98.8438	WGS84	Price et al. 2000
0.704612	0.0007	Human rib	19.6925	-98.8438	WGS84	Price et al. 2000
0.704608	0.0007	Human rib	19.6925	-98.8438	WGS84	Price et al. 2000
0.704664	0.0007	Human rib	19.6925	-98.8438	WGS84	Price et al. 2000
0.704652	0.0006	Human rib	19.6925	-98.8438	WGS84	Price et al. 2000
0.704663	0.0007	Human rib	19.6925	-98.8438	WGS84	Price et al. 2000
0.704641	0.0006	Human rib	19.6925	-98.8438	WGS84	Price et al. 2000
0.704558	0.0009	Human rib	19.6925	-98.8438	WGS84	Price et al. 2000
0.70464	0.0007	Human rib	19.6925	-98.8438	WGS84	Price et al. 2000
0.704672	0.0006	Human rib	19.6925	-98.8438	WGS84	Price et al. 2000
0.704611	0.0006	Human rib	19.6925	-98.8438	WGS84	Price et al. 2000
0.704662	0.0007	Human rib	19.6925	-98.8438	WGS84	Price et al. 2000
0.704616	0.0006	Human rib	19.6925	-98.8438	WGS84	Price et al. 2000
0.704603	0.0007	Human rib	19.6925	-98.8438	WGS84	Price et al. 2000

0.7047584	0.00001	Human long bone	19.6925	-98.8438	WGS84	Price et al. 2000
0.704658	0.00002	Human long bone	19.6925	-98.8438	WGS84	Price et al. 2000
0.70466	0.0008	Human long bone	19.6925	-98.8438	WGS84	Price et al. 2000
0.704826	0.0007	Human long bone	19.6925	-98.8438	WGS84	Price et al. 2000
0.704599	0.0009	Human tooth URM1	19.6925	-98.8438	WGS84	Price et al. 2000
0.704613	0.0008	Human femur	19.6925	-98.8438	WGS84	Price et al. 2000
0.704633	0.0007	Human tooth URM1	19.6925	-98.8438	WGS84	Price et al. 2000
0.704626	0.0008	Human femur	19.6925	-98.8438	WGS84	Price et al. 2000
0.70469	0.0006	Human femur	19.6925	-98.8438	WGS84	Price et al. 2000
0.704811	0.0006	Human femur	19.6925	-98.8438	WGS84	Price et al. 2000
0.704797	0.0008	Human femur	19.6925	-98.8438	WGS84	Price et al. 2000
0.704905	0.0007	Human femur	19.6925	-98.8438	WGS84	Price et al. 2000
0.704855	0.0006	Human femur	19.6925	-98.8438	WGS84	Price et al. 2000
0.705085	0.0007	Human femur	19.6925	-98.8438	WGS84	Price et al. 2000
0.704948	0.0011	Human femur	19.6925	-98.8438	WGS84	Price et al. 2000
0.704859	0.0007	Human femur	19.6925	-98.8438	WGS84	Price et al. 2000
0.7042	-	Human_tooth	19.628333	-101.57888	WGS84	Price et al. 2015
0.7052	-	Human_tooth	20.283333	-99.4	WGS84	Price et al. 2015
0.7077	-	Human_tooth	20.448056	-97.378056	WGS84	Price et al. 2015
0.7046	-	Human_tooth	19.6925	-98.8438	WGS84	Price et al. 2015
0.7046	-	Human_tooth	19.291667	-98.938889	WGS84	Price et al. 2015
0.7079	-	Human_tooth	19.445	-96.408889	WGS84	Price et al. 2015
0.7062	-	Human_tooth	18.816667	-97.283333	WGS84	Price et al. 2015
0.7074	-	Human_tooth	17.043889	-96.767778	WGS84	Price et al. 2015
0.7076	-	Human_tooth	18.716667	-96.15	WGS84	Price et al. 2015
0.7042	-	Human_tooth	18.466667	-95.433333	WGS84	Price et al. 2015
0.7036	-	Human_tooth	18.5	-95.233333	WGS84	Price et al. 2015
0.7085	-	Human_tooth	17.555	-94.4219	WGS84	Price et al. 2015
0.7074	-	Human_tooth	18.280081	-93.201753	WGS84	Price et al. 2015
0.7081	-	Human_tooth	18.27	-94.040278	WGS84	Price et al. 2015
0.7079	-	Human_tooth	17.483978	-92.046328	WGS84	Price et al. 2015
0.7079	-	Human_tooth	16.901219	-92.009675	WGS84	Price et al. 2015
0.708	-	Human_tooth	28.7	-100.52306	WGS84	Price et al. 2015
0.7079	-	Human_tooth	18.105392	-89.810829	WGS84	Price et al. 2015
0.7084	-	Human_tooth	19.35	-90.716667	WGS84	Price et al. 2015
0.7082	-	Human_tooth	18.833333	-90.4	WGS84	Price et al. 2015
0.7087	-	Human_tooth	20.523889	-90.009722	WGS84	Price et al. 2015
0.7089	-	Human_tooth	20.97	-89.62	WGS84	Price et al. 2015
0.7087	-	Human_tooth	20.683056	-88.568611	WGS84	Price et al. 2015
0.7089	-	Human_tooth	21.1425	-88.164722	WGS84	Price et al. 2015
0.7089	-	Human_tooth	21.6	-88.166667	WGS84	Price et al. 2015
0.7086	-	Human_tooth	20.891111	-88.136389	WGS84	Price et al. 2015
0.7082	-	Human_tooth	20.494722	-87.736111	WGS84	Price et al. 2015

0.708	-	Human_tooth	20.214722	-87.428889	WGS84	Price et al. 2015
0.7087	-	Human_tooth	17.2504	-88.9974	WGS84	Price et al. 2015
0.7081	-	Human_tooth	18.075	-88.558333	WGS84	Price et al. 2015
0.7086	-	Human_tooth	18.217356	-88.584731	WGS84	Price et al. 2015
0.707	-	Human_tooth	16.281111	-88.965	WGS84	Price et al. 2015
0.7151	-	not specified	17.083889	-89.133889	WGS84	Krueger 1985
0.70663	-	deer	14.84	-89.15	WGS84	Krueger 1985
0.70904	-	deer	14.84	-89.15	WGS84	Krueger 1985
0.70612	-	deer	14.84	-89.15	WGS84	Krueger 1985
0.70554	-	peccary	14.84	-89.15	WGS84	Krueger 1985
0.70576	-	peccary	14.84	-89.15	WGS84	Krueger 1985
0.70895	-	Puma	14.84	-89.15	WGS84	Krueger 1985
0.70632	-	Paca	14.84	-89.15	WGS84	Krueger 1985
0.707444	-	river snail shell	16.199294	-89.042035	WGS84	Freiwald 2011
0.707572	-	terrestial shell	17.297682	-88.80572	WGS84	Freiwald 2011
0.70763	-	land snail shell	16.761526	-89.122444	WGS84	Freiwald 2011
0.707712	-	iguana (iguanidae)	16.838796	-89.057830	WGS84	Freiwald 2011
0.707768	-	river snail shell	17.126107	-88.851322	WGS84	Freiwald 2011
0.707863	-	opossum	17.077779	-89.022306	WGS84	Freiwald 2011
0.708208	-	terrestial shell	17.103607	-89.104958	WGS84	Freiwald 2011
0.708219	-	toad (Bufonidae)	17.227144	-88.833334	WGS84	Freiwald 2011
0.708252	-	land snail shell	17.362762	-88.991435	WGS84	Freiwald 2011
0.708285	-	cow tooth enamel	17.13	-89.121	WGS84	Freiwald 2011
0.70832	-	opossum	17.131049	-89.048148	WGS84	Freiwald 2011
0.708342	-	lizard bone	17.019865	-89.096385	WGS84	Freiwald 2011
0.708366	-	land snail shell	17.17861	-88.677005	WGS84	Freiwald 2011
0.70838	-	snake bone	17.22489	-88.895270	WGS84	Freiwald 2011
0.708397	-	opossum	17.199729	-89.008765	WGS84	Freiwald 2011
0.708477	-	iguana (iguanidae)	17.086871	-89.141593	WGS84	Freiwald 2011
0.708527	-	toad (Bufonidae)	17.181858	-89.023310	WGS84	Freiwald 2011
0.708615	-	Anura bone	17.537348	-88.624032	WGS84	Freiwald 2011
0.708629	-	land snail shell	17.099538	-89.130343	WGS84	Freiwald 2011
0.708719	-	armadillo bone	17.086871	-89.141593	WGS84	Freiwald 2011
0.70882	-	rabbit (Sylvilagus)	17.297682	-88.80572	WGS84	Freiwald 2011
0.708912	-	iguana (iguanidae)	17.559868	-88.291196	WGS84	Freiwald 2011
0.708942	-	land snail shell	17.104529	-89.090040	WGS84	Freiwald 2011
0.709077	-	opossum	17.308564	-88.780109	WGS84	Freiwald 2011
0.710373	-	land snail shell	17.103659	-89.086864	WGS84	Freiwald 2011
0.710653	-	land snail shell	17.003968	-89.056142	WGS84	Freiwald 2011
0.711136	-	land snail shell	17.173726	-88.684095	WGS84	Freiwald 2011
0.711414	-	river snail shell	16.867018	-89.039116	WGS84	Freiwald 2011
0.711755	-	river snail shell	16.867018	-89.039116	WGS84	Freiwald 2011
0.713917	-	river snail shell	17.126107	-88.851322	WGS84	Freiwald 2011

0.71517	-	tree seed pod	17.055924	-88.580318	WGS84	Freiwald 2011
0.716212	-	toad (Bufonidae)	17.048941	-88.94818	WGS84	Freiwald 2011
0.716847	-	opossum (Didelphidae)	17.089852	-88.620838	WGS84	Freiwald 2011
0.724951	-	toad (Bufonidae)	16.992354	-88.96890	WGS84	Freiwald 2011
0.72552	-	Pine cone	16.992193	-88.938494	WGS84	Freiwald 2011
0.707394	-	terrestial shell	16.719983	-92.636278	WGS84	Freiwald 2011
0.707651	-	terrestial shell	16.719983	-92.636278	WGS84	Freiwald 2011
0.707747	-	terrestial shell	16.719983	-92.636278	WGS84	Freiwald 2011
0.706584	-	river snail shell	16.708325	-93.009840	WGS84	Freiwald 2011
0.707363	-	river snail shell	16.708325	-93.009840	WGS84	Freiwald 2011
0.707392	-	river snail shell	16.708325	-93.009840	WGS84	Freiwald 2011
0.707481	-	river snail shell	16.708325	-93.009840	WGS84	Freiwald 2011
0.707177	-	river snail shell	16.501132	-93.363339	WGS84	Freiwald 2011
0.707201	-	land snail shell	16.501132	-93.363339	WGS84	Freiwald 2011
0.708188	-	land snail shell	16.920833	-90.976665	WGS84	Freiwald 2011
0.708222	-	river snail shell	16.920833	-90.976665	WGS84	Freiwald 2011
0.707727	-	river snail shell	16.836665	-91.343893	WGS84	Freiwald 2011
0.707701	-	river snail shell	16.836665	-91.343893	WGS84	Freiwald 2011
0.704628	-	cow tooth enamel	14.900528	-92.392602	WGS84	Freiwald 2011
0.704663	-	caprinae tooth enamel	14.901045	-92.166113	WGS84	Freiwald 2011
0.704771	-	cow rib	14.889595	-92.479853	WGS84	Freiwald 2011
0.7051	-	terrestial shell	14.91849	-92.484032	WGS84	Freiwald 2011
0.707213	-	dog tooth enamel	15.698122	-93.210768	WGS84	Freiwald 2011
0.70768	-	dog bone	15.698122	-93.210768	WGS84	Freiwald 2011
0.707759	-	dog bone	15.698122	-93.210768	WGS84	Freiwald 2011
0.7082	-	bioavailable	16.920833	-90.976665	WGS84	Freiwald 2011
0.7077	-	bioavailable	16.836665	-91.343893	WGS84	Freiwald 2011
0.70438	-	KJ11-4	14.632279	-90.548528	WGS84	Wright et al. 2010
0.70432	-	KJ34-4	14.632279	-90.548528	WGS84	Wright et al. 2010
0.706	-	KJ24-4	14.632279	-90.548528	WGS84	Wright et al. 2010
0.70419	-	KJ21-2	14.632279	-90.548528	WGS84	Wright et al. 2010
0.70454	-	KJ33-2	14.632279	-90.548528	WGS84	Wright et al. 2010
0.7054	-	KJ41-2	14.632279	-90.548528	WGS84	Wright et al. 2010
0.70421	-	KJ42-2	14.632279	-90.548528	WGS84	Wright et al. 2010
0.70473	-	KJ43-2	14.632279	-90.548528	WGS84	Wright et al. 2010
0.70508	-	KJ44-2	14.632279	-90.548528	WGS84	Wright et al. 2010
0.70438	-	KJ45-2	14.632279	-90.548528	WGS84	Wright et al. 2010
0.70519	-	KJ46-2	14.632279	-90.548528	WGS84	Wright et al. 2010
0.70595	-	KJ46-4	14.632279	-90.548528	WGS84	Wright et al. 2010
0.70439	-	KJ47-2	14.632279	-90.548528	WGS84	Wright et al. 2010
0.7044	-	KJ48-2	14.632279	-90.548528	WGS84	Wright et al. 2010
0.7105	-	KJ49-2	14.632279	-90.548528	WGS84	Wright et al. 2010

0.70429	-	KJ50-2	14.632279	-90.548528	WGS84	Wright et al. 2010
0.70485	-	KJ51-2	14.632279	-90.548528	WGS84	Wright et al. 2010
0.70465	-	KJ52-2	14.632279	-90.548528	WGS84	Wright et al. 2010
0.70492	-	KJ52-4	14.632279	-90.548528	WGS84	Wright et al. 2010
0.7047	-	KJ53-2	14.632279	-90.548528	WGS84	Wright et al. 2010
0.70519	-	KJ54-2	14.632279	-90.548528	WGS84	Wright et al. 2010
0.7057	-	KJ54-4	14.632279	-90.548528	WGS84	Wright et al. 2010
0.70694	-	KJ55-2	14.632279	-90.548528	WGS84	Wright et al. 2010
0.70599	-	KJ56-2	14.632279	-90.548528	WGS84	Wright et al. 2010
0.70439	-	KJ18-4	14.632279	-90.548528	WGS84	Wright et al. 2010
0.7046	-	KJ32-4	14.632279	-90.548528	WGS84	Wright et al. 2010
0.70814	-	Human_tooth_nsp	17.221944	-89.622778	WGS84	Wright et al. 2012
0.70792	-	Human_tooth_nsp	17.221944	-89.622778	WGS84	Wright et al. 2012
0.70794	-	Human_tooth_nsp	17.221944	-89.622778	WGS84	Wright et al. 2012
0.70827	-	Human_tooth_nsp	17.221944	-89.622778	WGS84	Wright et al. 2012
0.70789	-	Human_tooth_nsp	17.221944	-89.622778	WGS84	Wright et al. 2012
0.70811	-	Human_tooth_nsp	17.221944	-89.622778	WGS84	Wright et al. 2012
0.70814	-	Human_tooth_nsp	17.221944	-89.622778	WGS84	Wright et al. 2012
0.70848	-	Human_tooth_nsp	17.221944	-89.622778	WGS84	Wright et al. 2012
0.70789	-	Human_tooth_nsp	17.221944	-89.622778	WGS84	Wright et al. 2012
0.70789	-	Human_tooth_nsp	17.221944	-89.622778	WGS84	Wright et al. 2012
0.70775	-	Human_tooth_nsp	17.221944	-89.622778	WGS84	Wright et al. 2012
0.70815	-	Human_tooth_nsp	17.221944	-89.622778	WGS84	Wright et al. 2012
0.70819	-	Human_tooth_nsp	17.221944	-89.622778	WGS84	Wright et al. 2012
0.70841	-	Human_tooth_nsp	17.221944	-89.622778	WGS84	Wright et al. 2012
0.70825	-	Human_tooth_nsp	17.221944	-89.622778	WGS84	Wright et al. 2012
0.70766	-	Human_tooth_nsp	17.221944	-89.622778	WGS84	Wright et al. 2012
0.70808	-	Human_tooth_nsp	17.221944	-89.622778	WGS84	Wright et al. 2012
0.70818	-	Human_tooth_nsp	17.221944	-89.622778	WGS84	Wright et al. 2012
0.70806	-	Human_tooth_nsp	17.221944	-89.622778	WGS84	Wright et al. 2012
0.7083	-	Human_tooth_nsp	17.221944	-89.622778	WGS84	Wright et al. 2012
0.70802	-	Human_tooth_nsp	17.221944	-89.622778	WGS84	Wright et al. 2012
0.70797	-	Human_tooth_nsp	17.221944	-89.622778	WGS84	Wright et al. 2012
0.70829	-	Human_tooth_nsp	17.221944	-89.622778	WGS84	Wright et al. 2012
0.70786	-	Human_tooth_nsp	17.221944	-89.622778	WGS84	Wright et al. 2012
0.70798	-	Human_tooth_nsp	17.221944	-89.622778	WGS84	Wright et al. 2012
0.70798	-	Human_tooth_nsp	17.221944	-89.622778	WGS84	Wright et al. 2012
0.70822	-	Human_tooth_nsp	17.221944	-89.622778	WGS84	Wright et al. 2012
0.70828	-	Human_tooth_nsp	17.221944	-89.622778	WGS84	Wright et al. 2012
0.70415	-	Human_tooth_nsp	17.221944	-89.622778	WGS84	Wright et al. 2012
0.70801	-	Human_tooth_nsp	17.221944	-89.622778	WGS84	Wright et al. 2012
0.70779	-	Human_tooth_nsp	17.221944	-89.622778	WGS84	Wright et al. 2012
0.70813	-	Human_tooth_nsp	17.221944	-89.622778	WGS84	Wright et al. 2012

0.70753	-	Human_tooth_nsp	17.221944	-89.622778	WGS84	Wright et al. 2012
0.70682	-	Human_tooth_nsp	17.221944	-89.622778	WGS84	Wright et al. 2012
0.70835	-	Human_tooth_nsp	17.221944	-89.622778	WGS84	Wright et al. 2012
0.70752	-	Human_tooth_nsp	17.221944	-89.622778	WGS84	Wright et al. 2012
0.7083	-	Human_tooth_nsp	17.221944	-89.622778	WGS84	Wright et al. 2012
0.7079	-	Human_tooth_nsp	17.221944	-89.622778	WGS84	Wright et al. 2012
0.7083	-	Human_tooth_nsp	17.221944	-89.622778	WGS84	Wright et al. 2012
0.70831	-	Human_tooth_nsp	17.221944	-89.622778	WGS84	Wright et al. 2012
0.70799	-	Human_tooth_nsp	17.221944	-89.622778	WGS84	Wright et al. 2012
0.70836	-	Human_tooth_nsp	17.221944	-89.622778	WGS84	Wright et al. 2012
0.70813	-	Human_tooth_nsp	17.221944	-89.622778	WGS84	Wright et al. 2012
0.71626	-	Human_tooth_nsp	17.221944	-89.622778	WGS84	Wright et al. 2012
0.70821	-	Human_tooth_nsp	17.221944	-89.622778	WGS84	Wright et al. 2012
0.70847	-	Human_tooth_nsp	17.221944	-89.622778	WGS84	Wright et al. 2012
0.70832	-	Human_tooth_nsp	17.221944	-89.622778	WGS84	Wright et al. 2012
0.70831	-	Human_tooth_nsp	17.221944	-89.622778	WGS84	Wright et al. 2012
0.70805	-	Human_tooth_nsp	17.221944	-89.622778	WGS84	Wright et al. 2012
0.70819	-	Human_tooth_nsp	17.221944	-89.622778	WGS84	Wright et al. 2012
0.70828	-	Human_tooth_nsp	17.221944	-89.622778	WGS84	Wright et al. 2012
0.70751	-	Human_tooth_nsp	17.221944	-89.622778	WGS84	Wright et al. 2012
0.70824	-	Human_tooth_nsp	17.221944	-89.622778	WGS84	Wright et al. 2012
0.70804	-	Human_tooth_nsp	17.221944	-89.622778	WGS84	Wright et al. 2012
0.70811	-	Human_tooth_nsp	17.221944	-89.622778	WGS84	Wright et al. 2012
0.70822	-	Human_tooth_nsp	17.221944	-89.622778	WGS84	Wright et al. 2012
0.70795	-	Human_tooth_nsp	17.221944	-89.622778	WGS84	Wright et al. 2012
0.70804	-	Human_tooth_nsp	17.221944	-89.622778	WGS84	Wright et al. 2012
0.70819	-	Human_tooth_nsp	17.221944	-89.622778	WGS84	Wright et al. 2012
0.708	-	Human_tooth_nsp	17.221944	-89.622778	WGS84	Wright et al. 2012
0.7085	-	Human_tooth_nsp	17.221944	-89.622778	WGS84	Wright et al. 2012
0.70825	-	Human_tooth_nsp	17.221944	-89.622778	WGS84	Wright et al. 2012
0.70822	-	Human_tooth_nsp	17.221944	-89.622778	WGS84	Wright et al. 2012
0.70809	-	Human_tooth_nsp	17.221944	-89.622778	WGS84	Wright et al. 2012
0.70797	-	Human_tooth_nsp	17.221944	-89.622778	WGS84	Wright et al. 2012
0.708	-	Human_tooth_nsp	17.221944	-89.622778	WGS84	Wright et al. 2012
0.7077	-	Human_tooth_nsp	17.221944	-89.622778	WGS84	Wright et al. 2012
0.70832	-	Human_tooth_nsp	17.221944	-89.622778	WGS84	Wright et al. 2012
0.70823	-	Human_tooth_nsp	17.221944	-89.622778	WGS84	Wright et al. 2012
0.7089	-	Human_tooth_nsp	17.221944	-89.622778	WGS84	Wright et al. 2012
0.7081	-	Human_tooth_nsp	17.221944	-89.622778	WGS84	Wright et al. 2012
0.70835	-	Human_tooth_nsp	17.221944	-89.622778	WGS84	Wright et al. 2012
0.70779	-	Human_tooth_nsp	17.221944	-89.622778	WGS84	Wright et al. 2012
0.7081	-	Human_tooth_nsp	17.221944	-89.622778	WGS84	Wright et al. 2012
0.70809	-	Human_tooth_nsp	17.221944	-89.622778	WGS84	Wright et al. 2012

0.70901	-	Human_tooth_nsp	17.221944	-89.622778	WGS84	Wright et al. 2012
0.70772	-	Human_tooth_nsp	17.221944	-89.622778	WGS84	Wright et al. 2012
0.70826	-	Human_tooth_nsp	17.221944	-89.622778	WGS84	Wright et al. 2012
0.7085	-	Human_tooth_nsp	17.221944	-89.622778	WGS84	Wright et al. 2012
0.70822	-	Human_tooth_nsp	17.221944	-89.622778	WGS84	Wright et al. 2012
0.70802	-	Human_tooth_nsp	17.221944	-89.622778	WGS84	Wright et al. 2012
0.7082	-	Human_tooth_nsp	17.221944	-89.622778	WGS84	Wright et al. 2012
0.70836	-	Human_tooth_nsp	17.221944	-89.622778	WGS84	Wright et al. 2012
0.70651	-	Human_tooth_nsp	17.221944	-89.622778	WGS84	Wright et al. 2012
0.70803	-	Human_tooth_nsp	17.221944	-89.622778	WGS84	Wright et al. 2012
0.70812	-	Human_tooth_nsp	17.221944	-89.622778	WGS84	Wright et al. 2012
0.70837	-	Human_tooth_nsp	17.221944	-89.622778	WGS84	Wright et al. 2012
0.70774	-	Human_tooth_nsp	17.221944	-89.622778	WGS84	Wright et al. 2012
0.70796	-	Human_tooth_nsp	17.221944	-89.622778	WGS84	Wright et al. 2012
0.70802	-	Human_tooth_nsp	17.221944	-89.622778	WGS84	Wright et al. 2012
0.70803	-	Human_tooth_nsp	17.221944	-89.622778	WGS84	Wright et al. 2012
0.7081	-	Human_tooth_nsp	17.221944	-89.622778	WGS84	Wright et al. 2012
0.70417	-	Human_tooth_nsp	17.221944	-89.622778	WGS84	Wright et al. 2012
0.70796	-	Human_tooth_nsp	17.221944	-89.622778	WGS84	Wright et al. 2012
0.70406	-	Human_tooth_nsp	17.221944	-89.622778	WGS84	Wright et al. 2012
0.70822	-	Human_tooth_nsp	17.221944	-89.622778	WGS84	Wright et al. 2012
0.70822	-	Human_tooth_nsp	17.221944	-89.622778	WGS84	Wright et al. 2012
0.70804	-	Ground/Surface water	21.57	-88.07	WGS84	Hodell et al. 2004
0.70841	-	Ground/Surface water	21.56	-88.18	WGS84	Hodell et al. 2004
0.70869	-	Ground/Surface water	21.44	-88.63	WGS84	Hodell et al. 2004
0.70854	-	Ground/Surface water	21.15	-89.68	WGS84	Hodell et al. 2004
0.70847	-	Ground/Surface water	21.09	-89.6	WGS84	Hodell et al. 2004
0.70895	-	plant	21.09	-89.6	WGS84	Hodell et al. 2004
0.70905	-	rock	21.09	-89.6	WGS84	Hodell et al. 2004
0.70912	-	soil	21.09	-89.6	WGS84	Hodell et al. 2004
0.70875	-	Ground/Surface water	20.67	-88.73	WGS84	Hodell et al. 2004
0.70806	-	Ground/Surface water	20.7	-89.36	WGS84	Hodell et al. 2004
0.70806	-	Ground/Surface water	20.66	-88.55	WGS84	Hodell et al. 2004
0.70811	-	Ground/Surface water	20.66	-88.8	WGS84	Hodell et al. 2004
0.70847	-	plant	20.65	-87.65	WGS84	Hodell et al. 2004
0.70812	-	Ground/Surface water	20.65	-87.65	WGS84	Hodell et al. 2004

0.70815	-	Ground/Surface water	20.64	-87.56	WGS84	Hodell et al. 2004
0.7082	-	Ground/Surface water	20.64	-87.56	WGS84	Hodell et al. 2004
0.70877	-	plant	20.59	-90.02	WGS84	Hodell et al. 2004
0.70856	-	soil	20.59	-90.02	WGS84	Hodell et al. 2004
0.70792	-	Ground/Surface water	20.59	-90.02	WGS84	Hodell et al. 2004
0.70896	-	Ground/Surface water	20.53	-87.22	WGS84	Hodell et al. 2004
0.70847	-	Ground/Surface water	20.52	-87.65	WGS84	Hodell et al. 2004
0.7087	-	plant	20.52	-87.65	WGS84	Hodell et al. 2004
0.70888	-	soil	20.52	-87.65	WGS84	Hodell et al. 2004
0.70809	-	Ground/Surface water	20.52	-87.65	WGS84	Hodell et al. 2004
0.7083	-	Ground/Surface water	20.27	-87.49	WGS84	Hodell et al. 2004
0.70917	-	rock	20.27	-87.49	WGS84	Hodell et al. 2004
0.7091	-	plant	20.27	-89.44	WGS84	Hodell et al. 2004
0.70901	-	rock	20.27	-89.44	WGS84	Hodell et al. 2004
0.70921	-	soil	20.27	-89.44	WGS84	Hodell et al. 2004
0.70839	-	Ground/Surface water	20.2	-87.5	WGS84	Hodell et al. 2004
0.70914	-	rock	20.2	-87.5	WGS84	Hodell et al. 2004
0.70775	-	Ground/Surface water	19.88	-88.77	WGS84	Hodell et al. 2004
0.70845	-	rock	18.69	-88.38	WGS84	Hodell et al. 2004
0.70763	-	Ground/Surface water	18.69	-88.38	WGS84	Hodell et al. 2004
0.70766	-	Ground/Surface water	18.69	-88.38	WGS84	Hodell et al. 2004
0.70767	-	Ground/Surface water	18.63	-88.46	WGS84	Hodell et al. 2004
0.70406	-	Ground/Surface water	18.42	-95.11	WGS84	Hodell et al. 2004
0.7078	-	shells	17.49	-92.05	WGS84	Hodell et al. 2004
0.70778	-	rock	17.4	-89.64	WGS84	Hodell et al. 2004
0.70798	-	plant	17.4	-89.64	WGS84	Hodell et al. 2004
0.70794	-	Ground/Surface water	17.39	-89.63	WGS84	Hodell et al. 2004
0.70766	-	rock	17.23	-89.15	WGS84	Hodell et al. 2004
0.70792	-	Ground/Surface water	17.23	-89.15	WGS84	Hodell et al. 2004
0.70802	-	Ground/Surface water	17.23	-89.6	WGS84	Hodell et al. 2004
0.70813	-	rock	17.23	-89.6	WGS84	Hodell et al. 2004
0.70784	-	plant	17.23	-89.6	WGS84	Hodell et al. 2004

0.70779	-	rock	17.22	-89.61	WGS84	Hodell et al. 2004
0.70791	-	plant	17.17	-89.06	WGS84	Hodell et al. 2004
0.70792	-	plant	17.17	-89.06	WGS84	Hodell et al. 2004
0.70778	-	rock	17.17	-89.06	WGS84	Hodell et al. 2004
0.70797	-	soil	17.17	-89.06	WGS84	Hodell et al. 2004
0.70778	-	rock	17.11	-89.68	WGS84	Hodell et al. 2004
0.71192	-	Ground/Surface water	17.09	-88.67	WGS84	Hodell et al. 2004
0.70757	-	Ground/Surface water	17.06	-89.4	WGS84	Hodell et al. 2004
0.70783	-	plant	17.06	-89.4	WGS84	Hodell et al. 2004
0.70772	-	rock	17.06	-89.4	WGS84	Hodell et al. 2004
0.70809	-	soil	17.06	-89.4	WGS84	Hodell et al. 2004
0.71514	-	Ground/Surface water	17.04	-88.98	WGS84	Hodell et al. 2004
0.70776	-	rock	17	-89.73	WGS84	Hodell et al. 2004
0.70739	-	Ground/Surface water	17	-89.73	WGS84	Hodell et al. 2004
0.70745	-	Ground/Surface water	17	-89.73	WGS84	Hodell et al. 2004
0.70767	-	rock	16.99	-89.69	WGS84	Hodell et al. 2004
0.70747	-	Ground/Surface water	16.99	-90.05	WGS84	Hodell et al. 2004
0.70783	-	Ground/Surface water	16.99	-89.69	WGS84	Hodell et al. 2004
0.70791	-	replicate	16.99	-89.69	WGS84	Hodell et al. 2004
0.70745	-	Ground/Surface water	16.98	-89.68	WGS84	Hodell et al. 2004
0.70757	-	plant	16.98	-89.68	WGS84	Hodell et al. 2004
0.70756	-	plant	16.98	-89.68	WGS84	Hodell et al. 2004
0.70775	-	soil	16.98	-89.68	WGS84	Hodell et al. 2004
0.70755	-	rock	16.98	-89.68	WGS84	Hodell et al. 2004
0.70749	-	Ground/Surface water	16.98	-89.68	WGS84	Hodell et al. 2004
0.70755	-	Ground/Surface water	16.97	-89.69	WGS84	Hodell et al. 2004
0.70779	-	rock	16.97	-89.69	WGS84	Hodell et al. 2004
0.70796	-	Ground/Surface water	16.95	-90.37	WGS84	Hodell et al. 2004
0.70824	-	Ground/Surface water	16.95	-90.37	WGS84	Hodell et al. 2004
0.70783	-	Ground/Surface water	16.92	-89.89	WGS84	Hodell et al. 2004
0.7079	-	Ground/Surface water	16.92	-89.89	WGS84	Hodell et al. 2004
0.70749	-	Ground/Surface water	16.92	-89.84	WGS84	Hodell et al. 2004
0.70752	-	Ground/Surface	16.92	-89.84	WGS84	Hodell et al. 2004

		water				
0.70833	-	Ground/Surface water	16.92	-90.42	WGS84	Hodell et al. 2004
0.70751	-	Ground/Surface water	16.92	-89.82	WGS84	Hodell et al. 2004
0.70746	-	Ground/Surface water	16.92	-89.83	WGS84	Hodell et al. 2004
0.70741	-	rock	16.91	-89.89	WGS84	Hodell et al. 2004
0.70745	-	Ground/Surface water	16.9	-89.77	WGS84	Hodell et al. 2004
0.70748	-	Ground/Surface water	16.9	-89.76	WGS84	Hodell et al. 2004
0.70744	-	Ground/Surface water	16.9	-89.78	WGS84	Hodell et al. 2004
0.70748	-	Ground/Surface water	16.9	-89.78	WGS84	Hodell et al. 2004
0.71275	-	Ground/Surface water	16.72	-88.42	WGS84	Hodell et al. 2004
0.70814	-	Ground/Surface water	16.7	-89.75	WGS84	Hodell et al. 2004
0.70737	-	rock	16.67	-89.71	WGS84	Hodell et al. 2004
0.70735	-	Ground/Surface water	16.64	-90.18	WGS84	Hodell et al. 2004
0.70778	-	Ground/Surface water	16.63	-89.6	WGS84	Hodell et al. 2004
0.70791	-	plant	16.63	-89.6	WGS84	Hodell et al. 2004
0.70777	-	rock	16.63	-89.6	WGS84	Hodell et al. 2004
0.70777	-	rock	16.63	-89.6	WGS84	Hodell et al. 2004
0.70746	-	Ground/Surface water	16.53	-90.19	WGS84	Hodell et al. 2004
0.70815	-	Ground/Surface water	16.47	-88.65	WGS84	Hodell et al. 2004
0.70751	-	Ground/Surface water	16.41	-90.11	WGS84	Hodell et al. 2004
0.70745	-	rock	16.39	-89.44	WGS84	Hodell et al. 2004
0.70764	-	Ground/Surface water	16.39	-89.44	WGS84	Hodell et al. 2004
0.70777	-	plant	16.39	-89.44	WGS84	Hodell et al. 2004
0.70777	-	rock	16.36	-90.11	WGS84	Hodell et al. 2004
0.7078	-	plant	16.36	-90.11	WGS84	Hodell et al. 2004
0.70764	-	Ground/Surface water	16.23	-89.1	WGS84	Hodell et al. 2004
0.70749	-	Ground/Surface water	16.18	-89.2	WGS84	Hodell et al. 2004
0.7079	-	rock	16.17	-89.41	WGS84	Hodell et al. 2004
0.70764	-	plant	16.15	-89.4	WGS84	Hodell et al. 2004
0.70693	-	Ground/Surface water	16.15	-89.4	WGS84	Hodell et al. 2004
0.70821	-	Ground/Surface	16.14	-90.18	WGS84	Hodell et al. 2004

		water				
0.7075	-	Ground/Surface water	16	-90.15	WGS84	Hodell et al. 2004
0.70742	-	Ground/Surface water	15.95	-89.24	WGS84	Hodell et al. 2004
0.70745	-	plant	15.95	-89.24	WGS84	Hodell et al. 2004
0.70745	-	Ground/Surface water	15.88	-90.19	WGS84	Hodell et al. 2004
0.70733	-	rock	15.88	-90.19	WGS84	Hodell et al. 2004
0.7075	-	plant	15.88	-90.19	WGS84	Hodell et al. 2004
0.70748	-	Ground/Surface water	15.83	-90.29	WGS84	Hodell et al. 2004
0.70773	-	rock	15.83	-90.29	WGS84	Hodell et al. 2004
0.7079	-	plant	15.73	-89.08	WGS84	Hodell et al. 2004
0.70777	-	Ground/Surface water	15.73	-89.08	WGS84	Hodell et al. 2004
0.70737	-	rock	15.68	-90.41	WGS84	Hodell et al. 2004
0.70767	-	plant	15.68	-90.41	WGS84	Hodell et al. 2004
0.70737	-	Ground/Surface water	15.68	-90.41	WGS84	Hodell et al. 2004
0.70788	-	Ground/Surface water	15.66	-89	WGS84	Hodell et al. 2004
0.70782	-	plant	15.54	-88.84	WGS84	Hodell et al. 2004
0.7075	-	Ground/Surface water	15.47	-90.37	WGS84	Hodell et al. 2004
0.70789	-	Ground/Surface water	15.42	-89.12	WGS84	Hodell et al. 2004
0.70719	-	Ground/Surface water	15.36	-90.48	WGS84	Hodell et al. 2004
0.70789	-	rock	15.36	-90.72	WGS84	Hodell et al. 2004
0.70791	-	rainfall	15.36	-90.72	WGS84	Hodell et al. 2004
0.7078	-	plant	15.36	-90.72	WGS84	Hodell et al. 2004
0.70774	-	Ground/Surface water	15.35	-90.66	WGS84	Hodell et al. 2004
0.70751	-	Ground/Surface water	15.34	-90.89	WGS84	Hodell et al. 2004
0.70459	-	rock	15.34	-90.89	WGS84	Hodell et al. 2004
0.70748	-	Ground/Surface water	15.34	-91.03	WGS84	Hodell et al. 2004
0.70726	-	plant	15.34	-91.03	WGS84	Hodell et al. 2004
0.70751	-	Ground/Surface water	15.33	-91	WGS84	Hodell et al. 2004
0.7169	-	rock	15.33	-91	WGS84	Hodell et al. 2004
0.70835	-	rock	15.32	-91.05	WGS84	Hodell et al. 2004
0.70736	-	rock	15.31	-91.06	WGS84	Hodell et al. 2004
0.7063	-	plant	15.31	-91.06	WGS84	Hodell et al. 2004
0.70727	-	plant	15.28	-89.07	WGS84	Hodell et al. 2004
0.70715	-	Ground/Surface	15.27	-91.12	WGS84	Hodell et al. 2004

		water				
0.70743	-	plant	15.27	-91.12	WGS84	Hodell et al. 2004
0.70631	-	plant	15.27	-91.12	WGS84	Hodell et al. 2004
0.71592	-	rock	15.27	-91.12	WGS84	Hodell et al. 2004
0.70793	-	plant	15.24	-91.15	WGS84	Hodell et al. 2004
0.70988	-	rock	15.22	-91.18	WGS84	Hodell et al. 2004
0.70655	-	plant	15.15	-89.33	WGS84	Hodell et al. 2004
0.70632	-	Ground/Surface water	15.03	-89.59	WGS84	Hodell et al. 2004
0.70621	-	plant	15.03	-89.59	WGS84	Hodell et al. 2004
0.70469	-	Ground/Surface water	14.97	-91.11	WGS84	Hodell et al. 2004
0.70431	-	plant	14.97	-91.11	WGS84	Hodell et al. 2004
0.70707	-	Ground/Surface water	14.95	-89.54	WGS84	Hodell et al. 2004
0.70663	-	rock	14.94	-89.83	WGS84	Hodell et al. 2004
0.70417	-	ash	14.93	-89.97	WGS84	Hodell et al. 2004
0.70714	-	Ground/Surface water	14.92	-89.97	WGS84	Hodell et al. 2004
0.70604	-	plant	14.92	-89.97	WGS84	Hodell et al. 2004
0.7058	-	rock	14.86	-89.22	WGS84	Hodell et al. 2004
0.70711	-	Ground/Surface water	14.86	-90.09	WGS84	Hodell et al. 2004
0.70725	-	Ground/Surface water	14.86	-89.32	WGS84	Hodell et al. 2004
0.7053	-	rock	14.85	-89.52	WGS84	Hodell et al. 2004
0.70461	-	plant	14.85	-89.52	WGS84	Hodell et al. 2004
0.72017	-	plant	14.84	-89.35	WGS84	Hodell et al. 2004
0.70633	-	Ground/Surface water	14.84	-89.15	WGS84	Hodell et al. 2004
0.70622	-	plant	14.84	-89.15	WGS84	Hodell et al. 2004
0.70639	-	plant	14.84	-89.15	WGS84	Hodell et al. 2004
0.70681	-	Ground/Surface water	14.83	-89.14	WGS84	Hodell et al. 2004
0.70644	-	Ground/Surface water	14.83	-89.14	WGS84	Hodell et al. 2004
0.7053	-	rock	14.83	-90.14	WGS84	Hodell et al. 2004
0.70528	-	rock	14.83	-90.14	WGS84	Hodell et al. 2004
0.70499	-	rock	14.8	-91.11	WGS84	Hodell et al. 2004
0.70607	-	plant	14.8	-90.27	WGS84	Hodell et al. 2004
0.70689	-	rock	14.74	-89.47	WGS84	Hodell et al. 2004
0.70553	-	plant	14.74	-89.47	WGS84	Hodell et al. 2004
0.70401	-	plant	14.7	-91.1	WGS84	Hodell et al. 2004
0.7039	-	rock	14.66	-91.2	WGS84	Hodell et al. 2004
0.70401	-	plant	14.66	-91.2	WGS84	Hodell et al. 2004
0.70421	-	Ground/Surface	14.64	-91.23	WGS84	Hodell et al. 2004

		water				
0.70419	-	Ground/Surface water	14.64	-91.23	WGS84	Hodell et al. 2004
0.70418	-	Ground/Surface water	14.64	-91.23	WGS84	Hodell et al. 2004
0.70417	-	Ground/Surface water	14.64	-91.23	WGS84	Hodell et al. 2004
0.70429	-	Ground/Surface water	14.64	-91.23	WGS84	Hodell et al. 2004
0.70418	-	plant	14.64	-91.23	WGS84	Hodell et al. 2004
0.70429	-	Ground/Surface water	14.55	-91.13	WGS84	Hodell et al. 2004
0.70428	-	plant	14.55	-91.13	WGS84	Hodell et al. 2004
0.70406	-	plant	14.55	-91.13	WGS84	Hodell et al. 2004
0.70392	-	ash	14.53	-90.77	WGS84	Hodell et al. 2004
0.70396	-	plant	14.53	-90.77	WGS84	Hodell et al. 2004
0.70492	-	Ground/Surface water	14.45	-90.53	WGS84	Hodell et al. 2004
0.70414	-	Ground/Surface water	14.38	-91.02	WGS84	Hodell et al. 2004
0.70395	-	plant	14.38	-91.02	WGS84	Hodell et al. 2004
0.70422	-	Ground/Surface water	14.37	-90.81	WGS84	Hodell et al. 2004
0.70414	-	Ground/Surface water	14.33	-91	WGS84	Hodell et al. 2004
0.70402	-	Ground/Surface water	14.3	-91.04	WGS84	Hodell et al. 2004
0.70407	-	Ground/Surface water	14.29	-90.97	WGS84	Hodell et al. 2004
0.70404	-	Ground/Surface water	14.27	-90.9	WGS84	Hodell et al. 2004
0.704	-	plant	14.27	-90.9	WGS84	Hodell et al. 2004
0.70406	-	Ground/Surface water	14.2	-90.71	WGS84	Hodell et al. 2004
0.70413	-	Ground/Surface water	14.14	-90.66	WGS84	Hodell et al. 2004
0.704	-	plant	14.14	-90.66	WGS84	Hodell et al. 2004
0.70406	-	Ground/Surface water	14.08	-91.05	WGS84	Hodell et al. 2004
0.70389	-	Ground/Surface water	14.07	-90.38	WGS84	Hodell et al. 2004
0.70429	-	Ground/Surface water	14.05	-90.34	WGS84	Hodell et al. 2004
0.7038	-	rock	14.05	-90.34	WGS84	Hodell et al. 2004
0.70408	-	plant	14.05	-90.34	WGS84	Hodell et al. 2004
0.70457	-	plant	13.93	-91.18	WGS84	Hodell et al. 2004
0.70888	-	Ground/Surface water	13.93	-91.16	WGS84	Hodell et al. 2004
0.70871	-	plant	13.93	-91.16	WGS84	Hodell et al. 2004

0.70905	-	limestone	21.091	-89.597	WGS84	Hodell et al. 2004
0.70847	-	Ground/Surface water	21.091	-89.597	WGS84	Hodell et al. 2004
0.70895	-	plant	21.091	-89.597	WGS84	Hodell et al. 2004
0.70912	-	soil	21.091	-89.597	WGS84	Hodell et al. 2004
0.70901	-	limestone	20.272	-89.436	WGS84	Hodell et al. 2004
0.7091	-	plant	20.272	-89.436	WGS84	Hodell et al. 2004
0.70921	-	soil	20.272	-89.436	WGS84	Hodell et al. 2004
0.70813	-	limestone	17.229	-89.602	WGS84	Hodell et al. 2004
0.70802	-	Ground/Surface water	17.229	-89.602	WGS84	Hodell et al. 2004
0.70784	-	plant	17.229	-89.602	WGS84	Hodell et al. 2004
0.70778	-	limestone	17.167	-89.061	WGS84	Hodell et al. 2004
0.70791	-	plant	17.167	-89.061	WGS84	Hodell et al. 2004
0.70792	-	plant	17.167	-89.061	WGS84	Hodell et al. 2004
0.70797	-	soil	17.167	-89.061	WGS84	Hodell et al. 2004
0.70772	-	limestone	17.055	-89.395	WGS84	Hodell et al. 2004
0.70757	-	Ground/Surface water	17.055	-89.395	WGS84	Hodell et al. 2004
0.70783	-	plant	17.055	-89.395	WGS84	Hodell et al. 2004
0.70809	-	soil	17.055	-89.395	WGS84	Hodell et al. 2004
0.70755	-	gypsum	16.977	-89.675	WGS84	Hodell et al. 2004
0.70745	-	Ground/Surface water	16.977	-89.675	WGS84	Hodell et al. 2004
0.70749	-	Ground/Surface water	16.977	-89.675	WGS84	Hodell et al. 2004
0.70757	-	plant	16.977	-89.675	WGS84	Hodell et al. 2004
0.70756	-	plant	16.977	-89.675	WGS84	Hodell et al. 2004
0.70775	-	soil	16.977	-89.675	WGS84	Hodell et al. 2004
0.70777	-	limestone	16.631	-89.604	WGS84	Hodell et al. 2004
0.70778	-	Ground/Surface water	16.631	-89.604	WGS84	Hodell et al. 2004
0.70791	-	plant	16.631	-89.604	WGS84	Hodell et al. 2004
0.70745	-	limestone	16.394	-89.444	WGS84	Hodell et al. 2004
0.70764	-	Ground/Surface water	16.394	-89.444	WGS84	Hodell et al. 2004
0.70777	-	plant	16.394	-89.444	WGS84	Hodell et al. 2004
0.70789	-	limestone	15.357	-90.723	WGS84	Hodell et al. 2004
0.7078	-	plant	15.357	-90.723	WGS84	Hodell et al. 2004
0.70736	-	limestone	15.307	-91.059	WGS84	Hodell et al. 2004
0.7063	-	plant	15.307	-91.059	WGS84	Hodell et al. 2004
0.7053	-	volcanic	14.851	-89.518	WGS84	Hodell et al. 2004
0.70461	-	plant	14.851	-89.518	WGS84	Hodell et al. 2004
0.70689	-	rock	14.736	-89.472	WGS84	Hodell et al. 2004
0.70553	-	plant	14.736	-89.472	WGS84	Hodell et al. 2004

0.70417	-	ash	14.926	-89.968	WGS84	Hodell et al. 2004
0.70604	-	plant	14.922	-89.966	WGS84	Hodell et al. 2004
0.70392	-	ash	14.53	-90.768	WGS84	Hodell et al. 2004
0.70396	-	plant	14.53	-90.768	WGS84	Hodell et al. 2004
0.7038	-	volcanic	14.053	-90.339	WGS84	Hodell et al. 2004
0.70408	-	plant	14.053	-90.339	WGS84	Hodell et al. 2004
0.7039	-	volcanic	14.662	-91.196	WGS84	Hodell et al. 2004
0.70401	-	plant	14.662	-91.196	WGS84	Hodell et al. 2004
0.7089	-	Tapir	21.091626	-89.595612	WGS84	Thornton 2011
0.7089	-	Peccary	21.091626	-89.595612	WGS84	Thornton 2011
0.7082	-	White-tailed deer	18.0805	-88.2971	WGS84	Thornton 2011
0.7083	-	White-tailed deer	18.0805	-88.2971	WGS84	Thornton 2011
0.7092	-	White-tailed deer	17.764207	-88.652233	WGS84	Thornton 2011
0.7094	-	White-tailed deer	17.764207	-88.652233	WGS84	Thornton 2011
0.7083	-	White-tailed deer	17.764207	-88.652233	WGS84	Thornton 2011
0.7074	-	White-tailed deer	17.764207	-88.652233	WGS84	Thornton 2011
0.7074	-	White-tailed deer	17.764207	-88.652233	WGS84	Thornton 2011
0.7084	-	White-tailed deer	17.764207	-88.652233	WGS84	Thornton 2011
0.7093	-	White-tailed deer	17.764207	-88.652233	WGS84	Thornton 2011
0.7091	-	White-tailed deer	17.764207	-88.652233	WGS84	Thornton 2011
0.7084	-	White-tailed deer	17.764207	-88.652233	WGS84	Thornton 2011
0.7084	-	White-tailed deer	17.764207	-88.652233	WGS84	Thornton 2011
0.7084	-	White-tailed deer	17.027778	-89.075278	WGS84	Thornton 2011
0.7117	-	White-lipped peccary	17.027778	-89.075278	WGS84	Thornton 2011
0.7087	-	Brocket deer	17.027778	-89.075278	WGS84	Thornton 2011
0.7088	-	Brocket deer	17.027778	-89.075278	WGS84	Thornton 2011
0.7082	-	Collared peccary	17.027778	-89.075278	WGS84	Thornton 2011
0.7085	-	Collared peccary	17.027778	-89.075278	WGS84	Thornton 2011
0.7282	-	Brocket deer	17.027778	-89.075278	WGS84	Thornton 2011
0.7202	-	White-tailed deer	17.027778	-89.075278	WGS84	Thornton 2011
0.7099	-	Tapir	17.027778	-89.075278	WGS84	Thornton 2011
0.7095	-	Tapir	17.027778	-89.075278	WGS84	Thornton 2011
0.7316	-	Collared peccary	17.027778	-89.075278	WGS84	Thornton 2011
0.7077	-	White-tailed deer	16.763081	-89.117813	WGS84	Thornton 2011
0.7076	-	White-tailed deer	16.763081	-89.117813	WGS84	Thornton 2011
0.7076	-	White-tailed deer	16.763081	-89.117813	WGS84	Thornton 2011
0.7079	-	White-tailed deer	16.763081	-89.117813	WGS84	Thornton 2011
0.7077	-	White-tailed deer	16.763081	-89.117813	WGS84	Thornton 2011
0.7076	-	Brocket deer	16.763081	-89.117813	WGS84	Thornton 2011
0.7076	-	Brocket deer	16.763081	-89.117813	WGS84	Thornton 2011
0.7131	-	Peccary	16.763081	-89.117813	WGS84	Thornton 2011
0.7076	-	Peccary	16.763081	-89.117813	WGS84	Thornton 2011

0.7077	-	White-tailed deer	16.763081	-89.117813	WGS84	Thornton 2011
0.7077	-	Peccary	16.763081	-89.117813	WGS84	Thornton 2011
0.7074	-	White-tailed deer	16.281923	-88.964024	WGS84	Thornton 2011
0.7076	-	White-tailed deer	16.281923	-88.964024	WGS84	Thornton 2011
0.7078	-	White-tailed deer	16.281923	-88.964024	WGS84	Thornton 2011
0.7074	-	Brocket deer	16.281923	-88.964024	WGS84	Thornton 2011
0.708	-	Deer	17.751999	-89.903126	WGS84	Thornton 2011
0.708	-	White-tailed deer	17.751999	-89.903126	WGS84	Thornton 2011
0.7075	-	White-tailed deer	17.004125	-89.890885	WGS84	Thornton 2011
0.7073	-	White-tailed deer	17.004125	-89.890885	WGS84	Thornton 2011
0.7072	-	White-tailed deer	17.004125	-89.890885	WGS84	Thornton 2011
0.7073	-	White-tailed deer	17.004125	-89.890885	WGS84	Thornton 2011
0.7075	-	Peccary	17.004125	-89.890885	WGS84	Thornton 2011
0.7075	-	White-tailed deer	17.004125	-89.890885	WGS84	Thornton 2011
0.7074	-	White-tailed deer	17.006342	-89.882222	WGS84	Thornton 2011
0.7069	-	White-tailed deer	17.006342	-89.882222	WGS84	Thornton 2011
0.7073	-	White-tailed deer	17.006342	-89.882222	WGS84	Thornton 2011
0.7075	-	Peccary	17.006342	-89.882222	WGS84	Thornton 2011
0.7076	-	White-tailed deer	17.006342	-89.882222	WGS84	Thornton 2011
0.7072	-	Peccary	17.179211	-91.255997	WGS84	Thornton 2011
0.7078	-	Peccary	17.179211	-91.255997	WGS84	Thornton 2011
0.7077	-	White-tailed deer	17.179211	-91.255997	WGS84	Thornton 2011
0.7077	-	White-tailed deer	17.179211	-91.255997	WGS84	Thornton 2011
0.7078	-	White-tailed deer	17.179211	-91.255997	WGS84	Thornton 2011
0.7078	-	White-tailed deer	17.179211	-91.255997	WGS84	Thornton 2011
0.7077	-	White-tailed deer	17.179211	-91.255997	WGS84	Thornton 2011
0.7076	-	White-tailed deer	17.179211	-91.255997	WGS84	Thornton 2011
0.7077	-	White-tailed deer	17.179211	-91.255997	WGS84	Thornton 2011
0.7066	-	White-tailed deer	16.411679	-90.277815	WGS84	Thornton 2011
0.7075	-	Peccary	16.411679	-90.277815	WGS84	Thornton 2011
0.7077	-	White-tailed deer	16.411679	-90.277815	WGS84	Thornton 2011
0.7077	-	White-tailed deer	16.411679	-90.277815	WGS84	Thornton 2011
0.7078	-	White-tailed deer	16.411679	-90.277815	WGS84	Thornton 2011
0.7076	-	Peccary	16.411679	-90.277815	WGS84	Thornton 2011
0.7074	-	White-tailed deer	16.347275	-90.188073	WGS84	Thornton 2011
0.7069	-	White-tailed deer	16.347275	-90.188073	WGS84	Thornton 2011
0.7077	-	Domestic dog	16.347275	-90.188073	WGS84	Thornton 2011
0.7076	-	Domestic dog	16.347275	-90.188073	WGS84	Thornton 2011
0.7073	-	White-tailed deer	16.00766	-90.039267	WGS84	Thornton 2011
0.7076	-	White-tailed deer	16.00766	-90.039267	WGS84	Thornton 2011
0.7075	-	White-tailed deer	16.00766	-90.039267	WGS84	Thornton 2011
0.7075	-	White-tailed deer	16.00766	-90.039267	WGS84	Thornton 2011
0.7073	-	White-tailed deer	16.00766	-90.039267	WGS84	Thornton 2011

0.7076	-	White-tailed deer	16.00766	-90.039267	WGS84	Thornton 2011
0.7073	-	Brocket deer	16.00766	-90.039267	WGS84	Thornton 2011
0.7074	-	White-lipped peccary	16.00766	-90.039267	WGS84	Thornton 2011
0.7074	-	Collared peccary	16.00766	-90.039267	WGS84	Thornton 2011
0.7074	-	White-tailed deer	16.00766	-90.039267	WGS84	Thornton 2011
0.7074	-	Peccary	16.00766	-90.039267	WGS84	Thornton 2011
0.7074	-	Collared peccary	16.00766	-90.039267	WGS84	Thornton 2011
0.7067	-	White-tailed deer	14.849725	-89.146783	WGS84	Thornton 2011
0.7089	-	White-tailed deer	14.849725	-89.146783	WGS84	Thornton 2011
0.7123	-	White-tailed deer	14.849725	-89.146783	WGS84	Thornton 2011
0.7046	-	White-tailed deer	14.849725	-89.146783	WGS84	Thornton 2011
0.7047	-	White-tailed deer	14.849725	-89.146783	WGS84	Thornton 2011
0.70686	-	LRM1	14.849725	-89.146783	WGS84	Price et al. 2010
0.70686	-	LRM3	14.849725	-89.146783	WGS84	Price et al. 2010
0.70688	-	URI1	14.849725	-89.146783	WGS84	Price et al. 2010
0.70688	-	URM1	14.849725	-89.146783	WGS84	Price et al. 2010
0.70688	-	LLM3	14.849725	-89.146783	WGS84	Price et al. 2010
0.70686	-	URI1	14.849725	-89.146783	WGS84	Price et al. 2010
0.70686	-	LRM1	14.849725	-89.146783	WGS84	Price et al. 2010
0.70686	-	LLM3	14.849725	-89.146783	WGS84	Price et al. 2010
0.70682	-	U_M3	14.849725	-89.146783	WGS84	Price et al. 2010
0.70644	-	L_I2	14.849725	-89.146783	WGS84	Price et al. 2010
0.70644	-	L_M3	14.849725	-89.146783	WGS84	Price et al. 2010
0.7089	-	bioavailable	21.45306	-88.31359	WGS84	Price et al. 2014
0.7089	-	bioavailable	21.14089	-88.14331	WGS84	Price et al. 2014
0.7086	-	bioavailable	20.99734	-88.04443	WGS84	Price et al. 2014
0.7083	-	bioavailable	20.51449	-87.73132	WGS84	Price et al. 2014
0.708	-	bioavailable	20.20807	-87.45941	WGS84	Price et al. 2014
0.7087	-	bioavailable	20.96355	-89.57688	WGS84	Price et al. 2014
0.7083	-	bioavailable	20.62433	-89.45633	WGS84	Price et al. 2014
0.7082	-	bioavailable	19.82614	-90.58227	WGS84	Price et al. 2014
0.7089	-	bioavailable	21.09873	-89.59821	WGS84	Price et al. 2014
0.7088	-	bioavailable	19.84799	-90.48833	WGS84	Price et al. 2014
0.7083	-	bioavailable	20.06625	-89.54406	WGS84	Price et al. 2014
0.7087	-	bioavailable	20.29826	-90.19775	WGS84	Price et al. 2014
0.7088	-	bioavailable	20.49906	-90.18676	WGS84	Price et al. 2014
0.7078	-	bioavailable	19.61154	-88.85742	WGS84	Price et al. 2014
0.7083	-	bioavailable	19.34716	-90.72002	WGS84	Price et al. 2014
0.7077	-	bioavailable	18.50367	-89.39561	WGS84	Price et al. 2014
0.7083	-	bioavailable	18.50044	-90.23071	WGS84	Price et al. 2014
0.7081	-	bioavailable	18.6098	-90.73059	WGS84	Price et al. 2014
0.7082	-	bioavailable	18.51833	-89.46611	WGS84	Price et al. 2014

0.7071	-	bioavailable	18.26116	-93.22169	WGS84	Price et al. 2014
0.7081	-	bioavailable	18.104087	-94.048462	WGS84	Price et al. 2014
0.7083	-	bioavailable	17.555	-94.4219	WGS84	Price et al. 2014
0.7079	-	bioavailable	17.50786	-92.005	WGS84	Price et al. 2014
0.7079	-	bioavailable	16.893916	-92.002258	WGS84	Price et al. 2014
0.7076	-	bioavailable	16.719983	-92.636278	WGS84	Price et al. 2014
0.7083	-	bioavailable	16.708325	-93.009840	WGS84	Price et al. 2014
0.7072	-	bioavailable	16.501132	-93.363339	WGS84	Price et al. 2014
0.7076	-	bioavailable	15.698122	-93.210768	WGS84	Price et al. 2014
0.7048	-	bioavailable	14.889595	-92.479853	WGS84	Price et al. 2014
0.7047	-	bioavailable	14.900528	-92.392602	WGS84	Price et al. 2014
0.7047	-	bioavailable	14.901045	-92.166113	WGS84	Price et al. 2014
0.7085	-	bioavailable	18.21735	-88.58473	WGS84	Price et al. 2014
0.7082	-	bioavailable	18.0805	-88.2971	WGS84	Price et al. 2014
0.7087	-	bioavailable	17.2	-88.967	WGS84	Price et al. 2014
0.7084	-	bioavailable	17.3627	-88.83333	WGS84	Price et al. 2014
0.7127	-	bioavailable	16.9695	-88.2315	WGS84	Price et al. 2014
0.707	-	bioavailable	16.2753	-88.9589	WGS84	Price et al. 2014
0.7077	-	bioavailable	16.7638	-89.1175	WGS84	Price et al. 2014
0.7079	-	bioavailable	17.753	-89.9189	WGS84	Price et al. 2014
0.708	-	bioavailable	17.2248	-89.611	WGS84	Price et al. 2014
0.7074	-	bioavailable	16.83	-90.019	WGS84	Price et al. 2014
0.7075	-	bioavailable	16.5269	-90.0604	WGS84	Price et al. 2014
0.7075	-	bioavailable	16.412	-90.1884	WGS84	Price et al. 2014
0.7075	-	bioavailable	15.8028	-90.2966	WGS84	Price et al. 2014
0.7042	-	bioavailable	14.642	-91.227	WGS84	Price et al. 2014
0.7052	-	bioavailable	14.632279	-90.548528	WGS84	Price et al. 2014
0.708	-	bioavailable	17.17921	-91.256	WGS84	Price et al. 2014
0.7042	-	bioavailable	14.3921	-91.1965	WGS84	Price et al. 2014
0.7041	-	bioavailable	14.9	-91.666	WGS84	Price et al. 2014
0.7061	-	bioavailable	15.2709	-89.0754	WGS84	Price et al. 2014
0.704	-	bioavailable	14.3803	-91.0108	WGS84	Price et al. 2014
0.7041	-	bioavailable	14.6458	-91.7361	WGS84	Price et al. 2014
0.7079	-	bioavailable	17.0619	-89.4056	WGS84	Price et al. 2014
0.7069	-	bioavailable	14.8497	-89.1467	WGS84	Price et al. 2014
0.70541	-	RM	20.365389	-103.82278	WGS84	Juarez 2008
0.70511	-	RP	21.289208	-102.50346	WGS84	Juarez 2008
0.70513	-	LM	21.289208	-102.50346	WGS84	Juarez 2008
0.70498	-	LM	21.289208	-102.50346	WGS84	Juarez 2008
0.70549	-	LM	19.432608	-99.133208	WGS84	Juarez 2008
0.7054	-	LM	20.630688	-103.29088	WGS84	Juarez 2008
0.70548	-	RM	20.347428	-103.89193	WGS84	Juarez 2008
0.70564	-	RM	20.659699	-103.34961	WGS84	Juarez 2008

0.70531	-	RM	19.662427	-103.08923	WGS84	Juarez 2008
0.70555	-	RM	25.749347	-100.28690	WGS84	Juarez 2008
0.70521	-	RM	21.125008	-101.68596	WGS84	Juarez 2008
0.70522	-	RM	20.5	-101.63333	WGS84	Juarez 2008
0.70506	-	LM	20.126456	-101.19334	WGS84	Juarez 2008
0.70461	-	RM	22.770925	-102.58325	WGS84	Juarez 2008
0.70489	-	RM	19.664748	-101.52327	WGS84	Juarez 2008
0.7035	0.0001	Basalt	8.740366	-82.947467	WGS84	Bern et al. 2007
0.704	0.0001	Vegetation	8.740366	-82.947467	WGS84	Bern et al. 2007
0.7041	-	Basalt	8.654151	-83.29392	WGS84	Bern et al. 2007
0.7042	0.0002	Vegetation	8.654151	-83.29392	WGS84	Bern et al. 2007
0.7034	-	Basalt	8.672912	-83.306352	WGS84	Bern et al. 2007
0.7039	0.0001	Vegetation	8.672912	-83.306352	WGS84	Bern et al. 2007
0.7037	-	Basalt	8.739352	-83.410767	WGS84	Bern et al. 2007
0.70415	0.00003	Vegetation	8.739352	-83.410767	WGS84	Bern et al. 2007
0.7038	0.0004	Basalt	9.403739	-84.158319	WGS84	Bern et al. 2007
0.7043	0.0003	Vegetation	9.403739	-84.158319	WGS84	Bern et al. 2007
0.7062	0.0002	Vegetation	8.621069	-83.734642	WGS84	Bern et al. 2005
0.7038	0.0006	Volcanic rocks	14.756337	-91.553417	WGS84	Pashkar et al. 1971
0.7042	0.0007	Volcanic rocks	14.616667	-91.183333	WGS84	Pashkar et al. 1971
0.7037	0.0005	basalt	14.286905	-90.562426	WGS84	Pashkar et al. 1971
0.7043	0.0006	rhyolite obsidian	14.286905	-90.562426	WGS84	Pashkar et al. 1971
0.7043	0.0003	rhyolite obsidian	15.15	-90.35	WGS84	Pashkar et al. 1971
0.7044	0.0004	rhyolite obsidian	14.368333	-90.42	WGS84	Pashkar et al. 1971
0.7046	0.0009	rhyodacite pumice	14.688864	-91.268644	WGS84	Pashkar et al. 1971
0.7031	0.0015	Volcanic rocks	14.47469	-90.880635	WGS84	Pashkar et al. 1971
0.7039	0.0012	Volcanic rocks	14.382307	-90.601507	WGS84	Pashkar et al. 1971
0.7037	0.0007	granodiorite	14.690671	-91.202521	WGS84	Pashkar et al. 1971
0.7071	0.0006	granite	14.286905	-90.562426	WGS84	Pashkar et al. 1971
0.7453	0.0007	Quartz-mica gneiss	15.083333	-90.75	WGS84	Pashkar et al. 1971
0.7395	0.0007	phyllite	14.782827	-90.793701	WGS84	Pashkar et al. 1971
0.7079	0.0014	granite	14.624467	-91.946576	WGS84	Pashkar et al. 1971
0.7052	0.0003	granite	14.286905	-90.562426	WGS84	Pashkar et al. 1971
0.7047	0.0007	phyllite	14.382307	-90.601507	WGS84	Pashkar et al. 1971
0.7067	0.0002	phyllite	14.39189	-91.193404	WGS84	Pashkar et al. 1971
0.7065	0.0007	rhyolite ignimbrite	14.39189	-91.193404	WGS84	Pashkar et al. 1971
0.7091	0.0006	argillite	14.589907	-90.715474	WGS84	Pashkar et al. 1971
0.7044	0.0004	obsidian dike	14.715037	-90.39507	WGS84	Pashkar et al. 1971
0.7045	0.0006	rhyolite ignimbrite	15.06977	-88.734965	WGS84	Pashkar et al. 1971
0.7175	0.0007	rhyolite ignimbrite	14.072275	-87.192136	WGS84	Pashkar et al. 1971
0.7125	0.001	rhyolite ignimbrite	14.073693	-86.418731	WGS84	Pashkar et al. 1971
0.7045	0.0002	rhyolite ignimbrite	14.43675	-89.18158	WGS84	Pashkar et al. 1971
0.7104	0.0004	rhyolite ignimbrite	14.804616	-88.162071	WGS84	Pashkar et al. 1971

0.7058	0.0004	rhyolite ignimbrite	14.798087	-87.338877	WGS84	Pashkar et al. 1971
0.7105	0.0006	granite gneiss	14.657211	-86.210767	WGS84	Pashkar et al. 1971
0.7257	0.0004	granite	13.720299	-86.508498	WGS84	Pashkar et al. 1971
0.7172	0.0008	phyllite	13.628904	-86.484491	WGS84	Pashkar et al. 1971
0.7049	0.0008	adesite	12.421877	-86.545117	WGS84	Pashkar et al. 1971
0.704	0.0005	Volcanic rocks	11.985278	-86.160833	WGS84	Pashkar et al. 1971
0.7053	0.0009	dacite ignimbrite	12.675723	-86.571617	WGS84	Pashkar et al. 1971
0.7035	0.0009	andesitic ignimbrite	12.230411	-86.099167	WGS84	Pashkar et al. 1971
0.7038	0.001	dacite	13.701754	-89.078258	WGS84	Pashkar et al. 1971
0.7041	0.001	andesite	13.813658	-89.632638	WGS84	Pashkar et al. 1971
0.70831	0.000014	Human_tooth_nsp	14.896267	-85.8709	WGS84	Warner 2016
0.70761	0.000015	Human_tooth_nsp	14.896267	-85.8709	WGS84	Warner 2016
0.70723	0.000012	Human_tooth_nsp	14.896267	-85.8709	WGS84	Warner 2016
0.71162	0.000016	Human_tooth_nsp	14.896267	-85.8709	WGS84	Warner 2016
0.71089	0.000015	Human_tooth_nsp	14.896267	-85.8709	WGS84	Warner 2016
0.71156	0.000013	Human_tooth_nsp	14.896267	-85.8709	WGS84	Warner 2016
0.71147	0.000012	Human_tooth_nsp	14.896267	-85.8709	WGS84	Warner 2016
0.71197	0.000012	Human_tooth_nsp	14.896267	-85.8709	WGS84	Warner 2016
0.71201	0.000014	Human_tooth_nsp	14.896267	-85.8709	WGS84	Warner 2016
0.70966	0.000013	Human_tooth_nsp	14.896267	-85.8709	WGS84	Warner 2016
0.71184	0.000015	Human_tooth_nsp	14.896267	-85.8709	WGS84	Warner 2016
0.70719	0.000013	Human_tooth_nsp	14.896267	-85.8709	WGS84	Warner 2016
0.71338	0.000014	Human_tooth_nsp	14.896267	-85.8709	WGS84	Warner 2016
0.71008	0.000016	Human_tooth_nsp	14.896267	-85.8709	WGS84	Warner 2016
0.70915	-	Ground/Surface water	20.59	-87.18	WGS84	Perry et al. 2009
0.70899	-	Ground/Surface water	21.22	-88.93	WGS84	Perry et al. 2009
0.70897	-	Ground/Surface water	20.53	-87.22	WGS84	Perry et al. 2009
0.70895	-	Ground/Surface water	21.35	-88.9	WGS84	Perry et al. 2009
0.70889	-	Ground/Surface water	20.88	-90.36	WGS84	Perry et al. 2009
0.70882	-	Ground/Surface water	21.3	-89.26	WGS84	Perry et al. 2009
0.70876	-	Ground/Surface water	21.17	-89.28	WGS84	Perry et al. 2009
0.70876	-	Ground/Surface water	20.67	-88.73	WGS84	Perry et al. 2009
0.70872	-	Ground/Surface water	21.23	-89.28	WGS84	Perry et al. 2009
0.70871	-	Ground/Surface water	21.17	-89.28	WGS84	Perry et al. 2009
0.7087	-	Ground/Surface water	21.44	-88.63	WGS84	Perry et al. 2009
0.70868	-	Ground/Surface	21.3	-89.26	WGS84	Perry et al. 2009

		water				
0.70867	-	Ground/Surface water	21.12	-90	WGS84	Perry et al. 2009
0.70865	-	Ground/Surface water	21.17	-89.28	WGS84	Perry et al. 2009
0.70865	-	Ground/Surface water	21.23	-89.28	WGS84	Perry et al. 2009
0.70861	-	Ground/Surface water	20.58	-89.59	WGS84	Perry et al. 2009
0.7086	-	Ground/Surface water	20.6	-89.28	WGS84	Perry et al. 2009
0.70857	-	Ground/Surface water	20.85	-90.24	WGS84	Perry et al. 2009
0.70854	-	Ground/Surface water	21.15	-89.68	WGS84	Perry et al. 2009
0.70852	-	Ground/Surface water	20.16	-87.55	WGS84	Perry et al. 2009
0.70848	-	Ground/Surface water	20.16	-87.55	WGS84	Perry et al. 2009
0.70848	-	Ground/Surface water	20.52	-87.65	WGS84	Perry et al. 2009
0.70848	-	Ground/Surface water	21.09	-89.6	WGS84	Perry et al. 2009
0.70844	-	Ground/Surface water	20.91	-88.87	WGS84	Perry et al. 2009
0.70844	-	Ground/Surface water	20.93	-89.02	WGS84	Perry et al. 2009
0.70842	-	Ground/Surface water	21.56	-88.18	WGS84	Perry et al. 2009
0.7084	-	Ground/Surface water	20.2	-87.5	WGS84	Perry et al. 2009
0.7084	-	Ground/Surface water	20.91	-88.87	WGS84	Perry et al. 2009
0.70834	-	Ground/Surface water	20.16	-87.55	WGS84	Perry et al. 2009
0.70834	-	Ground/Surface water	20.16	-87.55	WGS84	Perry et al. 2009
0.70833	-	Ground/Surface water	20.33	-89.66	WGS84	Perry et al. 2009
0.70832	-	Ground/Surface water	20.64	-90.21	WGS84	Perry et al. 2009
0.70832	-	Ground/Surface water	20.99	-88.6	WGS84	Perry et al. 2009
0.70831	-	Ground/Surface water	20.27	-87.49	WGS84	Perry et al. 2009
0.70831	-	Ground/Surface water	20.91	-88.87	WGS84	Perry et al. 2009
0.7083	-	Ground/Surface water	20.91	-88.87	WGS84	Perry et al. 2009
0.70829	-	Ground/Surface water	20.86	-90.38	WGS84	Perry et al. 2009

0.70829	-	Ground/Surface water	20.96	-88.6	WGS84	Perry et al. 2009
0.70828	-	Ground/Surface water	20.99	-88.6	WGS84	Perry et al. 2009
0.70827	-	Ground/Surface water	20.83	-89.9	WGS84	Perry et al. 2009
0.70827	-	Ground/Surface water	20.64	-90.21	WGS84	Perry et al. 2009
0.70827	-	Ground/Surface water	20.99	-88.6	WGS84	Perry et al. 2009
0.70817	-	Ground/Surface water	20.87	-88.63	WGS84	Perry et al. 2009
0.70816	-	Ground/Surface water	20.64	-87.56	WGS84	Perry et al. 2009
0.70813	-	Ground/Surface water	20.65	-87.56	WGS84	Perry et al. 2009
0.70813	-	Ground/Surface water	20.55	-90.43	WGS84	Perry et al. 2009
0.70812	-	Ground/Surface water	20.66	-88.8	WGS84	Perry et al. 2009
0.7081	-	Ground/Surface water	20.52	-87.65	WGS84	Perry et al. 2009
0.70807	-	Ground/Surface water	20.7	-89.36	WGS84	Perry et al. 2009
0.70807	-	Ground/Surface water	20.66	-88.55	WGS84	Perry et al. 2009
0.70805	-	Ground/Surface water	21.57	-88.07	WGS84	Perry et al. 2009
0.70804	-	Ground/Surface water	20.85	-90.28	WGS84	Perry et al. 2009
0.70798	-	Ground/Surface water	20.85	-90.28	WGS84	Perry et al. 2009
0.70798	-	Ground/Surface water	20.59	-90.02	WGS84	Perry et al. 2009
0.70787	-	Ground/Surface water	20.33	-89.66	WGS84	Perry et al. 2009
0.70786	-	Ground/Surface water	20.07	-89.05	WGS84	Perry et al. 2009
0.70782	-	Ground/Surface water	20.13	-88.92	WGS84	Perry et al. 2009
0.70781	-	Ground/Surface water	18.14	-88.68	WGS84	Perry et al. 2009
0.70778	-	Ground/Surface water	19.88	-88.77	WGS84	Perry et al. 2009
0.70776	-	Ground/Surface water	19.78	-88.74	WGS84	Perry et al. 2009
0.70776	-	Ground/Surface water	19.88	-88.77	WGS84	Perry et al. 2009
0.70769	-	Ground/Surface water	18.14	-88.68	WGS84	Perry et al. 2009
0.70768	-	Ground/Surface	18.63	-88.46	WGS84	Perry et al. 2009

		water				
0.70767	-	Ground/Surface water	18.69	-88.38	WGS84	Perry et al. 2009
0.70764	-	Ground/Surface water	18.69	-88.38	WGS84	Perry et al. 2009
0.70764	-	Ground/Surface water	18.65	-88.41	WGS84	Perry et al. 2009
0.70764	-	Ground/Surface water	18.65	-88.41	WGS84	Perry et al. 2009
0.708424	-	Burial-M1	15.216	-88.069	WGS84	Wells et al. 2014
0.708216	-	Burial-M1	15.324	-88.0422	WGS84	Wells et al. 2014
0.708631	-	Burial-M1	15.216	-88.069	WGS84	Wells et al. 2014
0.708191	-	Burial-M1	15.211	-88.069	WGS84	Wells et al. 2014
0.708025	-	Burial-M1	15.324	-88.0422	WGS84	Wells et al. 2014
0.708386	0.001	Coral	9.2502778	-79.840833	WGS84	Kirby et al. 2008
0.708371	0.0008	Coral	9.2502778	-79.840833	WGS84	Kirby et al. 2008
0.708404	0.0008	Pectinid	9.2502778	-79.840833	WGS84	Kirby et al. 2008
0.708386	0.0008	Pectinid	9.2502778	-79.840833	WGS84	Kirby et al. 2008
0.70825	0.0008	Bivalve	9.1966667	-79.811667	WGS84	Kirby et al. 2008
0.708502	0.0008	Ostrea sp.	9.0775	-79.747222	WGS84	Kirby et al. 2008
0.70845	0.0007	Pectinid	9.0775	-79.747222	WGS84	Kirby et al. 2008

APPENDIX B. CONTRIBUTING AUTHORS FOR BIOAVAILABLE SR DATA

Bern et al. 2007	Bern, C. R., Porder, S., & Townsend, A. R. (2007). Erosion and landscape development decouple strontium and sulfur in the transition to dominance by atmospheric inputs. *Geoderma*, *142*(3), 274-284.
Freiwald 2011	Freiwald, C. (2011). *Maya migration networks: Reconstructing population movement in the Belize River valley during the Late and Terminal Classic* (Vol. 72, No. 11).
Hodell et al. 2004	Hodell, D. A., Quinn, R. L., Brenner, M., & Kamenov, G. (2004). Spatial variation of strontium isotopes (87 Sr/86 Sr) in the Maya region: a tool for tracking ancient human migration. *Journal of Archaeological Science*, *31*(5), 585-601.
Juarez 2008	Juarez, C. A. (2008). Strontium and Geolocation, the Pathway to Identification for Deceased Undocumented Mexican Border-Crossers: A Preliminary Report. *Journal of forensic sciences*, *53*(1), 46-49.
Kirby et al. 2008	Kirby, M. X., Jones, D. S., & MacFadden, B. J. (2008). Lower Miocene stratigraphy along the Panama Canal and its bearing on the Central American Peninsula. *PLoS One*, *3*(7), e2791.
Krueger 1985	Krueger H. W. (1985). Sr isotopes and Sr/Ca in Bone. Paper presented at Bone Mineralization Conference, Warrenton, VA.
Pashkar et al. 1971	Pashkar, S. I. (1971). Biochemical studies in breeding corn for increased lysine and tryptophan. *Selektsiia I Semenovodstvo Kukuruzy*.
Perry et al. 2009	Perry, E., Paytan, A., Pedersen, B., & Velazquez-Oliman, G. (2009). Groundwater geochemistry of the Yucatan Peninsula, Mexico: constraints on stratigraphy and hydrogeology. *Journal of Hydrology*, *367*(1), 27-40.
Price et al. 2000	Price, T. D., Manzanilla, L., & Middleton, W. D. (2000). Immigration and the ancient city of Teotihuacan in Mexico: a study using strontium isotope ratios in human bone and teeth. *Journal of Archaeological Science*, *27*(10), 903-913.
Price et al. 2010	Price, T. D., Burton, J. H., Sharer, R. J., Buikstra, J. E., Wright, L. E., Traxler, L. P., & Miller, K. A. (2010). Kings and commoners at Copan: Isotopic evidence for origins and movement in the Classic Maya period. *Journal of Anthropological Archaeology*, *29*(1), 15-32.

Price et al. 2014	Price, T. D., Nakamura, S., Suzuki, S., Burton, J. H., & Tiesler, V. (2014). New isotope data on Maya mobility and enclaves at Classic Copan, Honduras. *Journal of Anthropological Archaeology*, *36*, 32-47.
Price et al. 2015	Price, T. D., Burton, J. H., Fullagar, P. D., Wright, L. E., Buikstra, J. E., & Tiesler, V. (2015). Strontium isotopes and the study of human mobility among the Ancient Maya. In *Archaeology and bioarchaeology of population movement among the Prehispanic Maya* (pp. 119-132). Springer International Publishing.
Thornton 2011	Thornton, E. K. (2011). Reconstructing ancient Maya animal trade through strontium isotope (87 Sr/86 Sr) analysis. *Journal of Archaeological Science*, *38*(12), 3254-3263.
Warner 2016	Warner, M. M. (2016). *A biogeochemistry approach to geographic origin and mortuary arrangement at the Talgua cave ossuaries, Olancho, Honduras* (Doctoral dissertation, Mississippi State University).
Wells et al. 2014	Wells, E. C., Davis-Salazar, K. L., Moreno-Cortes, J. E., Stuart, G. S., & Novotny, A. C. (2014). Analysis of the Context and Contents of an Ulua-Style Marble Vase from the Palmarejo Valley, Honduras. *Latin American Antiquity*, *25*(1), 82-100.
Wright et al. 2010	Wright, L. E., Valdés, J. A., Burton, J. H., Price, T. D., & Schwarcz, H. P. (2010). The children of Kaminaljuyu: Isotopic insight into diet and long-distance interaction in Mesoamerica. *Journal of Anthropological Archaeology*, *29*(2), 155-178.
Wright et al. 2012	Wright, L. E. (2012). Immigration to Tikal, Guatemala: Evidence from stable strontium and oxygen isotopes. *Journal of Anthropological Archaeology*, *31*(3), 334-352.

APPENDIX C. PREDICTION MAPS FOR EACH INDIVIDUAL

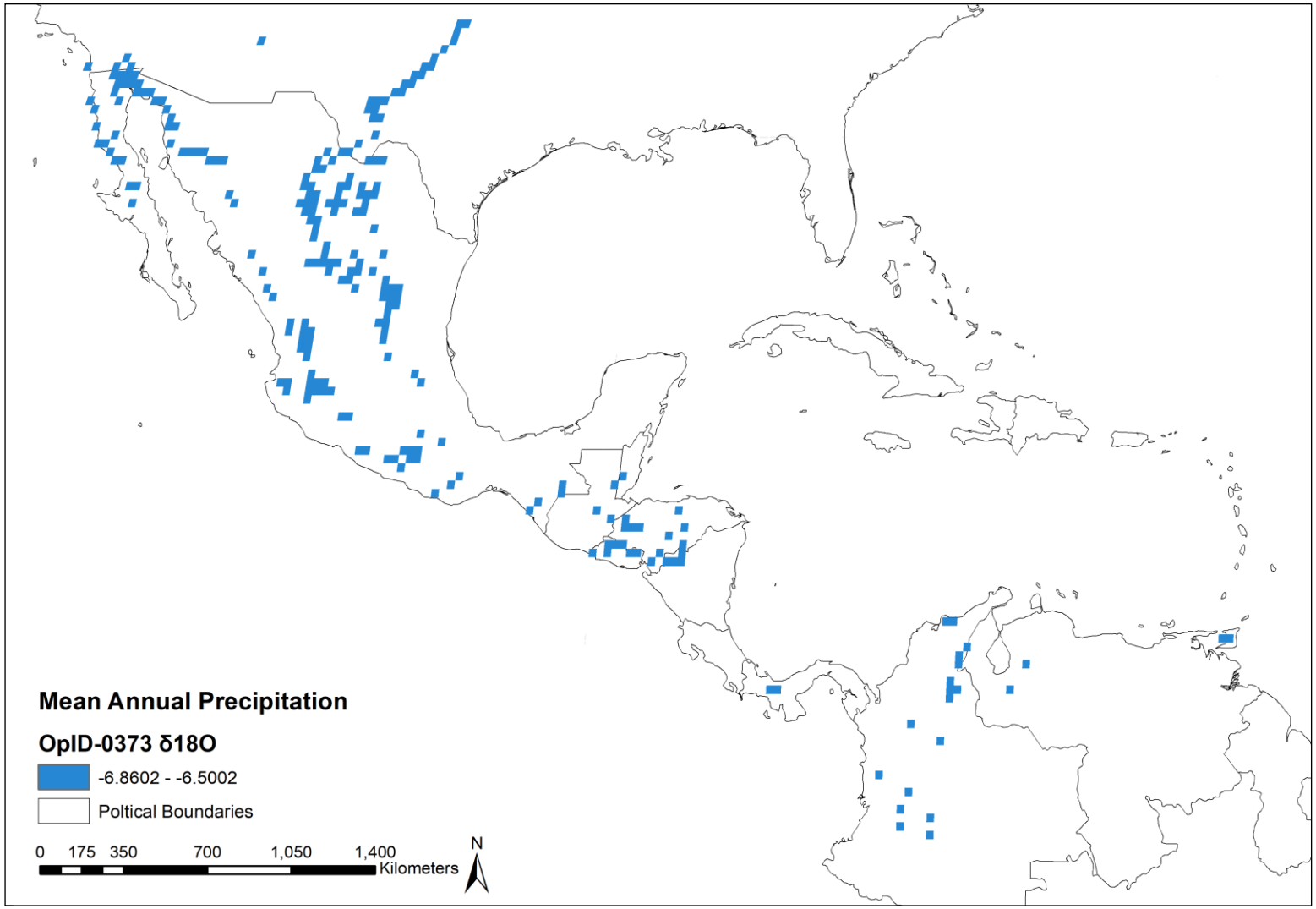

Figure C-1. Oxygen ($\delta^{18}O$) Prediction for OpID-0373. Raster by IsoMAP and map created in ArcMap 10.5.

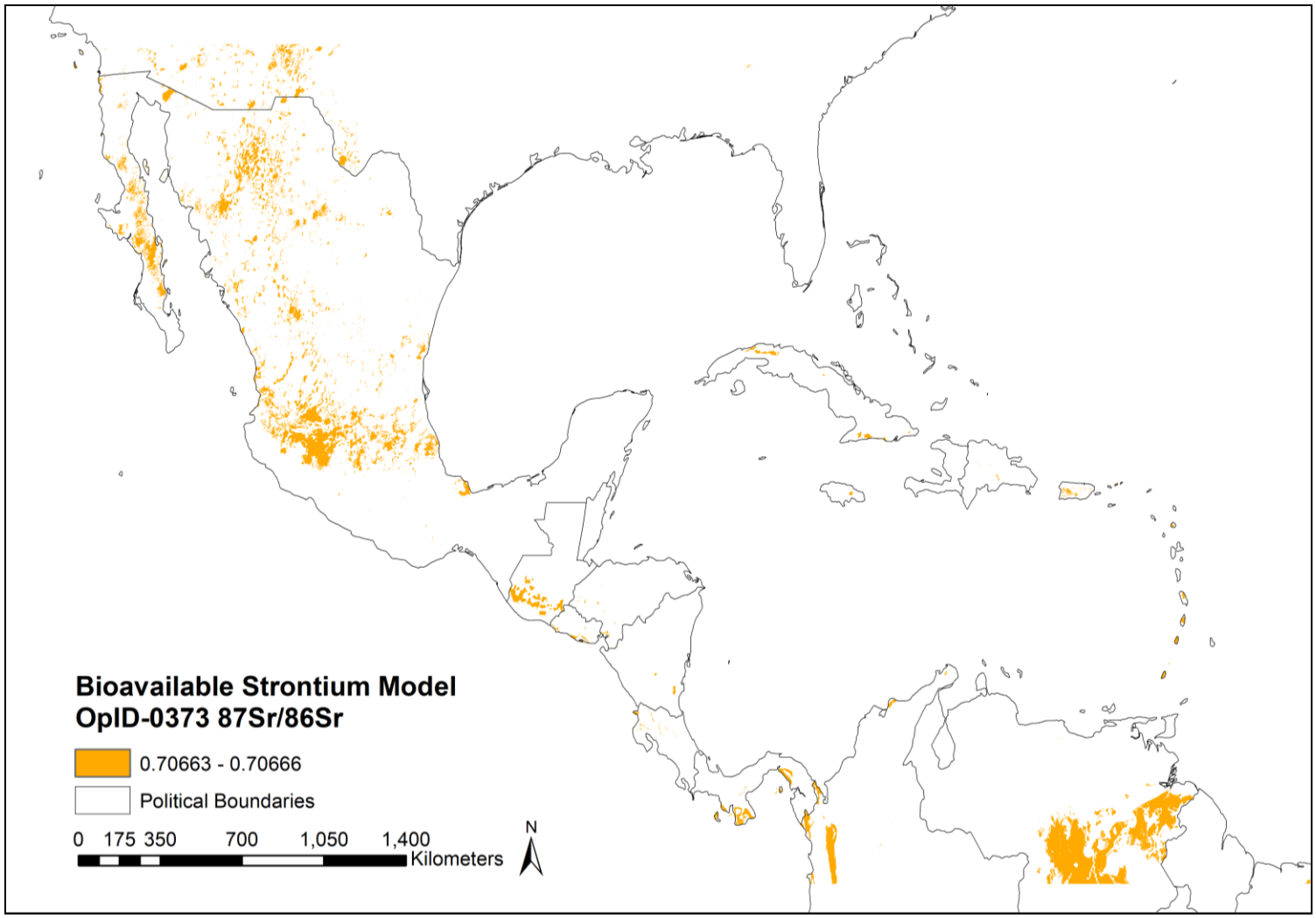

Figure C-2. Strontium ($^{87}Sr/^{86}Sr$) Prediction for OpID-0373. Raster provided by Bataille and map created in ArcMap 10.5.

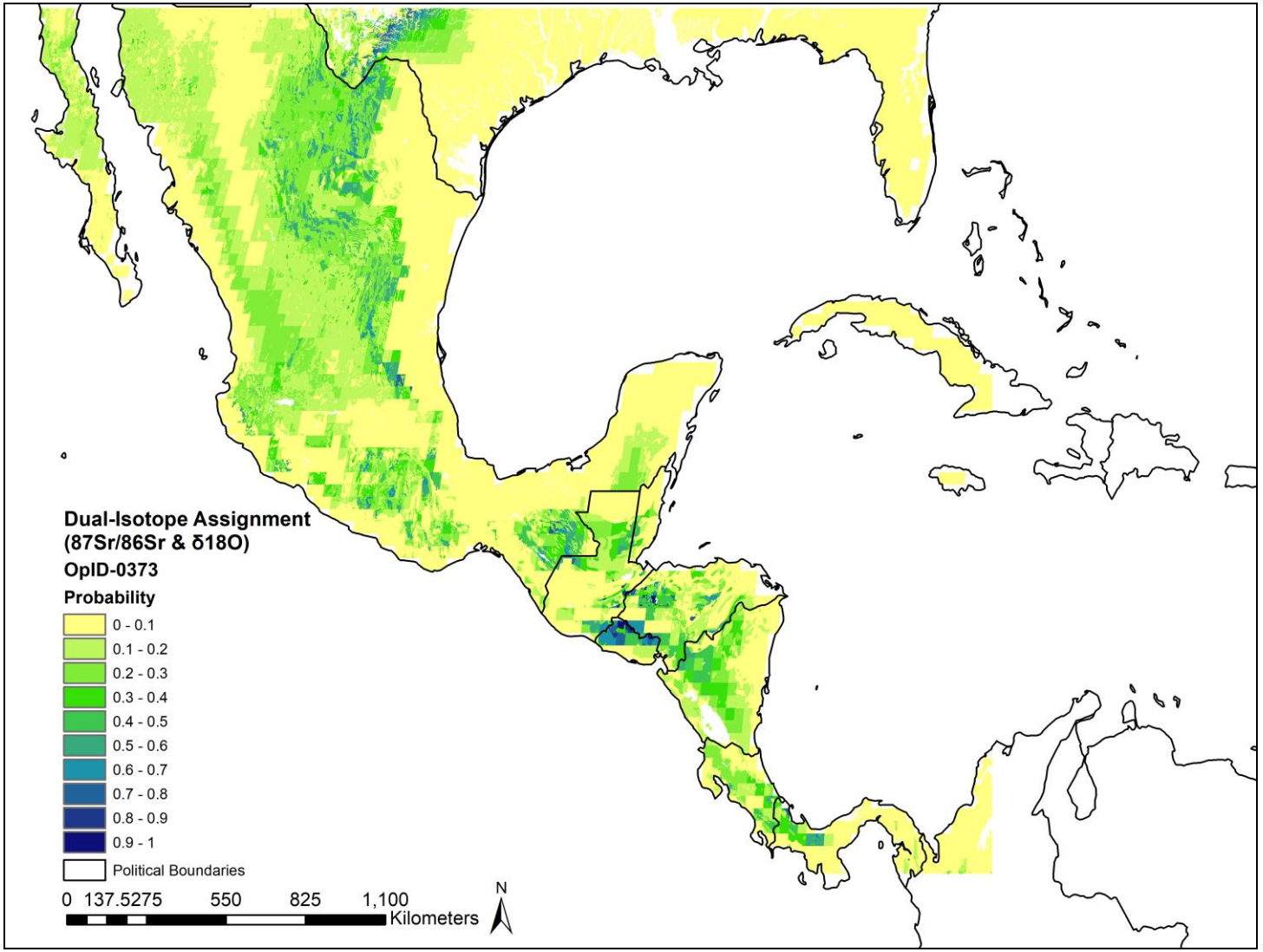

Figure C-3. Dual-Isotope ($^{87}Sr/^{86}Sr$ and $\delta^{18}O$) Prediction for OpID-0373. Assignment prediction map created in ArcMap 10.5.

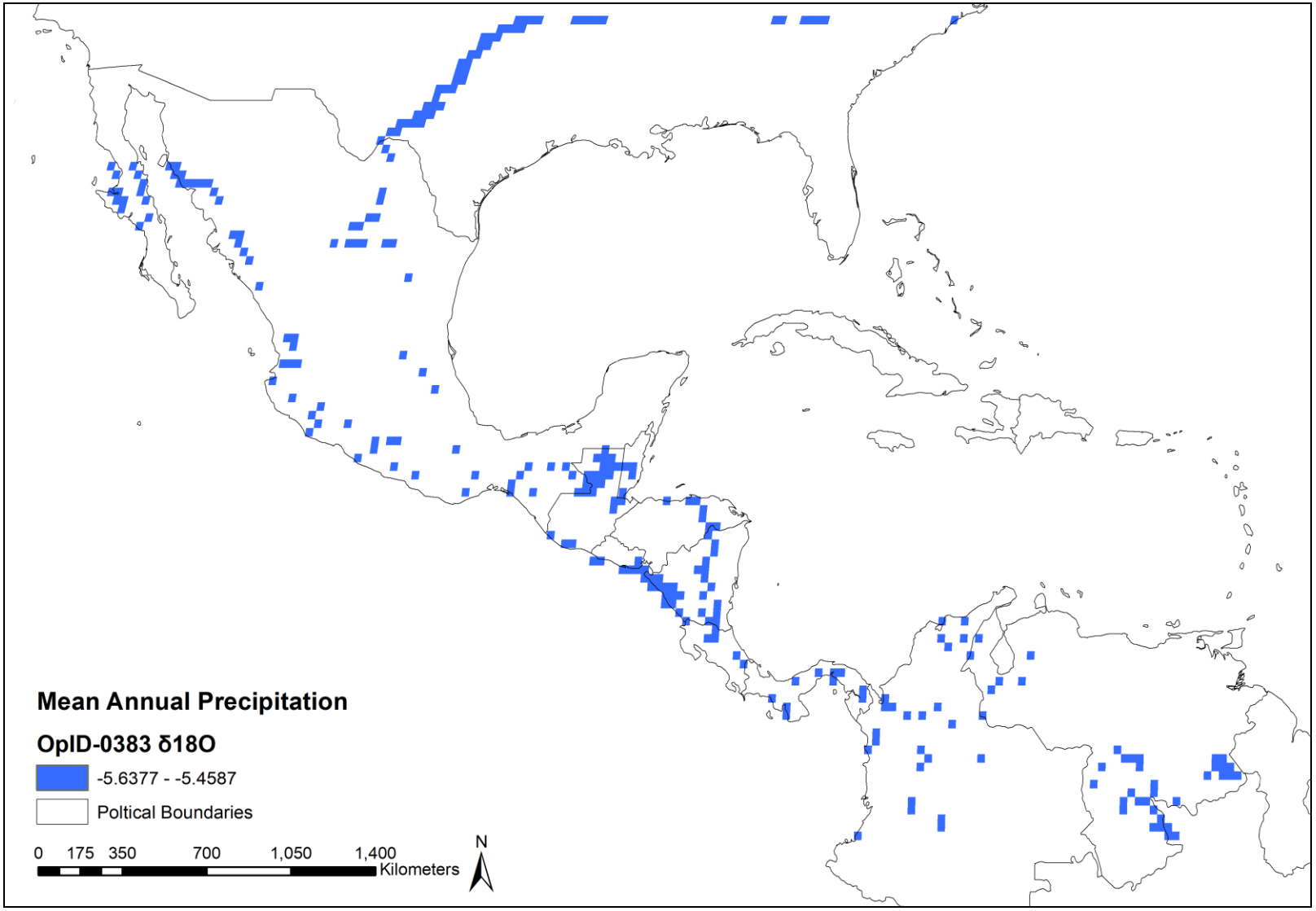

Figure C-4. Oxygen ($\delta^{18}O$) Prediction for OpID-0383. Raster by IsoMAP and map created in ArcMap 10.5.

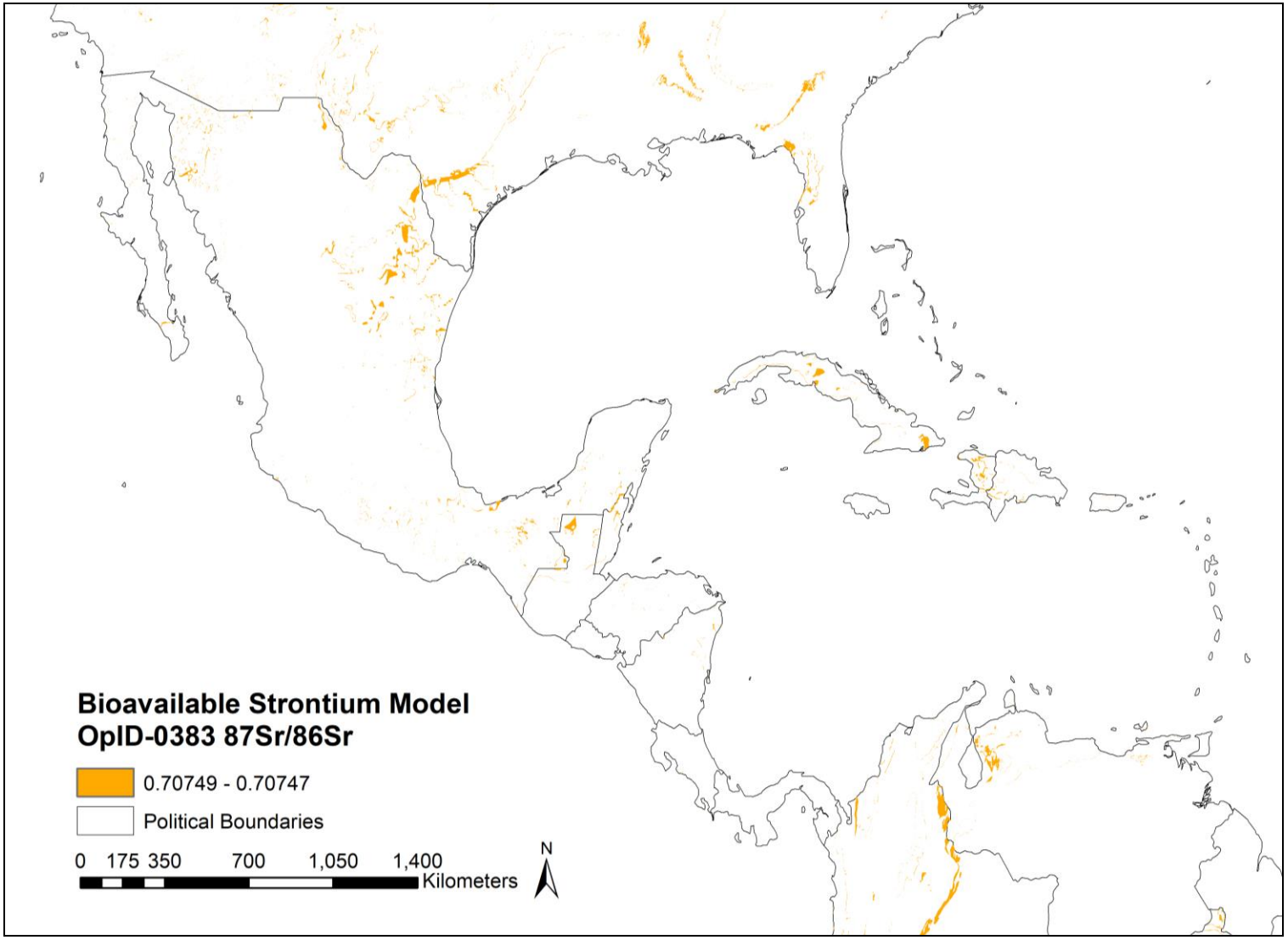

Figure C-5. Strontium ($^{87}Sr/^{86}Sr$) Prediction for OpID-0383. Raster provided by Bataille and map created in ArcMap 10.5.

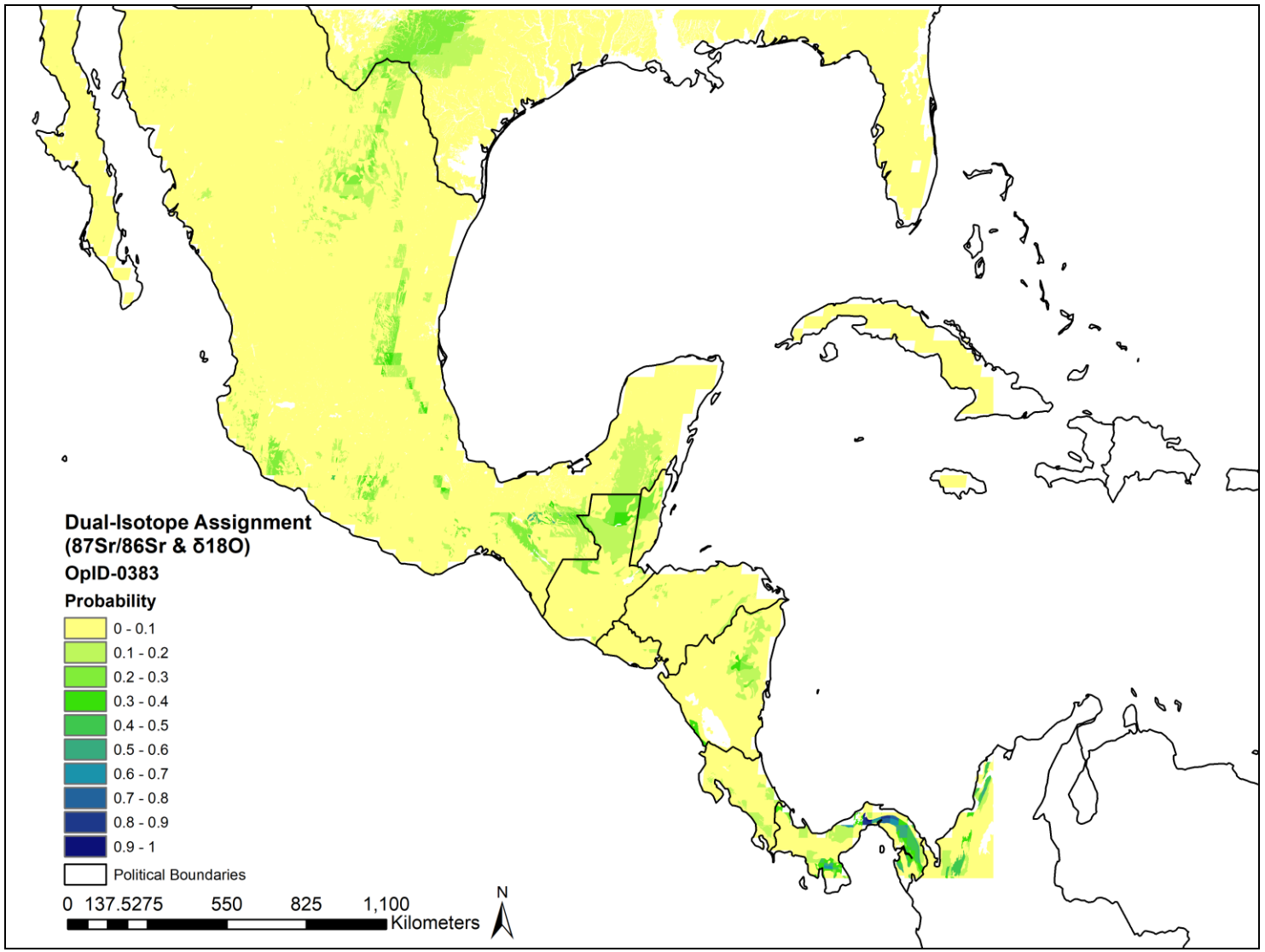

Figure C-6. Dual-Isotope ($^{87}Sr/^{86}Sr$ and $\delta^{18}O$) Prediction for OpID-0383. Assignment prediction map created in ArcMap 10.5.

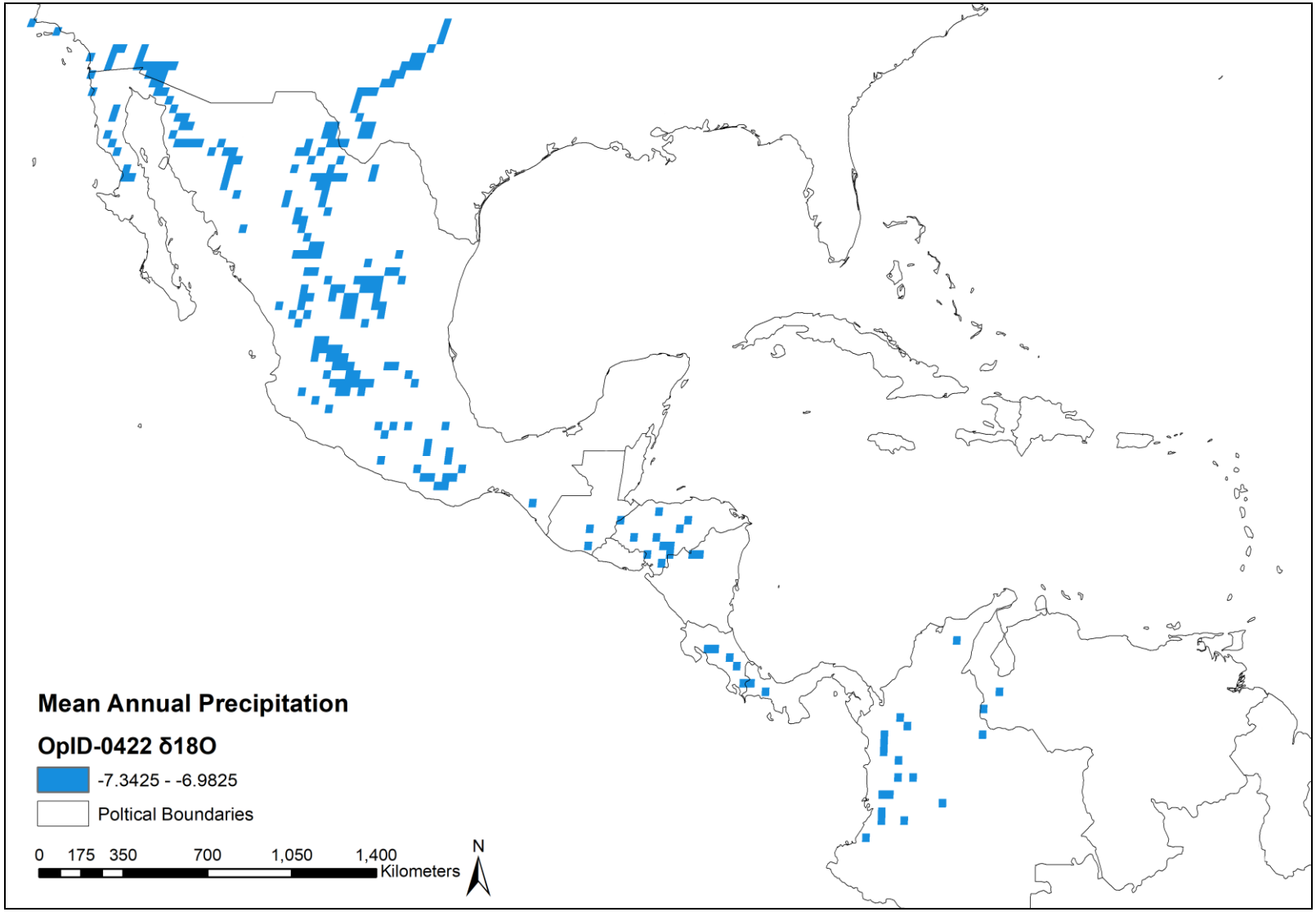

Figure C-7. Oxygen ($\delta^{18}O$) Prediction for OpID-0422. Raster by IsoMAP and map created in ArcMap 10.5.

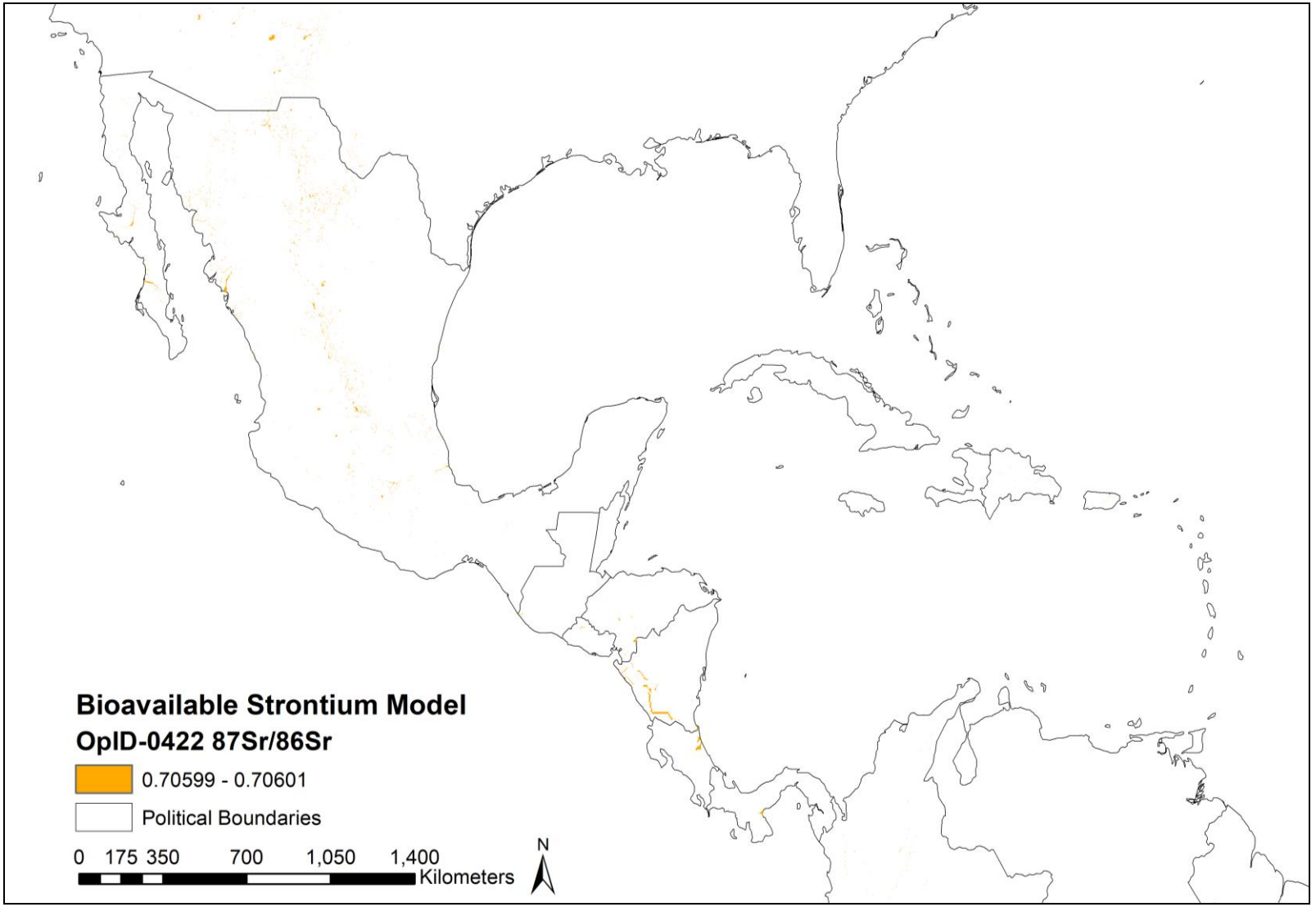

Figure C-8. Strontium ($^{87}Sr/^{86}Sr$) Prediction for OpID-0422. Raster provided by Bataille and map created in ArcMap 10.5.

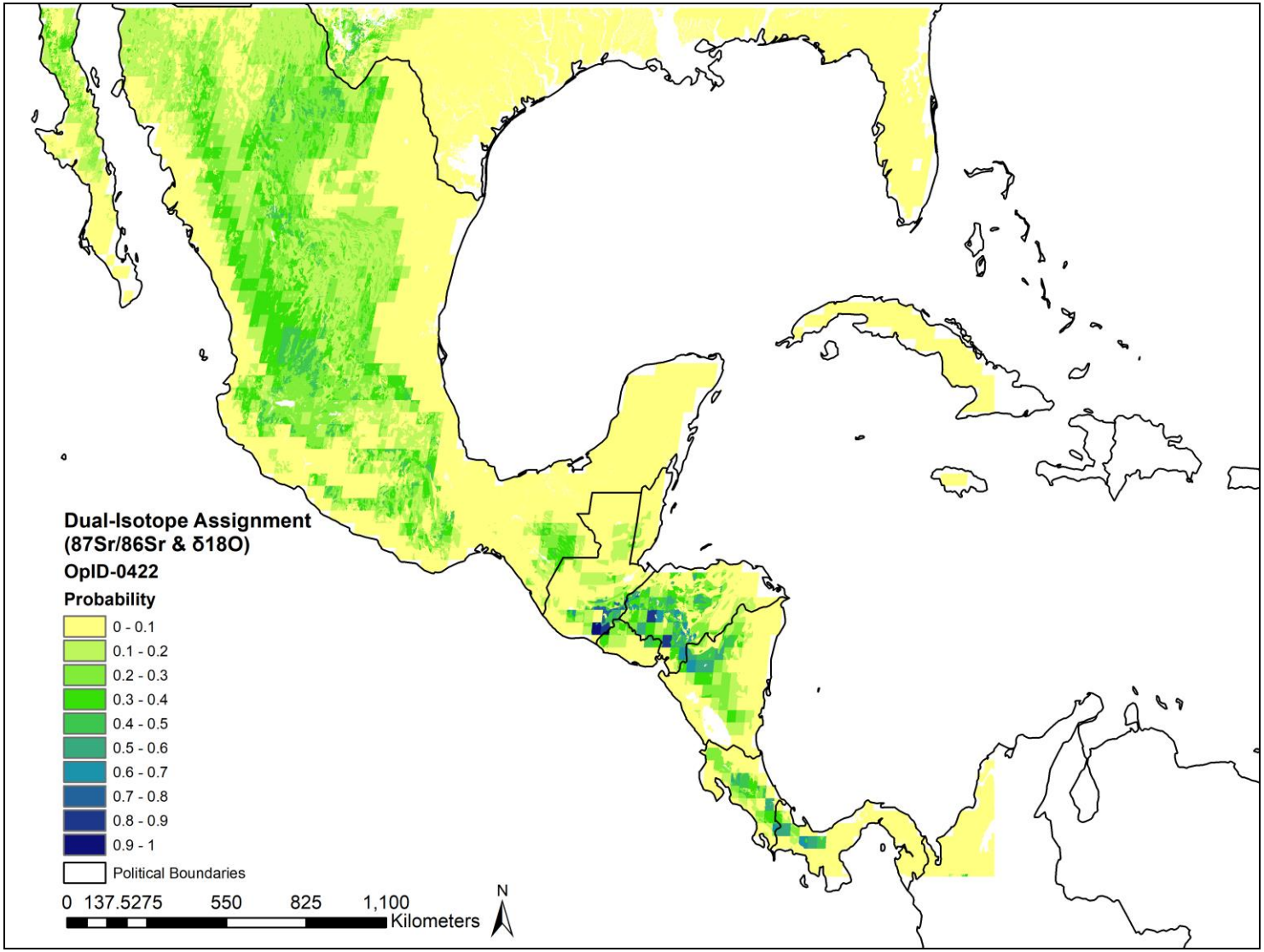

Figure C-9. Dual-Isotope ($^{87}Sr/^{86}Sr$ and $\delta^{18}O$) Prediction for OpID-0422. Assignment prediction map created in ArcMap 10.5.

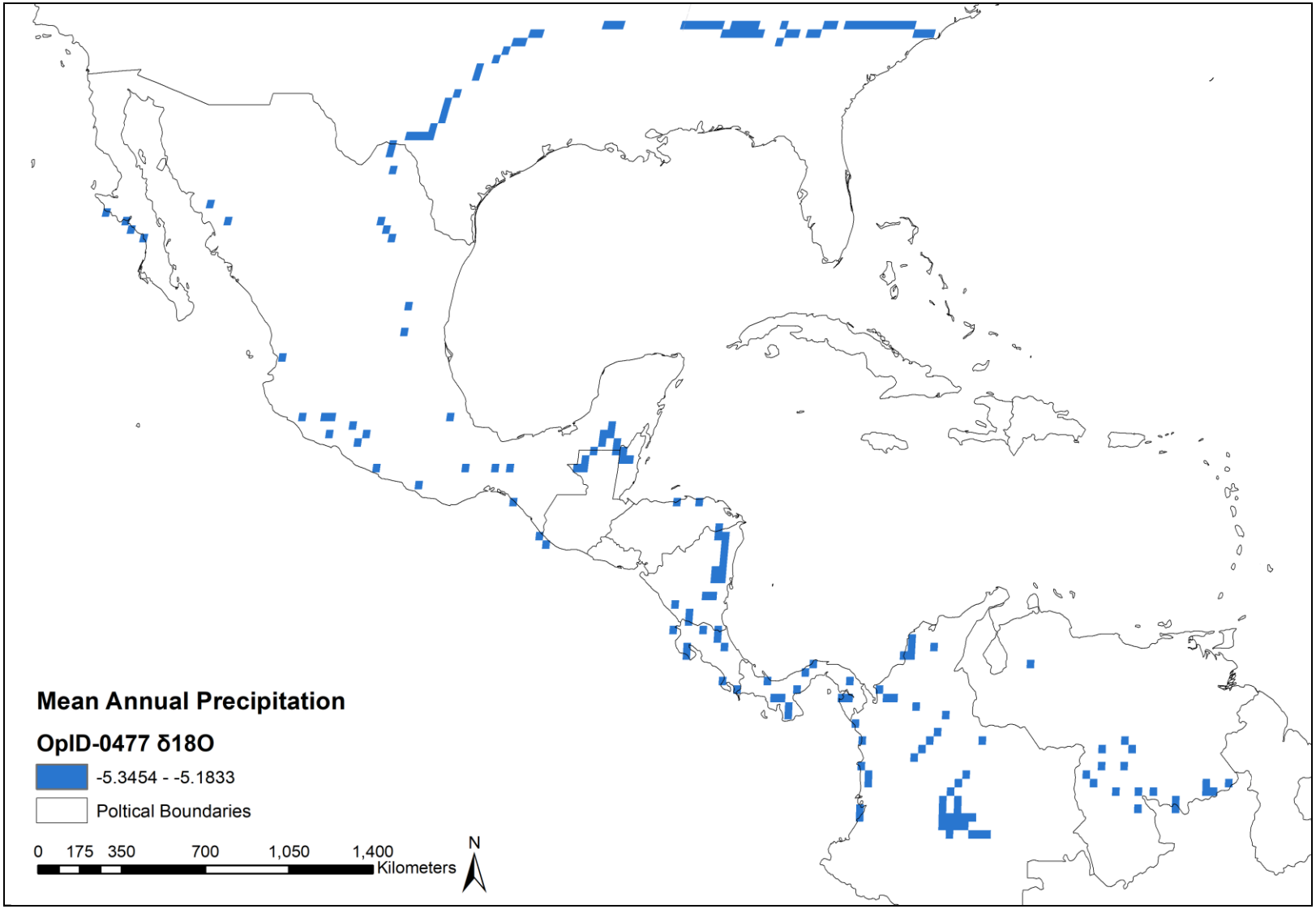

Figure C-10. Oxygen ($\delta^{18}O$) Prediction for OpID-0477. Raster by IsoMAP and map created in ArcMap 10.5.

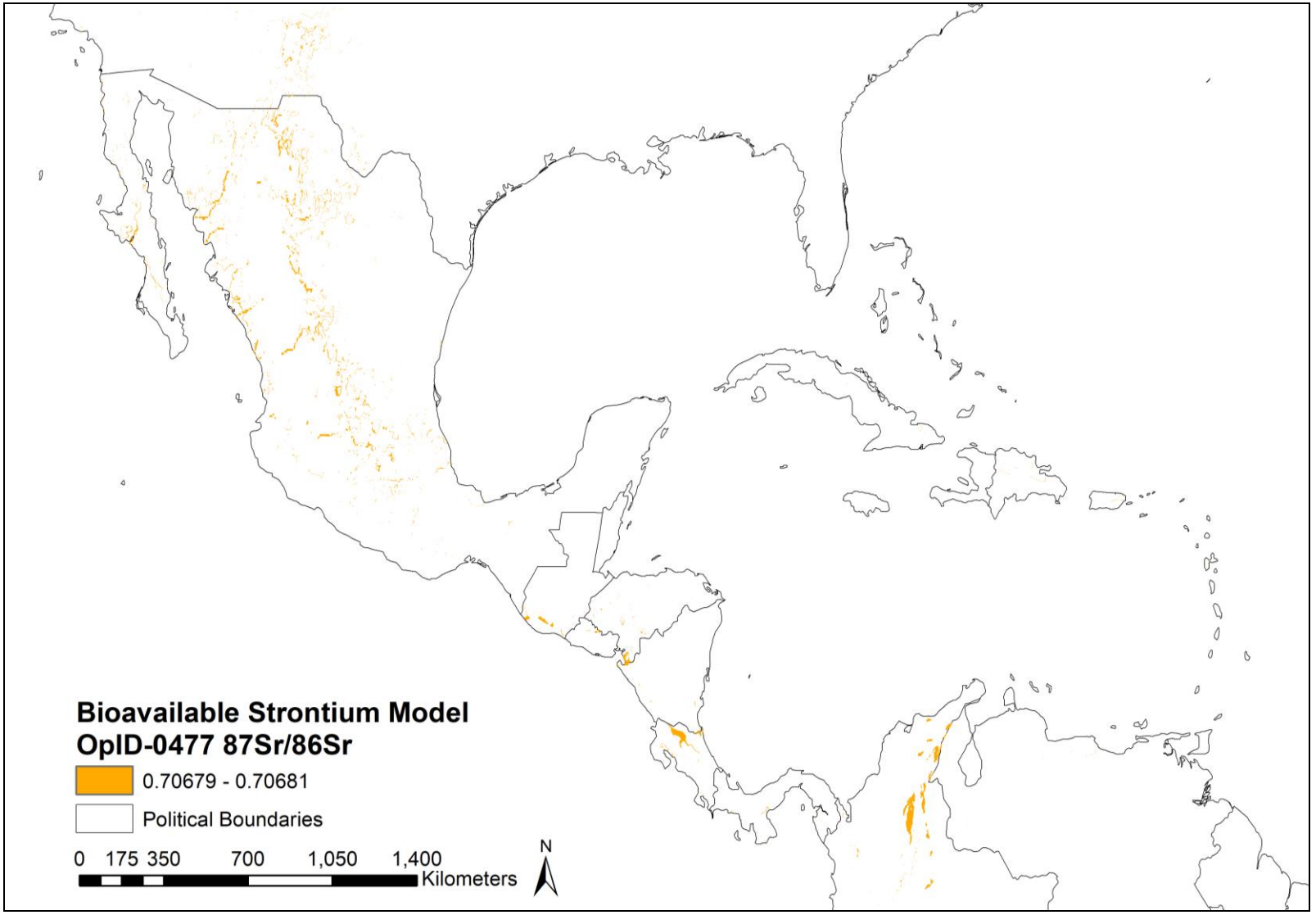

Figure C-11. Strontium ($^{87}Sr/^{86}Sr$) Prediction for OpID-0477. Raster provided by Bataille and map created in ArcMap 10.5.

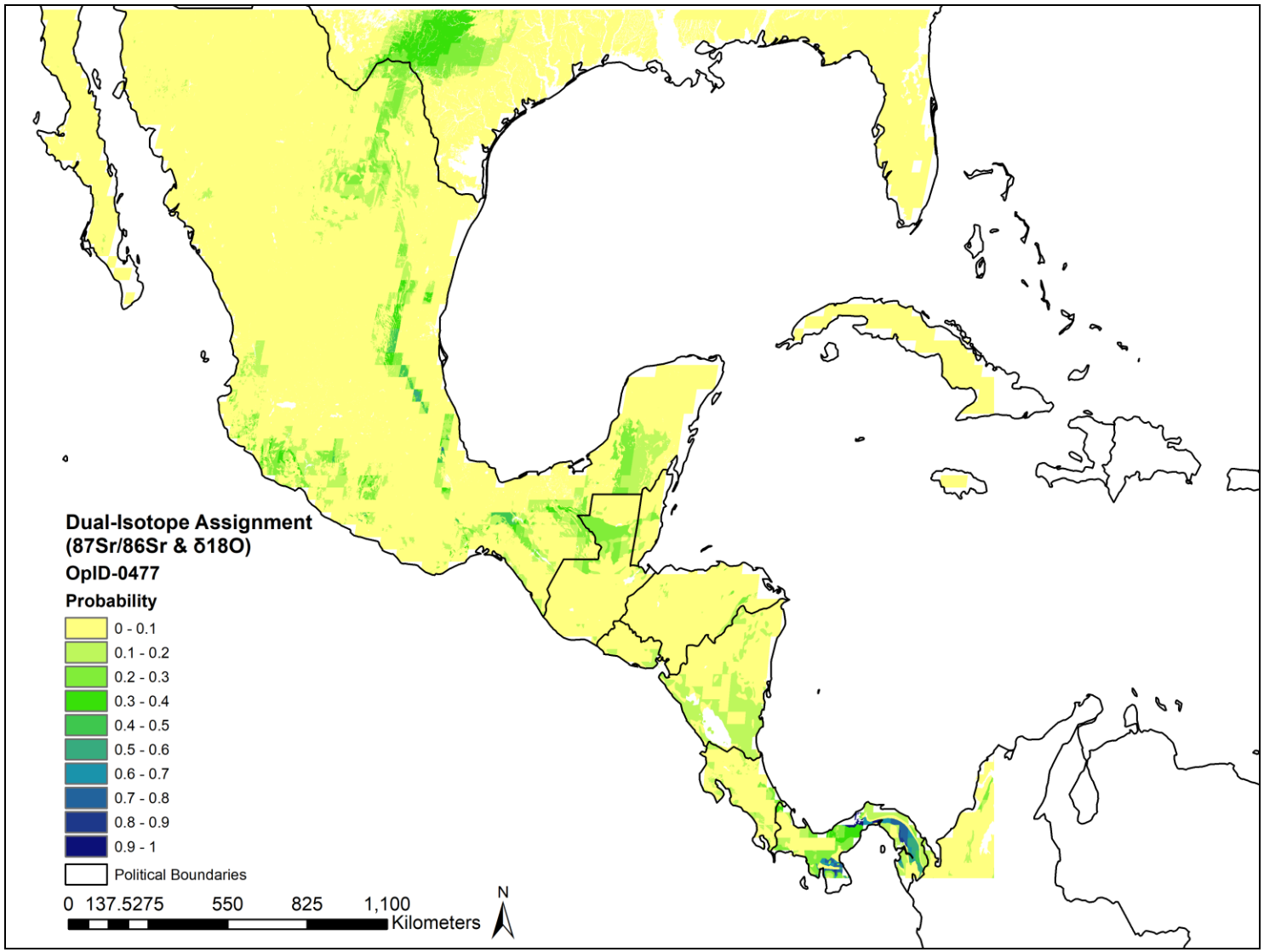

Figure C-12. Dual-Isotope ($^{87}Sr/^{86}Sr$ and $\delta^{18}O$) Prediction for OpID-0477. Assignment prediction map created in ArcMap 10.5.

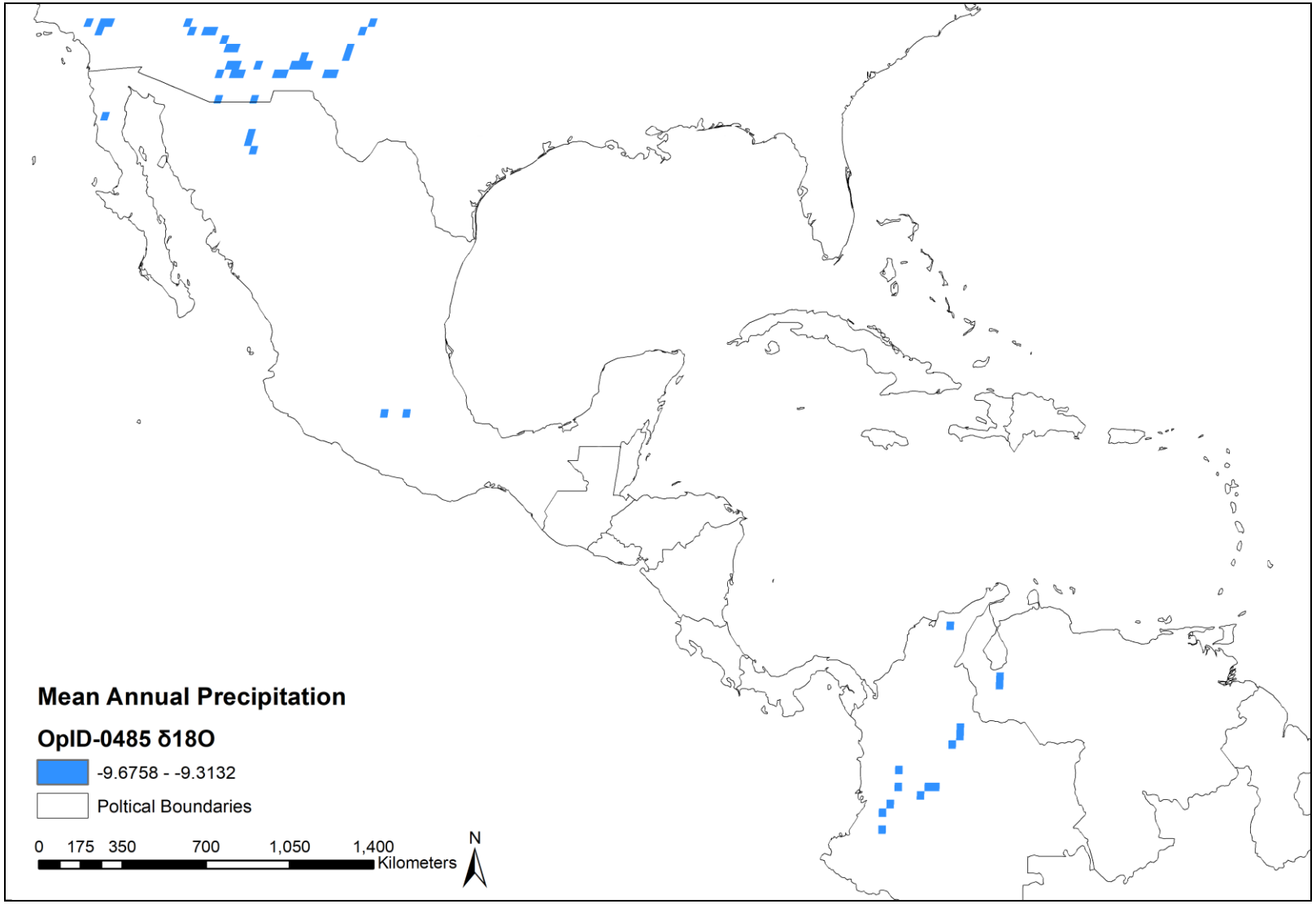

Figure C-13. Oxygen ($\delta^{18}O$) Prediction for OpID-0485. Raster by IsoMAP and map created in ArcMap 10.5.

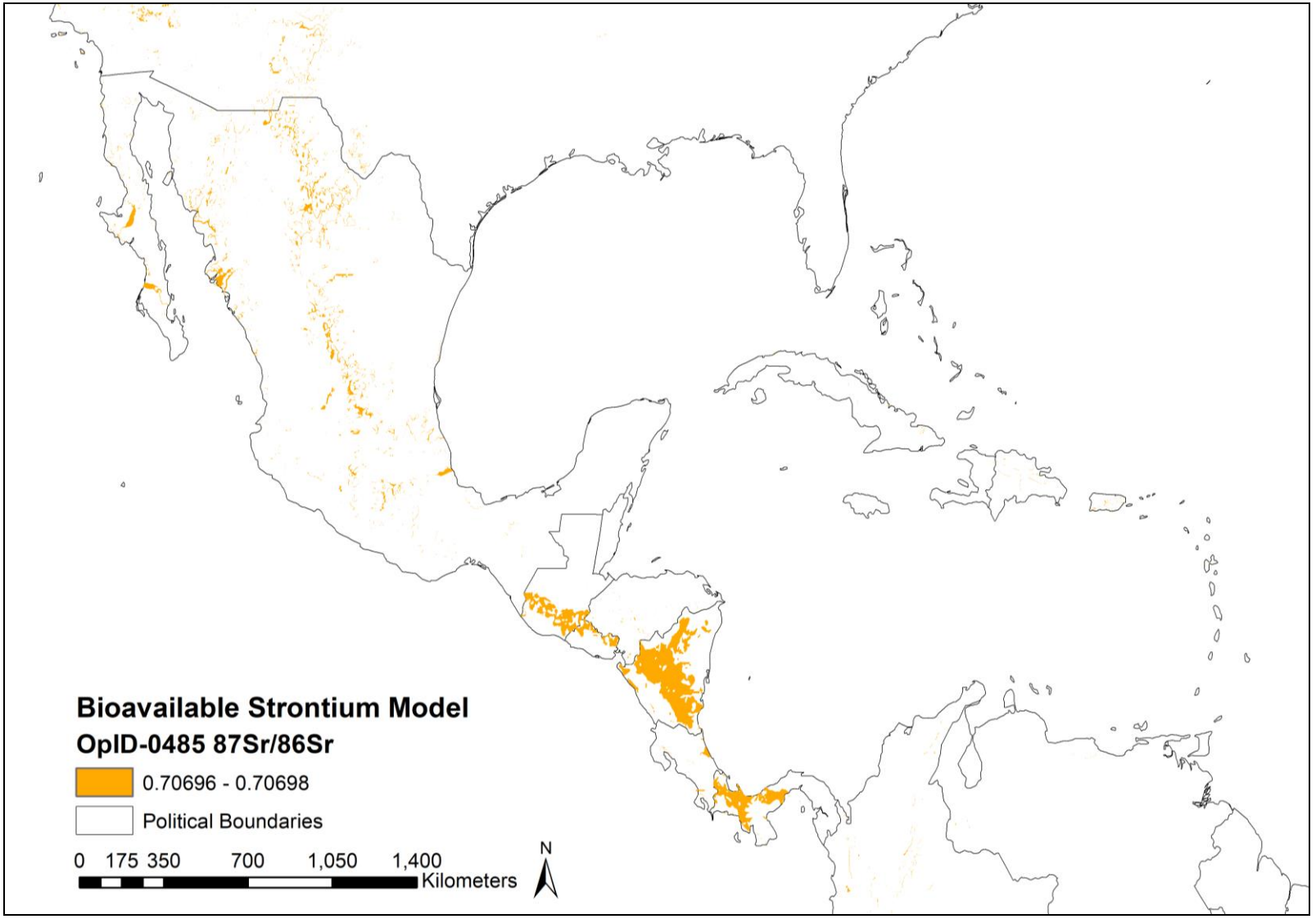

Figure C-14. Strontium ($^{87}Sr/^{86}Sr$) Prediction for OpID-0485. Raster provided by Bataille and map created in ArcMap 10.5.

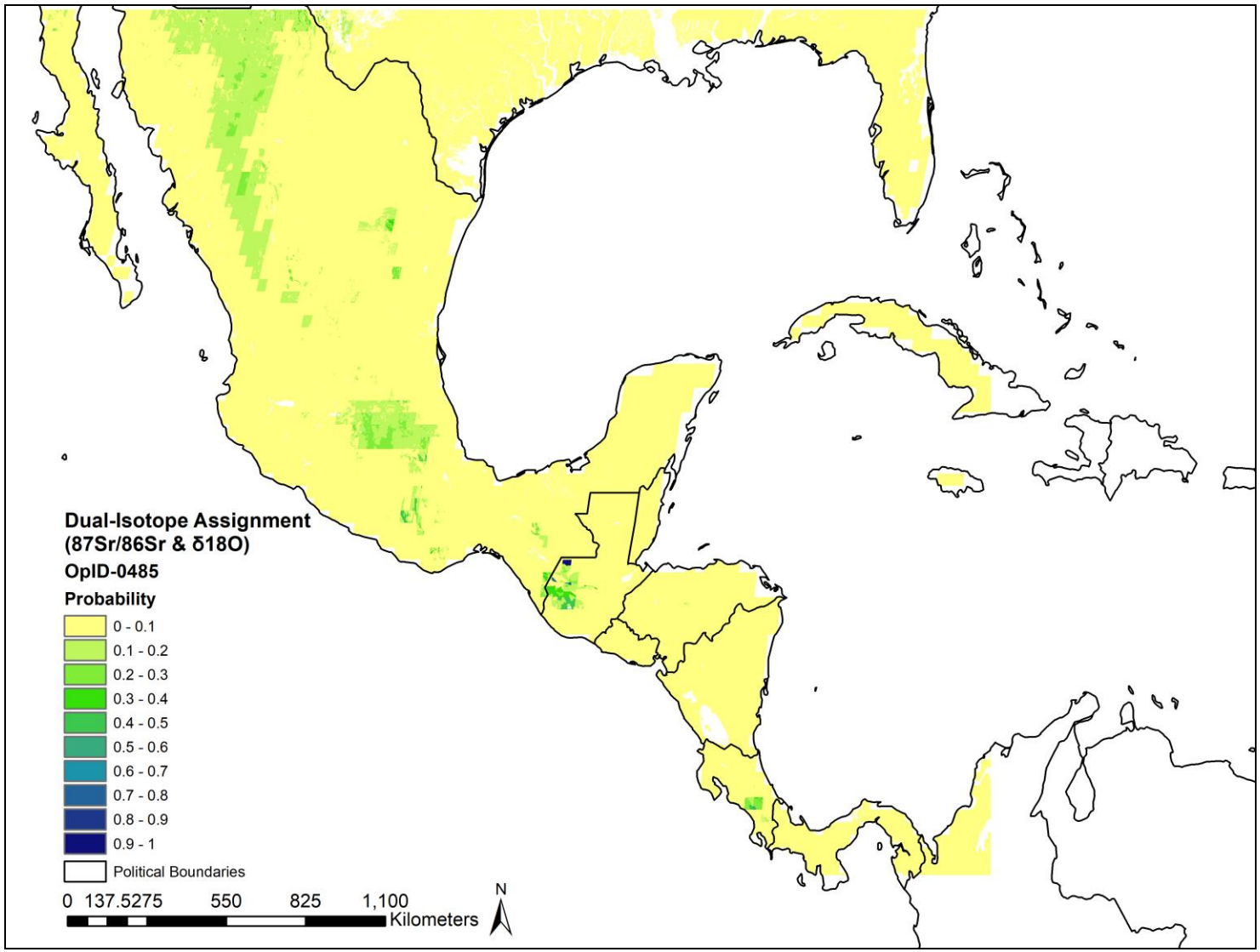

Figure C-15. Dual-Isotope ($^{87}Sr/^{86}Sr$ and $\delta^{18}O$) Prediction for OpID-0485. Assignment prediction map created in ArcMap 10.5.

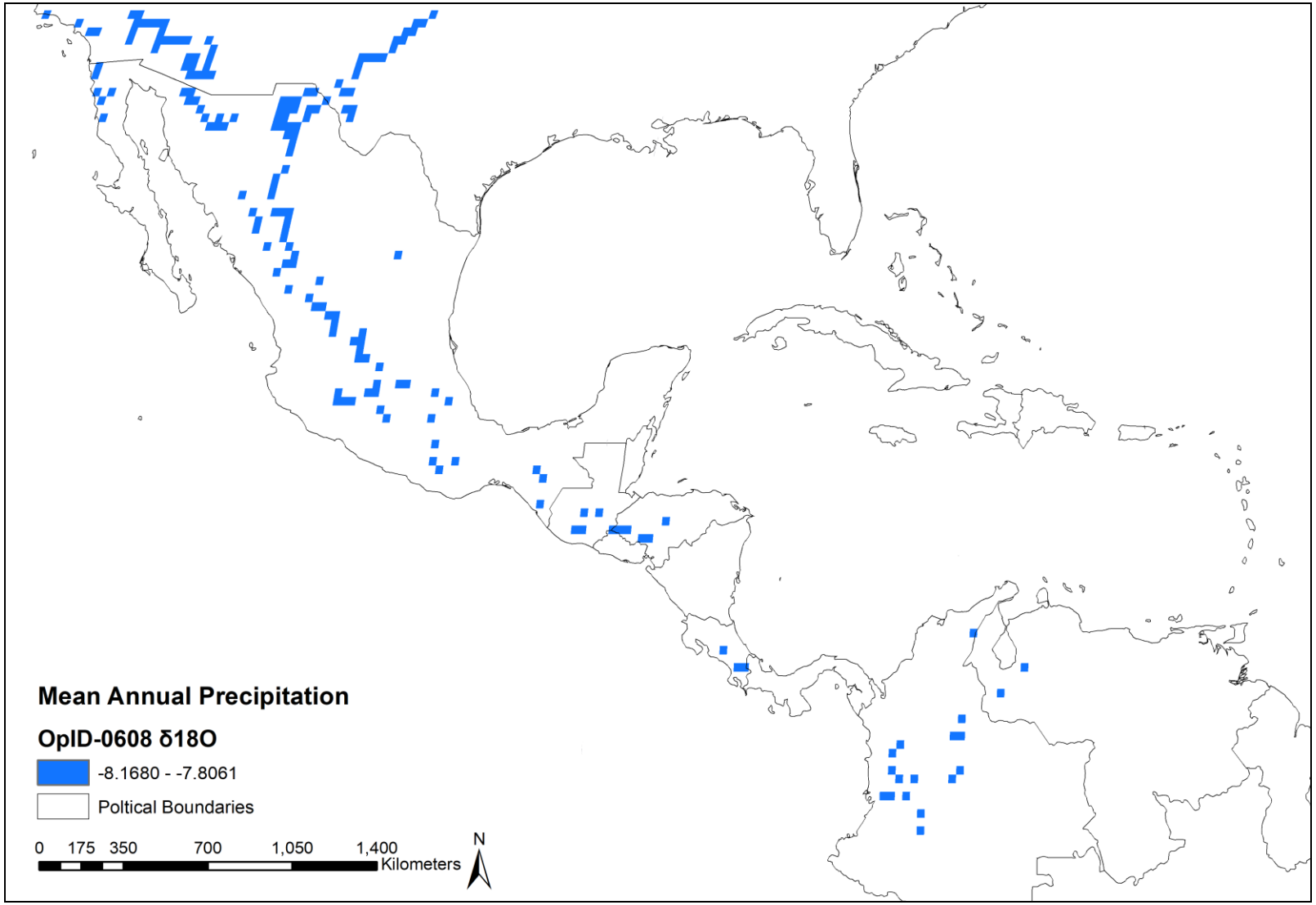

Figure C-16. Oxygen ($\delta^{18}O$) Prediction for OpID-0608. Raster by IsoMAP and map created in ArcMap 10.5.

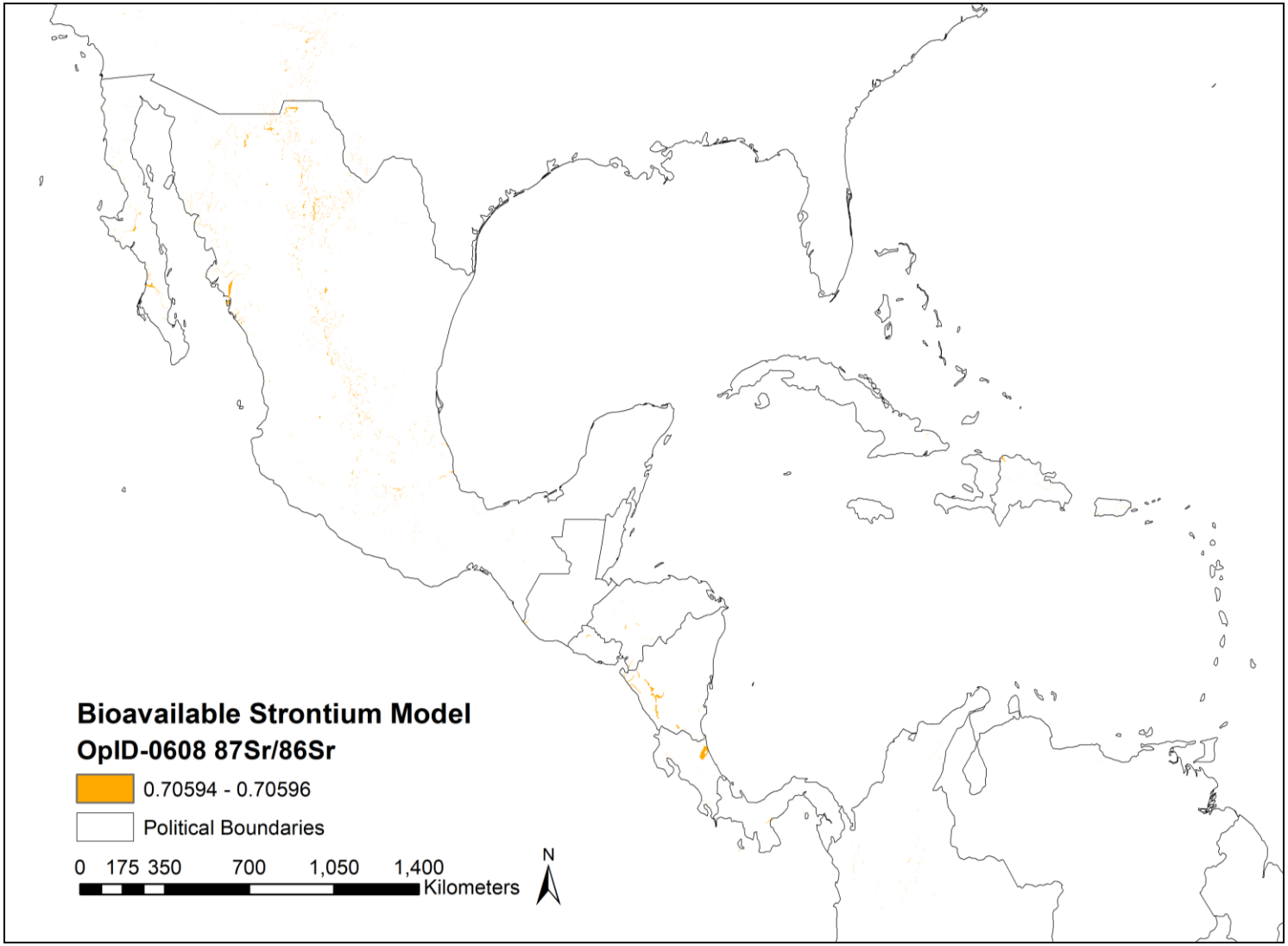

Figure C-17. Strontium ($^{87}Sr/^{86}Sr$) Prediction for OpID-0608. Raster provided by Bataille and map created in ArcMap 10.5.

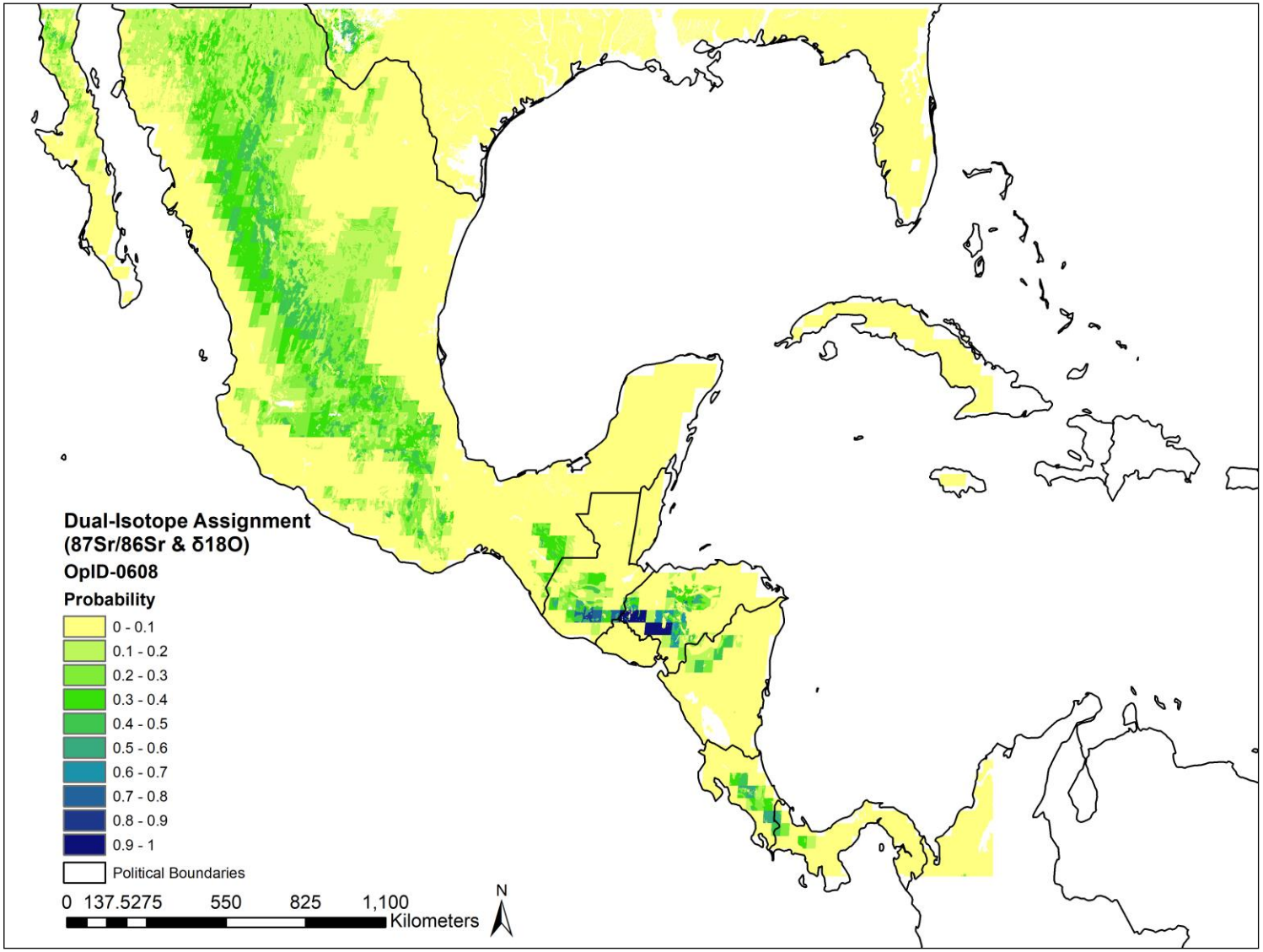

Figure C-18. Strontium ($^{87}Sr/^{86}Sr$) Prediction for OpID-0608. Raster provided by Bataille and map created in ArcMap 10.5.

LITERATURE CITED

Abd, E. (2011). *Using geographic information systems (gis) in spatial analysis of mortuary practices in the Kellis 2 Cemetery, Dakhleh Oasis, Egypt* (master's thesis). University of Central Florida.

Algee-Hewitt, B. F. (2016). Population inference from contemporary American craniometrics. *American Journal of Physical Anthropology*, *160*(4), 604-624.

Allison, C. E., & Francey, R. J. (1995). Recommendations for the reporting of stable isotope measurements of carbon and oxygen in CO_2 gas. *Reference and intercomparison materials for stable isotopes of light elements*, 154-164.

Ambrose, S. H. (1990). Preparation and characterization of bone and tooth collagen for isotopic analysis. *Journal of Archaeological Science*, *17*(4), 431-451.

Ambrose, S. H., & Norr, L. (1993). Experimental evidence for the relationship of the carbon isotope ratios of whole diet and dietary protein to those of bone collagen and carbonate. In *Prehistoric human bone* (pp. 1-37). Springer Berlin Heidelberg.

Anderson, B. E. (2008). Identifying the dead: methods utilized by the Pima County (Arizona) Office of the Medical Examiner for undocumented border crossers: 2001–2006. *Journal of Forensic Sciences*, *53*(1), 8-15.

Anderson BE & Spradley MK. 2016. The role of the anthropologists in the identification of migrant remains in the American southwest. Unpublished report. Texas: Texas State University, San Marcos, Anthropology Department.

Armelagos, G. J., & Gerven, D. P. V. (2003). A century of skeletal biology and paleopathology: contrasts, contradictions, and conflicts. *American Anthropologist*, *105*(1), 53-64.

Bartelink, E.J. & Eerkens, J.W. 2013. Sex-biased weaning and early childhood diet among middle Holocene hunter-gatherers in central California. *American Journal of Physical Anthropology,* 152:471-483.

Bartelink, E.J., Berg, G.E., Beasley, M.M., & Chesson, L.A. 2014. Application of stable isotope forensics for predicting region of origin of human remains from past wars and conflicts. *Annals of Anthropological Practice* 38(1):124-136.

Bartelink, E. J., Mackinnon, A. T., Prince-Buitenhuys, J. R., Tipple, B. J., & Chesson, L. A. (2016). Stable isotope forensics as an investigative tool in missing persons investigations. In *Handbook of Missing Persons* (pp. 443-462). Springer, Cham.

Bataille, C. P., & Bowen, G. J. (2012). Mapping $^{87}Sr/^{86}Sr$ variations in bedrock and water for large scale provenance studies. *Chemical Geology*, *304*, 39-52.

Bataille, C. P., Laffoon, J., & Bowen, G. J. (2012). Mapping multiple source effects on the strontium isotopic signatures of ecosystems from the circum-Caribbean region. *Ecosphere*, *3*(12), 1-24.

Bataille, C. P. (2017, June 20). Personal interview.

Beard, B. L., & Johnson, C. M. (2000). Strontium isotope composition of skeletal material can determine the birth place and geographic mobility of humans and animals. *Journal of Forensic Science*, *45*(5), 1049-1061.

Benson, S., Lennard, C., Maynard, P., & Roux, C. (2006). Forensic applications of isotope ratio mass spectrometry—a review. *Forensic Science International*, *157*(1), 1-22.

Bentley, R.A., R. Krause, T.D. Price, & B. Kaufmann. (2003). Human mobility at the early Neolithic settlement of Vaihingen, Germany: evidence from strontium isotope analysis. *Archaeometry*, 45, 471-486.

Bentley, R. A., T. D. Price, & E. Stephan. (2004). Determining the 'local' 87 Sr/86 Sr range for archaeological skeletons: a case study from Neolithic Europe. *Journal of Archaeological Science*, 31(4), 365-375.

Bentley, R. A., & C. Knipper. (2005). Geographical patterns in biologically available strontium, carbon and oxygen isotope signatures in prehistoric Southwest Germany. *Archaeometry*, 47(3), 629-44.

Bentley, R. A. (2006). Strontium isotopes from the earth to the archaeological skeleton: a review. *Journal of archaeological method and theory*, *13*(3), 135-187.

Bol, R., Marsh, J., & Heaton, T. H. (2007). Multiple stable isotope (18O, 13C, 15N and 34S) analysis of human hair to identify the recent migrants in a rural community in Southwest England. *Rapid Communications in Mass Spectrometry*, *21*(18), 2951-2954.

Bosl, C., Grupe, G., & Peters, J. 2006. A late Neolithic vertebrate food web based on stable isotope analyses. *International Journal of Osteoarchaeology*, 16(4):296-315.

Bowen, G. J. (2010). Statistical and geostatistical mapping of precipitation water isotope ratios. In *Isoscapes* (pp. 139-160). Springer Netherlands.

Bowen, G. J. (2013). Geographic assignment with stable isotopes in IsoMAP. *Methods in Ecology and Evolution*, 1-6.

Bowen, G. J. (2017, November 20). Personal Interview.

Budd, P., Millard, A., Chenery, C., Lucy, S., & Roberts, C. (2004). Investigating population movement by stable isotope analysis: a report from Britain. *Antiquity*, *78*(299), 127-141.

Burrough, P.A. & McDonnell, R. A. (1998). *Principles of Geographical Information Systems*. Oxford University Press, Oxford.

Byrd, A. M. (2016). *A GIS-based investigation into social violence and settlement patterns in the Gallina area of the American Southwest*. The University of New Mexico.

Carson, E. (2006). Maximum likelihood estimation of human craniometric heritabilities. *American Journal of Physical Anthropology*, *131*(2), 169-180.

Caspari, R. (2003). From types to populations: A century of race, physical anthropology, and the American Anthropological Association. *American Anthropologist*, *105*(1), 65-76.

Christensen, A. M., Passalacqua, N. V., & Bartelink, E. J. (2013). *Forensic Anthropology: Current methods and practice.* Elsevier.

Comar, C. L., Russell, R. S., & Wasserman, R. H. (1957). Strontium-calcium movement from soil to man. *Science 126*(3272):485-492.

DeLuca, L. A., McEwen, M. M., & Keim, S. M. (2010). United States–Mexico border crossing: Experiences and risk perceptions of undocumented male immigrants. *Journal of Immigrant and Minority Health*, *12*(1), 113-123.

Devor, E. J., McGue, M., Crawford, M. H., & Lin, P. M. (1986). Transmissible and nontransmissible components of anthropometric variation in the Alexanderwohl Mennonites: II. Resolution by path analysis. *American Journal of Physical Anthropology*, *69*(1), 83-92.

Edgar, H. J. (2013). Estimation of ancestry using dental morphological characteristics. *Journal of Forensic Sciences*, *58*(s1), 1-13.

Ehleringer, J. R., Bowen, G. J., Chesson, L. A., West, A. G., Podlesak, D. W., & Cerling, T. E. (2008). Hydrogen and oxygen isotope ratios in human hair are related to geography. *Proceedings of the National Academy of Sciences*, *105*(8), 2788-2793.

Ehleringer, J. R., Thompson, A. H., Podlesak, D. W., Bowen, G. J., Chesson, L. A., Cerling, T. E., Park, T., Dostie, P. & Schwarcz, H. (2010). A framework for the incorporation of isotopes and isoscapes in geospatial forensic investigations. In *Isoscapes* (pp. 357-387). Springer Netherlands.

Faure, G., & Powell, J. L. (1972). *Strontium isotope geology* (5). Berlin: Springer-Verlag.

Freiwald, C. (2011). *Maya migration networks: Reconstructing population movement in the Belize River valley during the Late and Terminal Classic* (Doctoral Dissertation) Retrieved from Academia. Edu. Vol. 72, No. 11.

Fry, B. (2006). *Stable isotope ecology*. New York: Springer.

Gill, G. W. (1998). Craniofacial criteria in the skeletal attribution of race. *Forensic osteology: Advances in the identification of human remains*. Springfield: Charles C. Thomas Publisher, Ltd.

Gravlee, C. C. (2009). How race becomes biology: embodiment of social inequality. *American Journal of Physical Anthropology*, *139*(1), 47-57.

Hefner, J. T. (2009). Cranial Nonmetric Variation and Estimating Ancestry. *Journal of Forensic Sciences, 54*(5), 985-995.

Hefner, J. T. & Ousley, S. D. (2014). Statistical classification methods for estimating ancestry using morphoscopic traits. *Journal of Forensic Sciences, 59(4),* 883-890.

Hefner, J. T., Spradley, M. K., & Anderson, B. (2014). Ancestry assessment using random forest modeling. *Journal of Forensic Sciences, 59(3),* 583-589.

Herrmann, N. P. & Devlin, J. B. (2008). Bone color as an interpretive tool of the depositional history of archaeological cremains. *The analysis of burned human remains*, *13*, 109-128.

Herz, N., & Garrison, E. G. (1997). *Geological methods for archaeology*. Oxford University Press.

Hillson, S. (2014). *Tooth development in human evolution and bioarchaeology*. Cambridge University Press.

Hoefs, J. (2008). *Stable isotope geochemistry*. Springer Science & Business Media.

Holmes, S. (2013). *Fresh fruit, broken bodies: Migrant farmworkers in the United States.* University of California Press.

Howells, W. W. (1995). Who's who in skulls: ethnic identification of crania from measurements. *Papers of the Peabody Museum of Archaeology and Ethnology, Harvard University*, 82. The Museum: Cambridge, MA.

Jantz, R. L. (2000). DISPOP Program.

Jantz, R. L., & Owsley, D. W. (2001). Variation among early North American crania. *American Journal of Physical Anthropology*, *114*(2), 146-155.

Jantz, R. L., & Ousley, S. D. (2005). FORDISC 3.0: personal computer forensic discriminant functions. *Knoxville, TN: University of Tennessee.*

Juarez, C. A. (2008). Strontium and geolocation, the pathway to identification for deceased undocumented Mexican border-crossers: A preliminary report. *Journal of Forensic Science*, *53*(1), 46-49.

Katzenberg, M. A. (2008). Stable isotope analysis: a tool for studying past diet, demography, and life history. *Biological Anthropology of the Human Skeleton, Second Edition*, 411-441.

Kennedy, K. A. (1995). But Professor, why teach race identification if races don't exist? *Journal of Forensic Science*, *40*(5), 797-800.

Klimentidis, Y. C., Miller, G. F., & Shriver, M. D. (2009). Genetic admixture, self-reported ethnicity, self-estimated admixture, and skin pigmentation among Hispanics and Native Americans. *American Journal of Physical Anthropology*, *138*(4), 375-383.

Knudson, K. J., T. A. Tung, K. C. Nystrom, T.D. Price, & P.D. Fullagar. (2005). The origin of the Juch'uypampa Cave mummies: strontium isotope analysis of archaeological human remains from Bolivia. *Journal of Archaeological Science*, 32, 903-913.

Knudson, K. J., & Buikstra, J. E. (2007). Residential mobility and resource use in the Chiribaya polity of Southern Peru: strontium isotope analysis of archaeological tooth enamel and bone. *International Journal of Osteoarchaeology*, 17, 563-580.

Knudson, K. J., Williams, S. R., Osborn, R., Forgey, K., & Williams, P. R. (2009). The geographic origins of Nasca trophy heads using strontium, oxygen, and carbon isotope data. *Journal of Anthropological Archaeology*, *28*(2), 244-257.

Laffoon, J. E., Sonnemann, T. F., Shafie, T., Hofman, C. L., Brandes, U., & Davies, G. R. (2017). Investigating human geographic origins using dual-isotope (87Sr/86Sr, δ18O) assignment approaches. *PloS one*, *12*(2), e0172562.

Longinelli, A. (1984). Oxygen isotopes in mammal bone phosphate: a new tool for paleohydrological and paeloclimatological research? *Geochemica et Cosmochimica Acta*, 48, 385-390.

Luz, B. & Y. Kolodny. (1985). Oxygen isotope variations in phosphate of biogenic apatites, IV mammal teeth and bone. *Eart and Planetary Science Letters*, 75, 29-36.

McMurry, J., & Fay, R.C. (2004). *Chemistry*. *4th edition.* Belmont, CA: Pearson Education.

Meehan, T. D., Giermakowski, J. T., & Cryan, P. M. (2004). GIS-based model of stable hydrogen isotope ratios in North American growing-season precipitation for use in animal movement studies. *Isotopes in environmental and health studies*, *40*(4), 291-300.

Miller, H. J. (2004). Tobler's first law and spatial analysis. *Annals of the Association of American Geographers*, *94*(2), 284-289.

Operation Identification. (2017, October 28). Retrieved from http://www.txstate.edu/anthropology/facts/outreach/opid.html

Ousley, S. D., & Jantz, R. L. (2005). FORDISC 3.1: computerized forensic discriminant functions. Knoxville (TN): The University of Tennessee.

Ousley, S. D., & Jantz, R. L. (2012). Fordisc 3 and statistical methods for estimating sex and ancestry. *A companion to forensic anthropology*. United Kingdom: Wiley & Sons.

Pestle, W. J., Crowley, B. E., & Weirauch, M. T. (2014). Quantifying inter-laboratory variability in stable isotope analysis of ancient skeletal remains. *PLoS one*, *9*(7), e102844.

Pima County Office of the Medical Examiner. (2016*). Annual Report 2016.* [Internet]. Available from https://webcms.pima.gov/UserFiles/Servers/Server_6/File/Government/Medical%20Examiner/Resources/Annual-Report-2016.pdfstats. Accessed: Jan 2017.

Price, T. D., Burton, J. H., Fullagar, P. D., Wright, L. E., Buikstra, J. E., & Tiesler, V. (2015). Strontium isotopes and the study of human mobility among the ancient maya. In *Archaeology and bioarchaeology of population movement among the Prehispanic Maya* (pp. 119-132). Springer International Publishing.

Price, T. D., Manzanilla, L., & Middleton, W. D. (2000). Immigration and the ancient city of Teotihuacan in Mexico: a study using strontium isotope ratios in human bone and teeth. *Journal of Archaeological Science*, *27*(10), 903-913.

Price, T. D., Burton, J. H., & Bentley, R. A. (2002). The characterization of biologically available strontium isotope ratios for the study of prehistoric migration. *Archaeometry, 44*(1), 117-135.

Ramey, R. & Juarez, C. A. (2018, April). *The challenges of forensic geolocation in the context of water insecurity in Mexico: understanding the relationships and limitations between isotopes in drinking water, teeth and hair.* Poster session presented at the meeting of the American Association of Physical Anthropology, Austin, TX.

Regan, L. A. (2006). *Isotopic determination of region of origin in modern peoples: Applications for identification of US war-dead from the Vietnam Conflict.* (Master's thesis). Retrieved from Florida University, Gainesville.

Relethford, J. H. (1994). Craniometric variation among modern human populations. *American Journal of Physical Anthropology*, *95*(1), 53-62.

Relethford, J. H. & Harding, R. M. (2001). Population genetics of modern human evolution. *Encyclopedia of Life Sciences*.

Relethford, J. H. (2010). Population-specific deviations of global human craniometric variation from a neutral model. *American Journal of Physical Anthropology*, *142*(1), 105-111.

Rhine, S. (1993). Skeletal criteria for racial attribution. *Annals of Anthropological Practice*, *13*(1), 54-67.

Rogerson, P. A. (2015). *Statistical methods for geography: a student's guide*. Sage.

Roseman, C. C., & Weaver, T. D. (2004). Multivariate apportionment of global human craniometric diversity. *American Journal of Physical Anthropology*, *125*(3), 257-263.

Sauer, N. J. (1992). Forensic anthropology and the concept of race: If races don't exist, why are forensic anthropologists so good at identifying them? *Social Science & Medicine*, *34*(2), 107-111.

Schoeninger, M. J., & DeNiro, M. J. (1984). Nitrogen and carbon isotopic composition of bone collagen from marine and terrestrial animals. *Geochimica et Cosmochimica Acta*, *48*(4), 625-639.

Schoeninger, M. J., & Moore, K. (1992). Bone stable isotope studies in archaeology. *Journal of World Prehistory*, *6*(2), 247-296.

Schwarcz, H. P., & Schoeninger, M. J. (1991). Stable isotope analyses in human nutritional ecology. *American Journal of Physical Anthropology*, *34*(S13), 283-321.

Sosa, T. S., A. Cucina, T. D. Price, J. H. Burton, & V. Tiesler. (2014). Maya coastal production, exchange, life stlye, and population mobility: a view from the port of Xcambo, Yucatan, Mexico. *Ancient Mesoamerica*, 25, 221-238.

Spradley, M. K. (2006). Biological anthropological aspects of the African diaspora; geographic origins, secular trends, and plastic versus genetic influences utilizing craniometric data. (Doctoral Dissertation). Retrieved from University of Tennessee, Knoxville. http://trace.tennessee.edu/utk_graddiss/1864.

Spradley, M. K. (2017, May 1). Personal interview.

Spradley, M. K. (2014). Toward Estimating Geographic Origin of Migrant Remains Along the United States-Mexico Border. *Annals of Anthropological Practice*, *38*(1), 101-110.

Spradley, M. K., Hamilton, M. D., & Giordano, A. (2012). Spatial patterning of vulture scavenged human remains. *Forensic Science International*, *219*(1-3), 57-63.

Spradley, M. K., Jantz, R. L., Robinson, A., & Peccerelli, F. (2008). Demographic change and forensic identification: problems in metric identification of Hispanic skeletons. *Journal of Forensic Sciences*, *53*(1), 21-28.

Spring, Ú. O. (Ed.). (2011). *Water resources in Mexico: scarcity, degradation, stress, conflicts, management, and policy* (Vol. 7). Springer Science & Business Media.

Tipple, B. J. (2015). Isotope Analyses of Hair as a Trace Evidence Tool to Reconstruct Human Movements: Combining Strontium Isotope with Hydrogen/Oxygen Isotope Data. (Technical Report). Retrieved from Department of Justice. (2011-DN-BX-K544).

Tobler, W. R. (1970). A computer movie simulating urban growth in the Detroit region. *Economic Geography*, *46*(sup1), 234-240.

Turner, B. L., Kamenov, G. D., Kingston, J. D., & Armelagos, G. J. (2009). Insights into immigration and social class at Machu Picchu, Peru based on oxygen, strontium, and lead isotopic analysis. *Journal of Archaeological Science*, *36*(2), 317-332.

United States Customs and Border Protection. (2016*). United States Border Patrol Southwest Border Sectors.* [Internet]. Available from http://www.cbp.gov/newsroom/media-resources/stats. Accessed: Jan 2017.

United States Customs and Border Protection. (2017*). United States Border Patrol Southwest Border Sectors.* [Internet]. Available from http://www.cbp.gov/newsroom/media-resources/stats. Accessed: Jan 2017.

Verzani, J. (2005). *Using R for introductory statistics*. CRC Press.

Warner, M. M. (2016). *A biogeochemistry approach to geographic origin and mortuary arrangement at the Talgua cave ossuaries, Olancho, Honduras.* (Master's thesis). Retrieved from Mississippi State.

Warner, M. M., Plemons, A. M., Herrmann, N. P., & Regan, L. A. (2018). Refining Stable Oxygen and Hydrogen Isoscapes for the Identification of Human Remains in Mississippi. *Journal of Forensic Sciences*, *63*(2), 395-402.

Wassenaar, L. I., Van Wilgenburg, S. L., Larson, K., & Hobson, K. A. (2009). A groundwater isoscape (δD, δ 18 O) for Mexico. *Journal of Geochemical Exploration*, *102*(3), 123-136.

West, J. B., Bowen, G.J., Dawson, T.E., Tu, K.P. (2010). Isoscapes: understanding movement, pattern, and process on Earth through isotope mapping. Netherlands: Springer.

West, J. B., Bowen, G. J., Cerling, T. E., & Ehleringer, J. R. (2006). Stable isotopes as one of nature's ecological recorders. *Trends in Ecology & Evolution*, *21*(7), 408-414.

Wunder, M. B., Kester, C. L., Knopf, F. L., & Rye, R. O. (2005). A test of geographic assignment using isotope tracers in feathers of known origin. *Oecologia*, *144*(4), 607-617.

Wunder, M. B., & Norris, D. R. (2008). Improved estimates of certainty in stable-isotope-based methods for tracking migratory animals. *Ecological Applications, 18*(2), 549-559.

Wunder, M. B. (2010). Using isoscapes to model probability surfaces for determining geographic origins. In *Isoscapes* (pp. 251-270). Springer Netherlands.

Wunder, M. B. (2012). Determining geographic patterns of migration and dispersal using stable isotopes in keratins. *Journal of Mammology*, 93(2), 360-367.

Wunder, M. (2017, June 21). Personal interview.